DETECTION OF UNDERWATER STIMULI IN CHAMBERED *NAUTILUS*

by

Christian P. Soucier

A dissertation submitted to the Graduate Faculty in Biology in partial fulfillment of the requirements for the degree of Doctor of Philosophy, The City University of New York

2006

This manuscript has been read and accepted for the Graduate Faculty in Biology in satisfaction of the dissertation requirements for the degree of Doctor of Philosophy

April 25th, 2006	Dr. Jennifer Basil
Date	Chair of Examining Committee
April 25th 2006	Dr. Richard Chappell
Date	Executive Officer

Dr. Christopher Braun, Hunter College, CUNY

Dr. John Chamberlain, Brooklyn College, CUNY

Dr. Matthew Perzanowski, Columbia University

Dr. Robert Rockwell, City College, CUNY

Dr. Richard Veit, College of Staten Island, CUNY

Supervisory Committee

THE CITY UNIVERSITY OF NEW YORK

Abstract

DETECTION OF UNDERWATER STIMULI IN CHAMBERED *NAUTILUS*

by

Christian P. Soucier

Advisor: Dr. Jennifer Basil

The marine environment is dominated by mechanical and acoustical energies such as water currents and vibrations. To respond to a given stimulus, marine organisms must collect information from their environment and subsequently process it. One such organism that may benefit from detecting these potential signals is the deep-water cephalopod, *Nautilus pompilius*. Two behavioral experiments were designed to test the sensory capabilities of *N. pompilius*. The first experiment exposed the animals to a series of angular accelerations and rotations to test the hypothesis that these animals are able to internalize environmental cues, such as hydrodynamic flow, perhaps with the aid of a canal (Kölliker's canal) that connects their statocyst to the exterior environment through an epidermal pore (an anatomical configuration that is unique within the Class Cephalopoda only to *Nautilus spp.*). As a measure of response to the stimulus, the positions of the hyponomes of the animals (funnels) were recorded throughout the experimental trials and their natural responses to angular acceleration were established. Results from the Angular-Accelerations Experiment indicated that only two of the 10 animals tested responded with compensatory movements in response to the rotating stimulus in the control condition. Analysis of all the animals suggested that when the animals were exposed to treatment conditions (unilateral and bilateral applications of petroleum jelly to the

area containing the epidermal pore), they responded by significantly re-positioning the hyponome either in the opposite direction (phase-shift) from that in the control condition or by maintaining the same direction but reducing the amplitude of the response. The second experiment tested the hypothesis that Chambered *Nautilus* are capable of responding to waterborne vibration — a sensory mechanism that had yet to be investigated. Animals were exposed to a vibrating bead that produced a range of displacements and velocities. Ventilation rate was used as a behavioral measure. Animals reduced their respiratory rate when exposed to vibrational stimuli: a decrease in respiration rate was significantly correlated to an increase in source-displacement (intensity) and source-velocity. Animals responded to stimuli in closer range by decreasing their ventilation rates even further.

For my wife, my mother, and most of all, for me.

Acknowledgements

It is with great pleasure that I am granted this opportunity to thank the following parties who have been instrumental in the completion of this project. First and foremost I would like to thank my advisor and mentor, Dr. Jennifer Basil, if not only for her wisdom and her intriguing ability to perceive the world through the eyes of the animal, but also for her patience and her never-ending tolerance as well. Secondly, I would like to thank my supervisory committee for all of their insights, explanations, teachings, and patience: Dr. Christopher Braun for his acoustical expertise; Dr. John Chamberlain for his knowledgeable critiques and constant flexibility; Dr. Neil Landman for all of his previous research, the opportunities he has afforded me, and his willingness to participate as an external reader; Dr. Matthew Perzanowski for his intellect and friendship; Dr. Robert "Rocky" Rockwell for his unmatched statistical knowledge and for making me part of the Annie Moore's family; and, finally, Dr. Richard Veit for his support and advice.

Next, I would like to thank the Laboratory of Invertebrate Behavioral Ecology of Brooklyn College/CUNY, and all of the individuals residing there who supported and assisted me throughout this entire process. Namely, graduates Kristine Kuroiwa-Bazzan, David Klein, and Robyn Crook, for their loyalty, their friendships, and all of their help, as well as undergraduates Michael Barach, Moses Feaster, and Daniel Hagler, for each of their needed contributions. I would also like to thank Dr. Martin Schreibman and the staff of the Aquatic Research and Environmental Assessment Center of Brooklyn College/CUNY (Jacob Raz, Chester Zarnoch, Doug "Man-Bear" Laing, and Robb Dickie) for the use of their facilities and creative solutions.

I would also like to recognize the institutional support I was granted throughout this process. A special thank you to Brooklyn College and the Department of Biology for keeping me employed throughout. Additionally, I would like to thank the American Museum of Natural History and the Sigma Xi Society for Scientific Research for the funding opportunities they provided me. Most of all, I would like to thank the Graduate Center of the City University of New York and Joan Reid and Dr. Richard Chappell of the Ph.D. Program in Biology for making this all possible.

Lastly, I would like to acknowledge each and every family member and friend that has supported me throughout this seemingly eternal process, with special regards to the Bishops of the Oblong Table. I treasure deeply the bonds that have been forged with each of you and truly appreciate all of your advice and encouragement. I want to give special thanks to my wife, Stephanie Vargas Soucier, for her graphical expertise and contributions as well as her support and patience. And, on a much sadder note, I would like to recognize one dear friend in particular, Louis Gelato, whose future and promise prematurely ended in January of 2005; Louis is a friend whom I shall never forget.

Table of Contents

List of Tables ..... **x**
List of Figures ..... **xi**
1.0 Introduction **1**
1.1 Natural History of the Chambered Nautilus **2**
1.2 Linear and Angular Acceleration Receptors **5**
1.3 Mechanics of Underwater Sound and Biological Relevance **8**
1.4 Previous Investigations and Current Research **11**
2.0 Angular Acceleration Experimental Overview **16**
2.1 Methods for Angular Acceleration Experiment **16**
2.1.1 Animals *16*
2.1.4 Data Collection and Analysis *21*
2.2 Results **23**
2.2.1 Overall behavior *23*
2.2.2 Individual Responses to Blocking Procedures *25*
2.3 Discussion **30**
3.0 Experimental Overview for Vibration Sensitivity Experiments **35**
Animals *36*
3.1 Methods for Source-Displacement Experiments **37**
3.1.1 Experimental Apparatus *37*
3.1.2 Vibrating Stimulus *37*
Instrument Calibration *39*
3.1.3 Experimental Procedures *39*
3.2 Methods for Frequency Sensitivity Experiment **40**
3.2.1 Experimental Apparatus *40*
3.2.2 Vibrating Stimulus *41*
3.2.3 Experimental Procedure *42*
3.3 Data Collection and Behavioral Analysis **42**
3.3.1 Statistical Analysis *43*
3.4 Overall Combined Results for All Experiments **44**
3.5 Results for Small Source-Displacement Experiment: Bead Displacement 0.01-0.13mm **47**
3.5.1 General Behavior *47*
3.5.2 Pooled Behavioral Analysis *48*
3.5.3 Behavioral Analyses of Individuals *49*
3.6 Results for Large Source-Displacement Experiment: Bead Displacement 0.08-1.12mm **53**
3.6.1 General Behavior *53*
3.6.2 Pooled Behavioral Analysis *54*
3.7 Results for Frequency Sensitivity Experiment: Range 10–1000Hz **57**
3.7.1 General Behavior *57*
3.7.2 Pooled Behavioral Analysis *57*
3.7.3 Behavioral Analyses of Individuals *60*

Table of Contents (continued)

3.8 Discussion..... 64
3.8.1 Possible Mechanisms of Transmission 66
3.8.2 Sample Size 68
3.8.3 Selection of 0.37mm Source-displacement for FSE..... 69
4.0 General Conclusions and Future Considerations 71
Literature Cited 124

List of Tables

Table 3.1. A list of six typical *Nautilus* behaviors, their corresponding index values, and their levels of measurement that were intended to be used in statistical analysis. Ventilation rate proved to be the only observable behavior and was therefore the only behavior that was incorporated into the analysis..... 93

Table 3.2. Table 3.2 lists changes in ventilation rate (VR) from the control mean for each stimulus and post-stimulus time bin according to three different experiments. Probability values are also given and maximum percentage values are bolded for each experiment..... 100

List of Figures

Figure 1.1. (A) Anterior view of a coleoid statocyst (*Octopus vulgaris*) depicting the macula and crista systems that are absent in *Nautilus*. (B) Anterior view of a *Nautilus* statocyst and the extension of Kölliker's canal to the exterior. Wavy line is an approximate demarcation of dorsal/ventral split (figure not to scale). 74

Figure 1.2. Lateral view of *Nautilus* depicting various external components with emphasis on the location of the epidermal pore that connects Kölliker's canal with the left statocyst. 75

Figure 2.1. Figure 2.1 is a schematic of the angular acceleration experimental apparatus; a.k.a. The SpinMaster. Components are listed as follows: a) 20-watt lamp, b) reversible motor with pulley, c) cylindrical tank with pulley, d) camera platform and camera, and e) animal harness. 76

Figure 2.2. Figure 2.2 is an image of an experimental animal extracted from video that shows the position of the hyponome (right-handed) during a counter clockwise rotation. The arrow approximately indicates the corresponding coordinates of measure for this frame. 77

Figure 2.3. Animal 1. Hyponome position in respect to a rotating stimulus for different blockage treatments. Increasing position values (0–360°) indicate a CCW rotation whereas decreasing values (360–0°) reflect a CW rotation. (+) Response values indicate hyponome positioning to the animal's left whereas (-) values indicate hyponome positioning to the animal's right. Compensatory responses are seen when the values of both variables are synchronized with respect to time. 78

Figure 2.4. Animal 11. Hyponome position in respect to a rotating stimulus for different blockage treatments. Increasing position values (0–360°) indicate a CCW rotation whereas decreasing values (360–0°) reflect a CW rotation. (+) Response values indicate hyponome positioning to the animal's left whereas (-) values indicate hyponome positioning to the animal's right. Compensatory responses are seen when the values of both variables are synchronized with respect to time. 79

Figure 2.5. Animal 7. Hyponome position in respect to a rotating stimulus for different blockage treatments. Increasing position values (0–360°) indicate a CCW rotation whereas decreasing values (360–0°) reflect a CW rotation. (+) Response values indicate hyponome positioning to the animal's left whereas (-) values indicate hyponome positioning to the animal's right. Compensatory responses are seen when the values of both variables are synchronized with respect to time. 80

Figure 2.6. Animal 9. Hyponome position in respect to a rotating stimulus for different blockage treatments. Increasing position values (0–360°) indicate a CCW rotation whereas decreasing values (360–0°) reflect a CW rotation. (+) Response values indicate hyponome positioning to the animal's left whereas (-) values indicate hyponome positioning to the animal's right. Compensatory responses are seen when the values of both variables are synchronized with respect to time. 81

List of Figures (continued)

Figure 2.7. Animal 10. Hyponome position in respect to a rotating stimulus for different blockage treatments. Increasing position values (0–360°) indicate a CCW rotation whereas decreasing values (360–0°) reflect a CW rotation. (+) Response values indicate hyponome positioning to the animal's left whereas (-) values indicate hyponome positioning to the animal's right. Compensatory responses are seen when the values of both variables are synchronized with respect to time. 82

Figure 2.8. Animal 2. Hyponome position in respect to a rotating stimulus for different blockage treatments. Increasing position values (0–360°) indicate a CCW rotation whereas decreasing values (360–0°) reflect a CW rotation. (+) Response values indicate hyponome positioning to the animal's left whereas (-) values indicate hyponome positioning to the animal's right. Compensatory responses are seen when the values of both variables are synchronized with respect to time. 83

Figure 2.9. Animal 3. Hyponome position in respect to a rotating stimulus for different blockage treatments. Increasing position values (0–360°) indicate a CCW rotation whereas decreasing values (360–0°) reflect a CW rotation. (+) Response values indicate hyponome positioning to the animal's left whereas (-) values indicate hyponome positioning to the animal's right. Compensatory responses are seen when the values of both variables are synchronized with respect to time. 84

Figure 2.10. Animal 4. Hyponome position in respect to a rotating stimulus for different blockage treatments. Increasing position values (0–360°) indicate a CCW rotation whereas decreasing values (360–0°) reflect a CW rotation. (+) Response values indicate hyponome positioning to the animal's left whereas (-) values indicate hyponome positioning to the animal's right. Compensatory responses are seen when the values of both variables are synchronized with respect to time. 85

Figure 2.11. Animal 6. Hyponome position in respect to a rotating stimulus for different blockage treatments. Increasing position values (0–360°) indicate a CCW rotation whereas decreasing values (360–0°) reflect a CW rotation. (+) Response values indicate hyponome positioning to the animal's left whereas (-) values indicate hyponome positioning to the animal's right. Compensatory responses are seen when the values of both variables are synchronized with respect to time. 86

Figure 2.12. Animal 8. Hyponome position in respect to a rotating stimulus for different blockage treatments. Increasing position values (0–360°) indicate a CCW rotation whereas decreasing values (360–0°) reflect a CW rotation. (+) Response values indicate hyponome positioning to the animal's left whereas (-) values indicate hyponome positioning to the animal's right. Compensatory responses are seen when the values of both variables are synchronized with respect to time. 87

List of Figures (continued)

Figure 2.13. Strength of Response (SOR) comparisons for all animals (N = 10) across all treatments. Probability values reflect significant differences of mean SOR between individual blocking treatments and the control. 88

Figure 3.1. Experimental setup for source-displacement experiments: a) top-view camera, b) oscilloscope, c) laptop computer, d) side-view camera, e) vibration absorption table, f) experimental tank with animal, and g) wall mount with mini-shaker and shaft/bead. 89

Figure 3.2. Fig. 3.2 is a screenshot of a computer-generated stimulus package that was used in the source-displacement experiments. Each signal is a composition of ten 2ms bursts of equal displacement amplitudes administered over a 5s period. Intervals consisting of 15s of silence were placed between each signal. 90

Figure 3.3. Experimental apparatus for frequency sensitivity experiments: a) oscilloscope, b) laptop computer, c) side-view camera, d) foam vibration absorption layer, e) experimental tank with animal, and f) wall mount with mini-shaker and attached shaft/bead. 91

Figure 3.4. Fig. 3.4 is a screen shot of a computer-generated representation of a randomized frequency presentation package (top). Arrows point to the bottom half of the figure that is a comparison between two different frequencies (10Hz and 1000Hz) of the same displacement amplitudes. 92

Figure 3.5. Bar graph depicts mean ventilation rates / 5s between control and stimulus treatments for all three experiments (N = 20). The asterisk indicates a significant difference from the control treatment. Error bars show mean ± 1.0 SE. 94

Figure 3.6. Bar graph depicts the average percent change in ventilation from the control to five stimulus and post-stimulus time categories. Each bin, except for the control, represents a 5s period of time that begins with the presentation of the stimuli and continues for 20s post-stimuli period. N = the number of 5s bins that were included in each category. Significant decreases between the control and stimuli bins were found for each of the five time categories. Error bars show mean ± 1.0 SE. 95

Figure 3.7. Bar graph depicts the percent change in ventilation/5s from the control for two distance categories over time. Each bin, except for the control, represents a 5s period of time that begins with the presentation of the stimulus and continues for 20s post-stimuli period (seven trials were included in the analysis). Significant decreases between the control and stimuli bins (marked by asterisks) were found for each of the <20cm categories and for the 5s Stimulus, 6–10s post-stimulus, and 16–20s post-stimulus categories (eight trials were included in the analysis). Error bars show mean ± 1.0 SE. 96

Figure 3.8. Figure 3.8 depicts the impact of the distance the animal is from the source on ventilation rate. Data shown is from two experiments, SSDE and LSDE, and accounts for 10 trials. Bead displacement refers to the distance traveled by the leading edge of the bead and does not include bead diameter. 97

List of Figures (continued)

Figure 3.9. Figure 3.9 shows the percent change in ventilation across five animals after exposure to randomized source velocities (N= 4 for the <20cm of the source and N = 1 for the >20cm). Significant decreases in ventilation from the control (0.00 m/s) were identified for 0.2 and 2.32m/s. 98
Figure 3.10. Bar graph depicts mean ventilation rates / 5s between control and stimulus treatments for all SSDE trials. The asterisk indicates a significant difference from the control treatment. Error bars show mean ± 1.0 SE. 99
Figure 3.11. Figure 3.11 compares ventilation responses to different stimulus and post-stimulus bins at different distances for each of three experiments. 101
Figure 3.12. Bar graph depicts mean ventilation rates / 5s between control and stimulus treatments for animal 2. The asterisk indicates a significant difference from the control treatment. Error bars show mean ± 1.0 SE. 102
Figure 3.13. Bar graph depicts mean ventilation rates / 5s between control and stimulus treatments for animal 7. The asterisk indicates a significant difference from the control treatment. Error bars show mean ± 1.0 SE. 103
Figure 3.14. Bar graph depicts mean ventilation rates / 5s between control and stimulus treatments for animal 9. The asterisk indicates a significant difference from the control treatment. Error bars show mean ± 1.0 SE. 104
Figure 3.15. Bar graph depicts mean ventilation rates / 5s between control and stimulus treatments for animal 5. No significant difference from the control treatment was found. Error bars show mean ± 1.0 SE. 105
Figure 3.16. Bar graph depicts mean ventilation rates / 5s between control and stimulus treatments for animal 6. No significant difference from the control treatment was found. Error bars show mean ± 1.0 SE. 106
Figure 3.17. Bar graph depicts mean ventilation rates / 5s between control and stimulus treatments for animal 4. No significant difference from the control treatment was found. Error bars show mean ± 1.0 SE. 107
Figure 3.18. Bar graph depicts mean ventilation rates / 5s between control and stimulus treatments for animal 10. No significant difference from the control treatment was found. Error bars show mean ± 1.0 SE. 108
Figure 3.19. Bar graph depicts mean ventilation rates / 5s between control and stimulus treatments for all LSDE trials. The asterisk indicates a significant difference from the control treatment. Error bars show mean ± 1.0 SE. 109
Figure 3.20. Bar graph depicts mean ventilation rates / 5s between control and stimulus treatments for animal 2. The asterisk indicates a significant difference from the control treatment. Error bars show mean ± 1.0 SE. 110
Figure 3.21. Bar graph depicts mean ventilation rates / 5s between control and stimulus treatments for animal 8. The asterisk indicates a significant difference from the control treatment. Error bars show mean ± 1.0 SE. 111
Figure 3.22. Bar graph depicts mean ventilation rates / 5s between control and stimulus treatments for animal 1. No significant difference from the control treatment was found. Error bars show mean ± 1.0 SE. 112

List of Figures (continued)

Figure 3.23. Bar graph depicts mean ventilation rates / 5s between control and stimulus treatments for animal 6. No significant difference from the control treatment was found. Error bars show mean ± 1.0 SE. 113
Figure 3.24. Bar graph depicts mean ventilation rates / 5s between control and stimulus treatments for animal 7. No significant difference from the control treatment was found. Error bars show mean ± 1.0 SE. 114
Figure 3.25. Bar graph depicts mean ventilation rates between control and stimulus treatments for all FSE trials. The asterisk indicates a significant difference from the control treatment. Error bars show mean ±1.0 SE. 115
Figure 3.26. Bar graph depicts mean ventilation rates between control and stimulus treatments for Animal 3 (control administered first). The asterisk indicates a significant difference from the control treatment. Error bars show mean ±1.0 SE. 116
Figure 3.27. Bar graph depicts mean ventilation rates between control and stimulus treatments for Animal 6 (control administered first). The asterisk indicates a significant difference from the control treatment. Error bars show mean ±1.0 SE. 117
Figure 3.28. Bar graph depicts mean ventilation rates between control and stimulus treatments for Animal 8 (control administered first). The asterisk indicates a significant difference from the control treatment. Error bars show mean ±1.0 SE. 118
Figure 3.29. Bar graph depicts mean ventilation rates between control and stimulus treatments for Animal 1 (control administered first). Pairwise comparisons revealed no significant difference from the control treatment. Error bars show mean ±1.0 SE. 119
Figure 3.30. Bar graph depicts mean ventilation rates between control and stimulus treatments for Animal 4 (stimulus administered first). The asterisk indicates a significant difference from the control treatment. Error bars show mean ±1.0 SE. 120
Figure 3.31. Bar graph depicts mean ventilation rates between control and stimulus treatments for Animal 11 (stimulus administered first). Pairwise comparisons revealed no significant difference from the control treatment. Error bars show mean ±1.0 SE. 121
Figure 3.32. Bar graph depicts mean ventilation rates between control and stimulus treatments for Animal 2 (stimulus administered first). Pairwise comparisons revealed no significant difference from the control treatment. Error bars show mean ±1.0 SE. 122
Figure 3.33. Bar graph depicts mean ventilation rates between control and stimulus treatments for Animal 9 (stimulus administered first). Pairwise comparisons revealed no significant difference from the control treatment. Error bars show mean ±1.0 SE. 123

"Nature first, then theory. Or, better, Nature and theory closely intertwined while you throw all your intellectual capital at the subject. Love the organisms for themselves first, then strain for general explanations, and, with good fortune, discoveries will follow."

E.O. Wilson from *Naturalist* – 1994

1.0 Introduction

Organisms that live in the ocean encounter an environment that is significantly different from what terrestrial animals routinely experience. Detection by sensory systems such as olfaction, equilibrium, vision, and acoustics vary drastically in their sensitivity from land to sea, and major differences can be noted for each: 1) olfactory stimuli do not necessarily exist in concentration gradients in either medium and the rate of diffusion in water decreases tenfold, 2) in water, the density of the medium and pressure differentials increase substantially, 3) the visual spectrum within the water column deteriorates with depth, and 4) vibrations travel more quickly underwater than in air and face less resistance.

Understanding how organisms cope with the variety of stimuli in the marine environment can reveal how sensory systems contribute to survival and reproduction. To respond to a given stimulus, marine organisms must somehow collect information from their environment and subsequently process it. Because the marine environment is dominated by mechanical and acoustical energies, such as water currents or vibrations (that may eventually be converted to sound waves), it is a reasonable assumption that many organisms benefit from the ability to detect and respond to these varying types of stimuli. One organism that may benefit from responding to such disturbances is the deep-water cephalopod, *Nautilus pompilius*.

In the last three decades, researchers have focused on identifying the sensory systems that contribute to the survival and functional ecology of cephalopods in general (Budelmann and Tu, 1997). *Nautilus* in particular has served as a model in studies of olfaction, vision, and equilibrium reception. Studies indicate that *Nautilus*, although predominantly chemotactic, are capable of using many sensory systems to complete basic survival tasks (*vision*, Muntz, 1994; (*equilibrium reception*, Budelmann, 1997, Neumeister and Budelmann, 1997; *olfaction*, Basil *et al*., 2000; Basil *et al.*, 2002; Basil *et al.*, 2005). Equilibrium reception has been investigated extensively (Neumeister and Budelmann, 1997), and the role of the statocyst in this system has been identified and described. However, the role of the Kölliker's canal has not been established. Using the chambered *Nautilus* as a model organism, two sets of experiments were designed to 1) determine if a particular component of the nautiloid equilibrium receptor system (Kölliker's canal) is used in the detection of rotary movements, and 2) determine if *Nautilus pompilius* is capable of extracting a signal from an underwater vibratory stimulus.

1.1 Natural History of the Chambered Nautilus

Nautilus pompilius is considered to be one of the oldest members of the class Cephalopoda (Phylum Mollusca). Presently, their genus represents less than 1% of the entire cephalopod population (Wood and O'Dor, 2000). Nautiluses are the only extant hard-shelled cephalopod and are therefore commonly used as a modern analog of the ellesmeroceratids, an ancestral lineage that dates back some 500 million years (Davis, 1987; Ward, 1987; Woodruff *et al.*, 1987; Wray *et al.*, 1995; but see Ward

and Saunders, 1997). *Nautilus* are predominantly bottom dwellers but are not restricted to the sediment (nektobenthic). In fact, they make daily vertical migrations at dawn and dusk along the coral reef slopes which they inhabit throughout the Indo-Pacific, including the Philippines, Palau, Fiji, Papua New Guinea, Australia, Samoa, and Tonga (O'Dor *et al*, 1993; Ward, 1987). Commonly found in depths of 150–300m, nautiluses are able to withstand pressures at depths of 750–830m before shell implosion occurs (Saunders and Landman, 1987; Jordan *et al.,* 1988). Nautiluses exhibit a solitary lifestyle. Unlike their coleoid counterparts (Octopuses, squids, and cuttlefishes), they are presumed to be carrion feeders (although Ward and Wicksten, 1980, disagree), focusing primarily on high-calcium items such as crustacean molt shells (Saunders and Landman, 1987; Ward, 1987). Their vertical migrations to the surface are thought to be responsible for basic feeding and mating activities and are most likely regulated by temperature (<24ºC) (Haven, 1977; Saunders and Spinosa, 1978; Ward, 1987; O'Dor *et al.*, 1993). *Nautilus* maintain buoyancy control during their migrations by detecting and adjusting to changes in hydrostatic pressure as little as 1atm and compensating with their locomotive system, the hyponome (Chamberlain, 1987; Jordan *et al.* 1988; O'Dor *et al.*, 1993).

Nautiluses (subclass Nautiloidea) are characterized as slow moving and non-visual, and in general their life strategies differ greatly from their highly visual relatives, octopuses, squids, and cuttlefish (subclass Coleoidea), who tend to live at shallower depths. Nautiluses are a long-lived species with life spans often extending into multiple decades (Landman and Cochran, 1987). Unlike the short juvenile stages of coleoids, reproductive maturity in nautiloids is reached at an average of 5.5 years

for both males and females (Martin *et al.,* 1978) and it has been suggested that this average may be as long as 10 years (Saunders, 1985; Landman and Cochran, 1987). After mating, female nautiluses lay up to 12 eggs that then gestate for 11 months (Mikami and Okutani, 1977; Saunders and Landman, 1987; Arnold *et al.,* 1990; Arnold *et al.*, 1993). In contrast, octopuses, squids, and cuttlefish are fast-swimming visual predators that are short lived and usually exhibit a semelparous lifestyle (Wood, 2002). They often reach reproductive maturity quickly and lay hundreds if not thousands of eggs in one reproductive season. A typical example of this strategy can be seen in the female pygmy cuttlefish, *Idiosepius paradoxus*, which reaches sexual maturity between 1.5–2 months and is capable of laying up to 1200 eggs within the following month (Shigeno and Yamamoto, 2002).

Aside from life-history strategies, nautiloids and coleoids differ greatly in their external morphology as well. Coleoids typically possess 8–10 appendages (arms, tentacles, or a combination of both) all of which are lined with mechanoreceptors and covered with chromatophores — pigment-containing organs surrounded by radial muscles that cover most of the body and can be independently contracted or relaxed to produce different visual patterns (Hanlon and Messenger, 1996; Cheng and Caldwell, 2000; Messenger, 2001). In comparison, nautiloids have 90–94 tentacles that are typically covered with mechanoreceptors and chemosensory cells. Their entire bodies are devoid of chromatophores (Hamada *et al*., 1980; Fukada, 1987; Ruth *et al.,* 2002). Coleoids have no external shell while nautiloids have a gas-filled external shell that is sectioned into chambers. The shell of *Nautilus* allows for buoyancy regulation by synchronizing two systems: 1) the ability to

maintain a low internal gas pressure relative to ambient pressure and 2) a ballast system using cameral fluid found inside the foremost chambers (Collins *et al.,* 1980; Jordan *et al.*, 1988). Coleoids possess highly developed eyes with lenses that allow the formation of distinct images. In contrast, the eyes of *Nautilus* lack a lens, and although capable of forming images, they are more suited for capturing as much light as possible in a dark environment, detecting wavelengths of bioluminescence in particular (Muntz, 1994a; Muntz, 1994b). Given the vast ecological, anatomical, and morphological differences between coleoids and nautiloids, it is a reasonable prediction that each group would emphasize and use sensory systems differently.

1.2 Linear and Angular Acceleration Receptors

For any organism to accurately orient in space, it must possess a system capable of detecting and interpreting various environmental cues. For instance, equilibrium receptors have evolved throughout the animal kingdom primarily to compensate for the one, physically constant mechanical force: inertia. Linear or gravity-based receptors called statocysts are present in almost all invertebrates (see Barber, 1968 for exceptions) but angular acceleration receptors (within the statocysts) have only been documented in decapod crustaceans and cephalopods (Barber, 1968; Budelmann and Tu, 1997; Popper *et al.*, 2001). These receptors vary in morphology and complexity, which may be correlated with the degree of behavioral complexity that the animal demonstrates in space. For example, fast-moving animals such as coleoids have developed more complex statocysts than slow-moving nautiloids probably because of their differences in lifestyles (Neumeister and Budelmann,

1997). Refining our focus to the differentiation of coleoid and nautiloid statocysts, two points can be inferred: (1) regardless of the complexity of the organ, the necessary tasks of spatial orientation are satisfactorily performed by each group, and (2) equilibrium receptors respond to mechanical forces of which gravity is just one; rotational accelerations and vibrations may also provide adequate stimuli to which these organs can respond, as previously demonstrated in the statocyst organs of certain octopod cephalopods (Williamson, 1988).

Young (1965) provided one of the first detailed descriptions of the central nervous system of *Nautilus*, concluding that it was more complex than any other non-cephalopod mollusc. He also suggested that the statocyst of *Nautilus* functioned not only as a gravity receptor, but could quite possibly respond to angular accelerations as well. Since then, multiple reviews have compared the structural diversity and functionality of cephalopod statocysts (Barber, 1968; Barber, 1969; Budelmann, 1977; Budelmann, 1988; Young, 1989). When comparing nautiloid equilibrium receptors to those of coleoids, *Nautilus* statocysts have historically been considered to be more primitive and are thought to represent the ancestral condition of extinct nautiloid forms (Barber, 1968). These conclusions are based on the anatomical differences between nautiloid and coleoid statocysts. Coleoid statocysts possess a crista/cupula system (Figure 1.1) capable of detecting angular accelerations and vibrations, and a macula/statolith system responsible for detecting linear accelerations. Both of these systems, however, are absent in *Nautilus* (Budelmann, 1977; Williamson, 1988; Young, 1989) (Fig. 1.1).

The statocysts of *Nautilus* are a pair of oval-shaped organs that are smaller in size than those of coleoids (Barber, 1968; Neumeister and Budelmann, 1997). The lumen within the statocyst is filled with endolymph fluid and is composed of four types of epithelial cells (two types of receptor hair cells, supporting cells, and ciliated cells). In each statocyst, polarized primary receptor hair cells number between 130,000–150,000, greatly outnumbering those of coleoids which possess between 3000–13,700 primary and secondary hair cells. Extending from each cell are kinocilia and microvilli that are responsible for generating action potentials based on stimulus intensity. The hair cells are divided into two groups (type A and type B) and are surrounded by supporting cells (Fig. 1.1). Type A hair cells possess 10–15 kinocilia per cell (each approximately 3.5–5μm) and occupy the ventral region of the lumen. Type B cells line the dorsal region of the organ and have 8–10 kinocilia per cell that are twice the length of type A kinocilia. Kinocilia of each cell type are surrounded by microvilli of equal length that increase the surface size of the cell and are less numerous on type A cells (Budelmann and Tu, 1997; Neumeister and Budelmann, 1997). The lumen is partially filled with numerous statoliths (statoconia) that are ovoid in shape, may or may not be fused together, and are denser than the surrounding medium. They range in size from 1.7–17.2μm and have a free-floating arrangement that resembles those found in certain bivalve (*Pecten maximus*; king scallop) and gastropod (*Lymnaea stagnalis*; pond snail) larval stages (Morris, 1989).

Another notable comparison made by Barber (1968) was that both groups of cephalopod statocysts contain a ciliated duct structure that is referred to as Kölliker's canal. Kölliker's canal in *Nautilus* is morphologically similar to the excretory ducts

found in the statocysts of other invertebrates with the exception that the canal walls are lined with cilia, a derived trait only found in cephalopods. Within Cephalopoda, a prominent difference is that this canal opens directly to the exterior in *Nautilus* via an epidermal pore located in the region above the rhinophore and below the pre-ocular tentacle (Figure 1.2), but this is not the case in coleoids (Young, 1965; Barber, 1968; Neumeister and Budelmann, 1997). Although Barber (1968) suggested that this structure contributes primarily to endolymph secretion, the exact function of this canal is poorly understood. Therefore, considering its proximity and connection to the animal's external environment, an element of this research was designed to determine if Kölliker's canal may also contribute to the sensory capability of the animal. Specifically, by aiding in the detection of rotary movements and potentially transmitting environmental information to the interior. Physiological studies have indicated that the cilia that line the walls of the canal itself are not innervated and probably do not function as part of a sensory mechanism (Neumeister and Budelmann, 1997). However, the same study acknowledges that further study of live tissue and cellular organization is necessary to verify this conclusion.

1.3 Mechanics of Underwater Sound and Biological Relevance

Sources of sound in the ocean include (but are not limited to) seismic activity, storm events, man-made contributions, and biological activity. For an animal to identify sound as a stimulus, it must be capable of extracting a signal from the ambient sound environment or, more accurately, from background noise (Rogers and Cox, 1988). Sound emission can originate from many different sources, but all sound

production begins in a similar fashion: a longitudinal propagating mechanical wave is generated by either a change in volume or a physical oscillation or movement. Disturbances that result from a change in volume and originate from a single pole, such as a pulsating sphere or the inflation of a teleost swim bladder, are usually referred to as a *monopole source*. *Dipole sources* are those that result from a disturbance in the medium in which the volume of the source remains constant and the signal has two points of origin. Typical examples of dipole sources are spheres that vibrate between two points or the sinusoidal movements of a fish moving through the water column (Kalmijn, 1988; Coombs, 1994).

Regardless of the source, the mechanics of a propagating sound wave are the same. Water molecules are initially displaced by a disturbance that creates adjacent regions of differing pressures. Consequently, a series of compression and rarefaction events extend both parallel and perpendicular from the source (Kinsler *et al*., 1982), the strength of which is dependent on acoustic intensity (the amount of energy per second flowing across a unit area). The frequency of the resulting signal is usually measured in cycles per second or Hertz, and is obtained by dividing the speed of sound in a given medium (1500 m/s in water) by the propagating wavelength (Everest, 2001). The acoustic fields created by this wave can be divided into two sections: the near-field (or local-flow field) and the far-field. The near-field is dominated by particle velocity, displacement, and acceleration, and is technically considered incompressible. Because of this, near-field measurements are normally treated as vector quantities since they have both magnitude and direction. As the propagating sound wave extends radially, it eventually detaches itself from the

source. This region is considered the far-field and can be more accurately measured in scalar quantities such as pressure and density that only reflect the magnitude of the signal. It is important to note that neither field is entirely exclusive of the other because both fields contain vector and scalar components; the major distinction is what components dominate which fields (Kalmijn, 1988; Roger and Cox, 1988).

Non-pelagic animals that live in bounded areas (the confines of which could be ocean bottoms, coral reefs, intertidal areas, etc.) operate primarily in the local-flow field simply because sound waves do not have adequate space to readily detach from the source. Pelagic animals, in contrast, frequently operate within both fields and have sensory systems adapted for adequate detection within each field that is dependent on their spatial location at any given point in time (Bleckmann, 1994). An example of the latter would be fishes that possess both lateral-line systems and otoliths, both of which serve as overlapping sensory systems. The lateral line detects low-frequency stimuli within only a few body lengths of the source, whereas the otolith organs (and other components of the inner ear) assume responsibility for acoustic reception from the outer reaches of the local-flow field well into the far-field (Kalmijn, 1988; Braun *et al.*, 2001). A similar model could be applied to nautiluses. A plausible mechanism might be that the immediate source (i.e., a group of snapping shrimp) could be detected through mechanoreceptors located on certain tentacles (Ruth *et al.*, 2002) while the progression of the wave through the remainder of the near-field into the far-field could be detected by equilibrium receptor organs such as the statocysts (Budelmann, 1988; Rogers and Cox, 1988). Since the statocysts contain statoconia that are denser than the surrounding endolymph, it is possible that

they could receive or be temporarily displaced by the signal, the movement of which may result in the bending of the polarized cilia that line the lumen wall.

1.4 Previous Investigations and Current Research

In *Nautilus*, the sensory systems that have been investigated to date include olfaction, vision, linear acceleration, and angular acceleration. Based on the dimly lit environment where nautiluses live, it has long been thought that olfaction is the primary sensory system used by these animals. Barber and Wright (1969), Hamada *et al.* (1980), Fukada (1987), Ward and Wicksten (1980), Saunders and Ward (1987), and Ruth *et al*. (2002) provided a detailed description of potential chemosensory organs including the rhinophores (olfactory pores located beneath each eyestalk), digital tentacles, and ocular tentacles and concluded that they are relatively unchanged from those of fossil nautiloids (Barber and Wright, 1969). Basil *et al.* (2000) conducted olfactory-orientation experiments and found that *Nautilus* are capable of detecting and tracking food odor from up to 10m. They are unable to successfully track an odor to its source without the use of their paired rhinophores, although their tentacles seem sensitive to the presence or absence of odor. Further research conducted by Basil *et al.* (2005) demonstrated that independent odor-stimulation of the rhinophore organs and digital tentacles initiate different tracking behaviors that correspond to far-field and near-field situations, respectively.

Vision in nautiloids has also been examined at length. Muntz (1991, 1994a, 1994b) developed a combination of anatomical and behavioral studies to compare vision between *Nautilus* and *Octopus*. These experiments confirmed that visual

acuity and sensitivity in *Octopus* are more sensitive than in *Nautilus*. These experiments also revealed that nautiluses are positively phototactic in their natural environment as well as within laboratory settings. Aside from demonstrating positive phototaxis, these data support the implication that *Nautilus* may rely on other sensory systems to complete basic survival tasks. Additional evidence has been provided by recent studies that establish that vision or oculomotor responses in *Nautilus* work in concert with gravity-based systems (statocysts) to compensate for linear accelerations (Budelmann and Tu, 1997).

Linear and angular acceleration systems have been the focus of multiple studies in octopuses, squids, and cuttlefish, but not nautiluses. Although it is widely accepted that *Nautilus* respond to gravity-based accelerations via the statocyst (Budelmann, 1975), it has not been demonstrated until recently that *Nautilus* respond to angular accelerations by means of the same organ. Neumeister and Budelmann (1997) measured funnel (hyponome) responses of *Nautilus* to an oscillating current that mimicked local flow around the vertical body axis of the animal. The positional responses of the hyponome of individuals with both statocysts left intact were compared to the responses of an individual in whom one statocyst had been removed. The results of this experiment indicated that post-operation animals with a statocyst removed were unable to demonstrate active behavioral responses (compensatory funnel movements) or passive behavioral responses (funnel-follow movements) to rotary movements within the first six hours of the statocyst operation. After 24 hours, passive behavior similar to that seen during the control was evident but compensatory behavior was not. The researchers attempted to repeat the experiments with animals

that had undergone bilateral removal of the statocysts but none of the surgeries were successful.

These results may not be surprising based on the assumption that mobile animals in aqueous habitats must possess some mechanism of detecting spatial and temporal information to perform compensatory orientation. However, these findings empirically challenge the notion that the statocysts of *Nautilus* are inferior to those of coleoids in terms of their equilibrium reception. In addition, the potential role of Kölliker's canal in detecting rotary movements was never investigated and a plausible hypothesis may be that it is used to transmit environmental information from the exterior of the animal to the interior. Multiple mechanisms of transmission may be possible but, based on current anatomical evidence of the canal (lack of innervated cilia), it is unlikely that it sends direct signals to the statocyst nerve. It is more likely that the canal may somehow regulate pressure between the statocyst and the ambient environment or possibly act as a filter for incoming signals. These reactions may influence endolymph flow and/or hair-cell movement within the lumen and ultimately affect the behavioral response to angular accelerations.

Furthermore, there is the possibility that the *Nautilus* statocyst may be capable of performing other functions that have previously been demonstrated in coleoids, such as vibration detection. Williamson (1988) tested vibration sensitivity in the northern octopus, *Eledone cirrosa*, and determined that the hair-cell sensitivity within the statocyst of the octopus demonstrated sensitivity to a minimum particle displacement of 0.12μm (three of four orders of magnitude less sensitive than what average fishes can detect). These results led to the conclusion that the statocyst of *E.*

cirrosa could not be typically considered as an auditory organ when compared to the auditory systems of fish (whereas the term "auditory" typically refers to far-field detection typically dominated by pressure components) but that the threshold sensitivities were similar to other aquatic invertebrates. More importantly, these results demonstrated that this organ is sensitive to biologically relevant vibrations (Klages *et al*., 2002 noted that the deep-water amphipod, *Eurythenes gryllus*, produces particle displacements of 0.05–0.3µm between 70–200Hz when feeding and swimming) and that the threshold of sensitivity is most likely governed by the ecology of the organism. Williamson (1988) suggested that the vibration-sensitivity threshold of a pelagic species may differ from a substrate-dwelling animal because the background noise levels of their environments or stimuli requirements may differ. This can also be viewed in an evolutionary context as a predator-defense mechanism. Moynihan (1985) hypothesized that less sensitive vibration thresholds may enhance coleoid survival by lessening the effect of intense acoustic emissions that odontocete predators (toothed whales, dolphins, and porpoises) use to disorient their prey. Williamson (1988) also alluded to the possibility that vibration sensitivity need not be confined simply to the statocyst, further suggesting that certain mechanoreceptors may be sensitive to vibration as well, but never hypothesized exactly as to how this system may be used.

It is this line of logic that has formed to the basis of the hypotheses that suggest that *Nautilus* may be capable of detecting underwater vibration. Although the statocysts of nautiluses are considered to be more primitive than those of coleoids, perhaps their extreme external morphological differentiation from other coleoids has

prevented the evolution of such a complex organ because their contrasting life-style has not deemed it necessary. A pertinent example of these morphological differences is that nautiluses have 94 tentacles covered in mechanoreceptors compared to the eight or ten appendages of coleoids (Pojeta and Gordon, 1985; Fukada, 1987; Ruth *et al.*, 2002). Another example, and perhaps a more acoustically relevant one, is the gas-filled external shell of the chambered *Nautilus*. Although this shell and its chambers are primarily thought to compensate for buoyancy, principles of underwater acoustics dictate that (whether evident to the animal or not) it may also double as a resonating chamber, thereby potentially nullifying the need for the development of a more complex receptor organ.

2.0 Angular Acceleration Experimental Overview

The overall goal of this experiment was to determine if unilateral or bilateral blockage of Kölliker's canal impacts the ability of *Nautilus* to respond to angular accelerations. I hypothesized that communication between the statocyst and the external environment was possible, and that it could be prevented by administering a noninvasive epidermal-pore-blockage to the region of Kölliker's canal. Movements of the animal's funnel were tracked and measured to determine the net direction of the funnel in response to the rotating stimulus. The prediction, using a within-subject design, was that the response of the animals to the control condition in which no pores were blocked should be markedly different than the response in any or all of the blocked conditions.

2.1 Methods for Angular Acceleration Experiment

2.1.1 Animals

Ten wild-caught adult *Nautilus pompilius* originally collected in the Philippines were housed in a recirculating system at the Aquatic Research and Environmental Assessment Center (AREAC) at Brooklyn College of the City University of New York. The animals were divided into two groups and kept in a closed system that consisted of two 140-gallon polyethylene tanks filled with artificial sea water (Instant Ocean™). Both tanks were joined together and connected to a 25-gallon biofilter that contained additional aeration and filtration media. The animals were kept at constant temperature of 17º C and at a salinity level of 32–34 ppt. Fish heads (*Tilapia sp.*) were used as a primary food source and rations were

administered every third day. Daily checks of water quality (temperature, salinity, DO, pH, calcium, alkalinity, ammonia, nitrite, nitrate, and phosphate) were conducted to monitor the system and maintain the health of the animals (pH levels ranged between 8–8.4 and ammonia and nitrates/nitrates were generally near zero). Trace elements in the form of a calcium/alkalinity liquid buffer system (B-Ionic™) were added on a weekly basis (75ml of each component) to maintain the necessary levels of calcium.

2.1.2 Experimental Apparatus for Response to Angular Accelerations Experiment

To create an experimental arena in which rotary movements of both animal and water could be controlled, a cylindrical Plexiglas™ tank with an inner diameter of 27cm and a height of 43cm was attached to a turntable (15cm diameter) that was connected to a torque motor-driven pulley system (Fig.2.1). An 11.14cm pulley (diameter) was attached to a reversible AC powered motor that was used to control the direction and velocity of the turntable. A PVC harness was constructed to restrain the animal within the tank and a silicon mold of the animal's shell was formed and inserted into the harness to serve as an additional restraint. To ensure that the animal remained stationary during each trial, the harness was attached to a plastic nut-and-bolt assembly that was connected to a fitted acrylic crossbeam and mounted to the top of the tank (Fig. 2.1). External visual cues were controlled for by placing a black cardboard curtain around the entire tank. Directional arrows were constructed out of red masking tape and attached to the inside of the curtain to serve as directional indicators to the observer during video analysis. Although it could be argued that the arrows themselves might have served as a visual cue, the incorporation of them into

the experimental design can be justified in that 1) Muntz (1987) demonstrated that *Nautilus* can only detect wavelengths that fall between 400nm and 570nm; the wavelength of the color of the arrows falls between 600nm and 700nm and 2) even if the animals could detect the arrows, the cues remained constant throughout each of the trials for each of the animals. A digital video camcorder (Canon ZR 65 MC) connected to an external monitor was mounted to the turntable, aimed directly at the hyponome, and used to record each trial. An adjustable 20W desk lamp was placed 0.5m above the tank during each trial to provide proper lighting for the camera and, as with the arrows mentioned previously, served as a constant experimental factor.

2.1.3 Procedures for Angular Acceleration Experiment

Temporary Epidermal-Pore-Blocking Procedure for Kölliker's Canal

Trials were conducted on ten separate days occurring between 05/27/2004 and 07/15/2004, between 0830h and 1630h. Each animal served as its own control and was exposed to four separate experimental treatments: 1) no pores blocked (control/sham), 2) left pore blocked, 3) right pore blocked, and 4) both pores blocked. Each blocking procedure was completed by applying a small amount of petroleum jelly to the general area located beneath the pre-ocular tentacle, where the pore has been described (refer to Fig. 1.3). An inert dye (Rhodadmine B, Sigma C.I. 45170) was added to the petroleum compound to ensure the identification of proper application. Both a wooden dowel and the male end of a plastic cable tie were used as application instruments and proper sham techniques were employed in controls to control for any handling and applicator effects. Basil *et al.* (2000) demonstrated that

this procedure was completely reversible due to the short dissolution time of the petroleum jelly (< 1h).

Before each procedure, an animal was first transported in a 5-gallon bucket and was then placed in a 10-gallon holding tank prior to the application of the block. Each container was filled with water drawn from the animal's home tank to prevent unintended chemical cueing. Once the animal was placed in the holding tank, the application instrument was prepared by first disinfecting it with a 95% EtOH solution and then coating it with the petroleum/dye mixture (unless a sham application was being administered at which time the instrument was simply disinfected). To properly access the area necessary to perform the pore block, the animal was removed from the water and inverted briefly, allowing better access to the target region since gravity prevented the animal from retracting its hood completely. Animals were never kept out of the water for more than 45s per attempt and no more than three consecutive attempts per animal were needed. Once the blocks or shams were successfully administered, the animal was moved from the holding tank to the experimental tank (also filled with water from the home tank) to begin habituation. After completion of each trial, the experimental arena was drained and rinsed with fresh (tap) water to remove any individual olfactory cues. There were concerns that inverting the animal might affect statocyst function. Therefore, potential effects of animal inversion and statoconia displacement within the statocyst were addressed by pre-trial habituation (10min) that allowed time for the settlement of the statoconia since their specific density is greater than that of the endolymph. Additionally, all

animals were treated in an identical fashion so, if an effect was evident, it would affect the entire sample population and would be evident in the sham-treated animals.

Additional Experimental Procedures

Prior to the start of the trial, each animal was placed into the experimental tank and allowed to habituate for 10min. If an animal expelled the petroleum block during the habituation period, the animal was removed and the block was reapplied after which the animal was returned to the experimental tank and allowed to re-habituate. To control for order effects, animals were randomly grouped together according to predetermined pore-blockage presentation orders (four groups in total, each of which began with a different pore-blockage).

After habituation, each animal was subjected to alternating rotations of the angular acceleration device that served as a step-stimulus, during which time the positional responses of the hyponome were recorded. The entire step-stimulus was defined as the directional acceleration from zero to peak velocity, the deceleration from peak velocity to zero, the acceleration from zero to peak velocity in the opposite direction, and, lastly, the deceleration from peak velocity to zero. The rotations occurred at a frequency of 0.03Hz and had a maximum spinning velocity of approximately $20° \ s^{-1}$ around the vertical axis of the animal. Each animal was exposed to 10 alternating rotations, experiencing a total of five clockwise (CW) and five counterclockwise (CCW) spins during each trial. Initial starting directions were alternated between trials for each animal as well as between animals overall, to control for order effects. Each directional spin was approximately 18s long and total trial lengths for each blockage condition were 3min. Therefore, after the completion

of all four blockage trials, each animal experienced 40 individual directional rotations (ten for each blockage treatment condition), that were sequentially aligned so that no two spins in the same direction occurred one after another. No animal was tested more than once in a 24-hour period.

2.1.4 Data Collection and Analysis

Experimental trials were collected with digital camcorders and uploaded to an external hard drive (Western Digital 160G, Lake Forest, California) so they could be analyzed using Video Analysis 1 software (VA1). The computer software (freeware) was supplied by Dr. Bill Tietjen of Bellarmine University, Louisville, Kentucky (http://cas.bellarmine.edu/tietjen/DownLoads/computer_programs_for_data_colle.htm). For each trial, X-Y coordinate data were sequentially recorded at 0.5s intervals that corresponded to the furthest dorsal point of the animal's hyponome, provided that a clear observation could be made (Fig. 2.2). Out of a total of 14,386 observations, coordinate data were collected for 13,215 points or 91.9% of the total observations made. Coordinate data were then transformed to reflect the angular differential that originated from the center of rotation, D_{cor}, which is defined as the point marking the middle of the interior end of the tunnel that is formed by the animal's hyponome, irrespective of the actual position of the hyponome itself. This was accomplished by using the equation: $D_{cor} = \text{Arctan}(x/y)*(y/|y|)*(180/\pi)$, where the term $(y/|y|)$ adjusts for directional polarity and $(180/\pi)$ transforms the maximum angular response to 90º (if the hyponome is positioned directly along the x-axis to the animal's left) or -90º (if the hyponome is positioned directly along the x-axis to the animal's right). All values were then converted into an index measuring the strength of response (SOR) by

dividing D_{cor} by 90. An index value of 0 indicates that the hyponome is positioned somewhere along the y-axis and is perpendicular to the animal's center of rotation (which, theoretically, would only produce vertical movements), whereas large values (1 being the maximum) indicate stronger rotational responses as the hyponome is moved closer to the x-axis and is not vertically aligned with the animal's center of rotation.

The terms "left-handed" and "right-handed" are used henceforth to describe the average directional positioning of the hyponome for each individual during a given treatment (e.g., positive values reflect that the overall positional preference of the hyponome is to the animal's left side and negative values indicate that the average positional response is to the animal's right side. Directional preferences (both combined and individual) observed during the control condition served as an indicator of natural side preferences under normal conditions and were then used as a baseline to compare changes in both individual and overall behaviors in different blockage conditions.

Additional terms such as "compensatory" and "funnel-follow" refer to the active or passive behavior of the animal determined by its funnel position. A compensatory response is defined as one that would expel water in the same direction that the animal is rotating in order to counteract the rotation. A funnel-follow response is defined a passive behavior where the position of the animal's hyponome is set so that water is expelled in the opposite direction of the spin, thereby making no attempt to counteract the motion. Directional values were separated by treatment (control, left block, right block, and both block) and direction (CW1-5 or CCW1-5),

with the number following the direction corresponding to its temporal occurrence within the trial. Directional data were collected and then plotted over a theoretical stimulus curve that was based on the rotational speed of the experimental apparatus. The curve was created using actual spinning frequencies that were the same for each trial and by incorporating estimated rise and fall times of the step-stimulus. Stimulus curves were identical for each animal and comparison of responses to the curve was used to establish phase-locked relationships between both variables. Any additional statistics reported were analyzed using SPSS v.11.5 and supporting graphics were created using Microsoft Excel 2002.

2.2 Results

2.2.1 Overall behavior

Animals responded differently in these experiments depending upon the rotation of the animal's environment, as measured by the direction of movement of their hyponome. The initial hypothesis was that each animal would demonstrate a uniform positional response in coordination with the direction it was spinning. This however was not the case after evaluating responses within 10 trials — the control condition therefore proved to be an unreliable source of baseline behavioral data. In 50% of the trials, animals showed no apparent response to the stimulus since no phase-locked trend between stimulus and behavior could be established. In the remaining five trials, three of the animals demonstrated anti-phase behavior (funnel-follow) and only two demonstrated clear compensatory or in-phase behavior when coupled to the stimulus. Descriptions of these responses will be therefore limited to

only the two animals that demonstrated compensatory behavior during the control treatment since the remaining eight animals failed to demonstrate compensatory behavior during the control. This suggests that the stimulus was ineffective or that the handling of animals affected their ability to respond to the stimulus effectively.

Statistical analysis was based on hyponome-position data collected at 0.5s intervals and overall values for a given treatment or spinning direction are based on the average strength of those responses (mean SOR). Descriptions of the time-based dynamical movements of the hyponome are also given. No treatment order effects were observed in any of the trials.

Another observation worth noting was that there was a natural preference for left-handed placement of the hyponome under control conditions. As indicated by the mean SOR throughout the course of each trial, this lateral preference was observed in eight of the ten animals during the control treatment. The remaining two of the ten animals demonstrated a right-handed response after exposure to the same treatment. Initially, it was thought that this was a direct result of the animal's hyponome configuration, as two different arrangements have been noted during these experiments. The hyponome is comprised of overlapping mantle tissue and the side from which the mantle tissue overlaps, either the animal's left or right, differs between individuals. To my knowledge, this discovery has not been previously reported in the literature and may contribute to the observed laterality expressed by these individuals, although no statistical support for this hypothesis was found during the analyses.

2.2.2 Individual Responses to Blocking Procedures

Statistical Note

A statistically conservative approach was used when evaluating the results of all univariate ANOVA tests and pairwise comparisons (*post hoc t*-tests) between treatments for each animal. A Bonferroni correction was applied to reduce the overall error rate. The significance level was adjusted by sequentially dividing the *p* value (.05) by the total number of tests and then ordering the F statistical value from largest to smallest. For example, if seven animals were compared individually, the individual with the highest F statistic or lowest *p* value would be held to an error rate of .007 as opposed to .05 (as .05 / 7 = .007). The next highest F statistic would be held to an error rate of .008 (as .05 / 6 = .008), and so forth. This correction was applied to each experiment where individual results were reported.

Animals that demonstrated compensatory, in-phase responses during the control

Animal 1: Animal 1 demonstrated clear in-phase compensatory behavior throughout the entire control trial. When both pores were blocked, however, the animal maintained a strong anti-phase following behavior for nearly the entire trial. Left blockage and right blockage treatment conditions revealed more ambiguous responses from the control but phase-shifts were still apparent throughout a majority of both trials suggesting a switch to a passive funnel-follow response when treated (Figure 2.3). An ANOVA was conducted that revealed significant variance between conditions with regard to spinning direction (CW: $p = <.001$, $F = 111.902$; CCW: $p =$

<.001, F = 182.151). *Post hoc t*-tests further revealed significant differences between the control and each of the blocking conditions when separated by spinning direction.

For CW rotations, the animal averaged compensatory responses during two treatments, control and right blockage, with a mean SOR of -.334 during the control and a mean SOR of -.033 during the right pore block. The animal demonstrated funnel-follow behavior during the remaining two treatments averaging a SOR of .523 during the left-pore blockage and a mean SOR of .445 during the both-pore blockage procedure. All pairwise comparisons between the control and the blocking treatments were significant at the <.001 level. During CCW rotations, the Animal 1 averaged compensatory responses only during the control treatment (x = .543) and exhibited anti-phase behavior during each of the other treatments (left x = -.393, right x = -.372, both x = -.332). All pairwise comparisons between the control and the blocking treatments were significant at the <.001 level.

During the control condition, observations of dynamical movements of the hyponome suggested that this animal frequently alternated between weak and strong compensatory responses throughout the entire trial. Animal 1 only exhibited continuous funnel-follow behavior during seventh rotation (or the fourth CCW rotation) and then reverted back to compensatory behavior during the remaining three rotations. The animal exhibited funnel-follow behavior for both left unilateral and bilateral pore blockage conditions, with the most consistent trends evident during the bilateral blockage. The right pore blockage treatment elicited multiple behavioral shifts from compensatory to funnel-follow throughout the first 110 seconds of the

trial but the responses were much less consistent than that of any of the other treatments, making it difficult to establish any general trend.

Animal 11: Animal 11 also demonstrated a clear in-phase compensatory behavior throughout approximately the last 2.5 minutes of the control trial. In contrast to the previous animal, a similar in-phase compensatory response was seen when the animal had both pores blocked but the amplitude of the response decreased. Left blockage and right blockage treatment conditions revealed no easily discernible phase-shift but a weighted directional response was observed as the animal averaged a right-handed hyponome position during each of the trials (Figure 2.4). An ANOVA was conducted that revealed significant differences between treatment conditions with regard to spinning direction (CW: $p = <.001$, $F = 86.936$; CCW: $p = <.001$, $F = 360.498$). *Post hoc t*-tests additionally revealed significant differences between the control and all but one of the blocking conditions when separated by spinning direction.

For CW rotations, the animal averaged compensatory responses during all four treatments (control x = -.124, left x = -.621, right x = -.413, and both x = -.187) although no defined stimulus-SOR coupled responses could be seen in the unilateral blocking conditions. Pairwise comparisons between the control and all blocking treatments were significant at the <.001 level with the exception of the both-pore blocking procedure which was not significant. During CCW rotations, the Animal 1 averaged compensatory responses during the control and bilateral blockage treatments (control x = .300 and both x = .153) and exhibited anti-phase behavior during both unilateral blockage treatments (left x = -.796 and right x = -.383). All

pairwise comparisons between the control and the blocking treatments were significant at the <.001 level.

Time-based dynamic positional responses of the hyponome during the control condition were similar to those of Animal 1 with the exception that Animal 11 had less of a tendency to alternate between strong and weak compensatory behaviors, maintaining typically strong positional responses for approximately the last 120 seconds of the trial. Both unilateral blockage treatments evoked similar behavioral patterns as the animal maintained a relatively strong right-handed position regardless of the spinning direction. Both compensatory and funnel-follow behaviors were observed throughout the course of the trial but switching between behaviors during the same rotation did not happen frequently, although more common during the last 100 seconds of the left pore blockage treatment. In contrast to Animal 1, Animal 11 exhibited compensatory behavior throughout most of the bilateral blockage treatment, switching between behaviors during the last four CCW rotations and rarely during any of the CW rotations. Although similar behavior was seen during the control treatment, the amplitude of the responses was smaller when the animal was exposed to the bilateral blockage treatment.

Animals that demonstrated anti-phase responses during the control

Animals 7, 9, and 10 exhibited anti-phase (funnel-follow) behavior during each of the control treatment trials suggesting that the stimulus had little effect on these animals since active responses throughout the trials were rare. No consistent patterns in response to the effects of manipulation could be seen either within or between subjects and, even if they were found to exist, no active behavioral response

was demonstrated during the control treatments. Any attempt to compare SOR results to other treatment conditions would be inappropriate. Figure 2.5, Figure 2.6, and Figure 2.7 show behavioral responses over time for all three animals to each treatment condition in relation to the stimulus.

Animals that demonstrated no phase-coupled response during the control

Animals 2, 3, 4, 6, and 8 demonstrated no clear phase-coupled responses during any of the control treatments. Although differences exist between treatments both within-subject and between-subject, the failure to establish a behavioral baseline within the control suggests that the stimulus may not have been effective for any of these five animals and subsequent comparison of varying treatment effects is not warranted and are only discussed for descriptive purposes.

Two of the five animals demonstrated a left-handed directional preference during the majority of the control trial whereas the remaining three animals exhibited continuous switching of the hyponome between CW and CCW directions, but with no obvious synchronization with the stimulus. For the remaining conditions, each animal exhibited either a directional preference or anti-phase behavior, with four of five animals (all but animal 6) displaying passive anti-phase behavior during the bilateral blockage. Two of the animals, Animal 2 and Animal 8 exhibited funnel-follow behavior during each of the three blockage conditions. Figure 2.8 through Figure 2.12 show temporal-based behavioral responses of all five animals to each treatment condition in relation to the stimulus.

As an additional note, an analysis was performed that compared the mean SOR across all animals (N = 10) without coupling the responses to the stimulus.

Significant differences in mean responses were found to exist between each blocking treatments and the control (Student's *t*-test, $p = <.001$ for each treatment comparison) suggesting that hyponome positioning was affected by each blocking procedure (Figure 2.13). Since the responses that were analyzed were not based on a time scale or coupled to the rotating stimulus, they cannot serve as a proper measure of dynamic behavior, active or passive, and are therefore not discussed further.

2.3 Discussion

With the exception of the two animals that demonstrated compensatory responses to angular accelerations, these experiments have not produced convincing evidence to suggest that *Nautilus* are somehow capable of internalizing information gathered from external environmental cues via superficial structures located beneath the eyestalk. This discussion will therefore first focus on the two animals that responded to the baseline stimulus conditions. Both of the animals that exhibited definitive compensatory behaviors during the control treatment significantly altered their hyponome positioning during blockage conditions. It is important to note that the actual directional preference for each animal has no bearing on the interpretation of these results since it has already been established that these animals exhibit high levels of inter-animal variation, and that the focus should be placed on deviations from active behavioral responses such as compensatory funnel movements.

In both animals, bilateral blocking evoked a clear passive response trend that is nearly phase-shifted 180° from the control response, suggesting that the treatment

somehow prevents each animal from responding as it would in an unaltered state. Unilateral blockage treatments produced similar trends to the bilateral procedures, although the anti-phase relationship of the treatment response to the stimulus was less synchronized (this was more evident in Animal 11 than Animal 1). However, responses of both animals to the unilateral blockages still demonstrated that the treatment greatly impaired the animals' ability to respond in a continuously active manner as in the control condition. Given this observation, one could assume that the behavioral response is at least partially based on the transmission of an external signal to the interior — a transmission that is somehow disrupted once the animal is exposed to a unilateral block. Perhaps the animals can detect a difference in internal statocyst pressures between sides and that any external mechanoreceptors that may normally compensate are affected by the block and become incapacitated. Such a mechanism could account for the seemingly weighted (Animal 11 demonstrated a lateral positional preference of the hyponome to the left during both unilateral blocking procedures) or delayed positional responses of the hyponome that were exhibited by Animal 1 during the unilateral blockage procedures. Additional support for such a mechanism is supported by the observation that the behavior of animals with bilateral blockages is an even more dramatic (and synchronized) departure from the control. These data suggest that ability of each animal was somehow incapacitated by the treatment and that may be a result of simultaneously inactivating epidermal mechanosensors on both sides of the animal or possibly preventing the signal from activating sensory hairs within the statocyst. Speculation as to the relevance of these behaviors *in situ* is challenging since direct observations from the wild are lacking.

However, the fact that these animals are able to respond by actively re-positioning their funnel is of extreme relevance within a sensory context as it further defines the capabilities of these animals and may encourage future work.

A more pressing speculation, however, is one that centers on the inability to elicit and identify a baseline behavioral response from eight of the ten animals tested. The speed of rotation as a stimulus most likely imposes the greatest limitations on eliciting compensatory behavior during the control treatment. In this experiment, rotating speeds were much lower than what has been used in previous experiments (Neumeister and Budelmann, 1997) and may not have been adequate to evoke a response from 80% of the animals tested. Perhaps the two animals that did respond had lower sensitivity thresholds than the others. Also, the presentation of the stimulus was step-based as opposed to sinusoidal which may have somehow impacted the animals' abilities to respond, either by confounding the signal presentation by reversing direction or by prematurely truncating it.

Another limiting factor in this experiment was the treatment. Although seemingly effective in two of the trials, it is difficult to argue that the blockage of Kölliker's canal is the only limiting factor in the treatment simply because it was not the only structure affected by the treatment. Mechanoreceptors are found on the base of the rhinophore and may exist in the surrounding epidermal region, all of which may have been inadvertently obstructed during the application of the petroleum jelly or at some point during the trial. Also, as explained previously, pre-trial animal inversion may have interfered with treatment responses, further complicating the results. These possibilities can not be overlooked and, in light of this, make it

difficult to arrive at any conclusion that would identify the canal as the only contributing structure. The same reasoning dictates that it surely cannot be discounted either. Future experiments should focus on the physiological isolation of only the canal and not the surrounding tissue.

It is likely that statocyst-based sensory mechanism capable of detecting internal pressure differences or external hydrodynamic signals would be of tremendous value in the wild. These animals could use such a mechanism in conjunction with other systems to avoid predation or spatially orient themselves. There may be foraging implications as well since these animals may use hydrodynamic cues to locate prey (especially those found along the structures of a coral reef in depths where vision may be severely restricted). These tactics are employed by other members of Cephalopoda whose statocysts appear to be more complex, but importantly, fundamentally different. Perhaps the anatomical uniqueness of the *Nautilus* statocyst compensates for the lack of physiological sophistication seen in other members of the Class, and by their using an alternate yet simplified mechanism, allows them to accomplish similar goals.

In view of the larger scope of future work, the possibility that these animals are affected by the application of the blockages to the designated areas still exists and cannot be dismissed as was witnessed in two of the 10 animals tested. Although these results were not conclusive given within the context of this experiment, it seems that future work addressing a similar hypothesis is well warranted and could provide valuable insight into the functional ecology of this animal. This experiment should be treated as a model for future experiments that examine the role of Kölliker's canal

and mechanoreceptors near the rhinophore in the ability of the Chambered *Nautilus* to respond to angular accelerations.

3.0 Experimental Overview for Vibration Sensitivity Experiments

The overall approach of these experiments was to use a cascading experimental design to determine if *Nautilus* can sense waterborne vibrations. I hypothesized that *Nautilus* were capable of detecting and responding to vibratory stimuli and that they may be sensitive to changes in signal intensities and velocities. The first step was to characterize the responses of nautiluses, if any, to vibrational stimuli. They were therefore initially tested with a range of stimuli that covered a broad array of frequencies and source-displacements (a vibrating bead). This was accomplished by varying the amplitude of the stimulus by using a number of short high-energy pulses ("clicks"). These "clicks" were presented in a repeating series over a specified length of time, with each click separated by a period of silence (a "pulse train"). If the nautiluses demonstrated a discernible response pattern to any stimuli in these initial experiments (Small Source-Displacement Experiment and Large Source-Displacement Experiment, hereafter referred to as SSDE and LSDE, respectively), that information could be incorporated into the design of the Frequency Sensitivity Experiment (FSE) for which an appropriate stimulus-displacement value could be identified and then used as a constant variable throughout the experiment. The source-displacement experiments (SSDE and LSDE) were conducted on separate occasions, using the same animals over a two-month span, to accurately test a broad range of source-displacements. No animal was tested twice within a 48h period.

The Frequency Sensitivity Experiment (FSE) was designed to test the response of nautiluses to varying frequencies of the same displacement and to determine the response of *Nautilus* to increasing/decreasing particle velocities.

Unlike the SSDE and LSDE experiments, select frequencies were randomly presented in continuous 5s increments (as opposed to short pulses) each of which was separated by a specified period of silence. This experiment was conducted over the course of 24 hours.

Animals

Eleven wild-caught adult *Nautilus pompilius* originally collected in the Philippines were housed in a recirculating system at the Aquatic Research and Environmental Assessment Center (AREAC) at Brooklyn College of the City University of New York. The animals were divided into two groups and kept separately in a closed system that consisted of two 140-gallon polyethylene tanks filled with artificial sea water (Instant Ocean™). Both tanks were joined together and connected to a 25-gallon biofilter that contained additional aeration and filtration media. The animals were kept at constant temperature of 17º C and at a salinity level of 32-34 ppt. Fish heads (*Tilapia sp.*) were used as a primary food source and rations were administered every third day. Daily checks of water quality (temperature, salinity, DO, pH, calcium, alkalinity, ammonia, nitrite, nitrate, and phosphate) were conducted to monitor the system and maintain the health of the animals. Trace elements in the form of a calcium/alkalinity liquid buffer system (B-Ionic™) was added on a weekly basis (75ml of each component) to maintain the necessary levels of calcium.

3.1 Methods for Source-Displacement Experiments

3.1.1 Experimental Apparatus

In both source-displacement experiments (small and large), the experimental arena was a rectangular Plexiglas™ tank (51cm L x 25.4cm W x 31.7cm H), containing ~30cm standing water (Figure 3.1). To control for ambient background noise, an insulated and isolated basement room was selected to run the trials. Within the room, the tank was placed on a vibration-absorption table that was constructed from a granite slab (151cm L x 56cm W x 3cm H). The slab was placed atop 12 tennis balls that were separately set in plastic rings and spaced evenly across a metal desk (115cm H x 77cm W x 73.5cm L).

Two digital cameras (Sony Digital Handycam, model DCR-VX1000), mounted on tripods, were used to record each trial and provide both top and side views. One was positioned 1.5m in front of the long-axis of the tank and the other was placed 1m above the tank. To prevent visual contact between the animals and the observers, and to control for inadvertent cuing, a removable blind was placed along three sides of the tank. Only the area containing the apparatus was illuminated with one fluorescent overhead light bulb. Experimenters remained at least 3m from the uncovered portion of the tank and did not move in front of it during the trials

3.1.2 Vibrating Stimulus

To create a dipole source, a spherical acrylic bead (18.95mm in SSDE and 9.44mm in LSDE) was mounted to an aluminum shaft (length 17cm, diameter 2mm), which was bent at a 90° angle, and attached to a mini-shaker (Bruël & Kjaer vibration exciter, model 4810). The mini-shaker was fixed to a wall-mounted frame and

positioned inside of the tank, such that the bead was located in the middle of all three spatial axes. Pulse trains were delivered using a Gateway 450S laptop computer (2.0 GHz Pentium 4M processor) and signal outputs were monitored with an oscilloscope (Tenma, model 72-320). Displacement values were based on biological relevance determined by existing literature (see introduction) and divided into two overlapping ranges, presented in two separate experiments. This format was chosen to minimize habituation to the stimulus and to prevent animal stress resulting from extended trial times (which would be necessary to present the entire range of displacements adequately). The smaller values were tested in the SSDE and ranged from 0.01mm to 0.13mm, whereas the larger values were tested in the LSDE and ranged from 0.08mm to 1.12mm. For the Large Source-Displacement Experiment, a stereo receiver (Kenwood, model VR-615) was used to amplify the signal, thereby increasing the source-displacement.

Stimulus signals were created using SigGenRP v.4.4 stimulus design software from Tucker-Davis Technologies. Stimulus presentations were compiled and edited using CoolEdit Pro v.2.1 from Syntrillium Software Corporation (recently acquired by Adobe Systems Inc., San Jose, California and renamed Adobe Audition v.1.5). Each of the stimulus pulse trains were 5s long and included ten 2ms clicks of the same amplitude, separated by nine 0.553s intervals of silence (Fig. 3.2). Stimulus pulses and their respective source-displacements were measured and calibrated prior to the experiment using a Metrolight laser micrometer, model Alpha XO3. All pulse trains were included only once in each of the trial sequences. Their presentation

orders were randomized using the Microsoft Excel 2002 random-number-generator function.

Instrument Calibration

As a procedural note at the time of instrumental calibration (instrument resolution was .003mm), signals differing slightly in amplitude sometimes produced the same displacements after being rounded to the third decimal place, indicating that the differences in some of the computer-generated signals were extraordinarily small and may not be distinguishable by my current methods of measurement from each other. However, the difference in these signals is so minute that it is unlikely that any behavioral differences between displacements would be detectable, especially within the lower range of displacements presented (*i.e.,* 0.01–0.08mm).

3.1.3 Experimental Procedures

Trials were conducted on three separate days between the hours of 1300h and 1700h for SSDE. LSDE took place over two days between the hours of 1100h and 1800h. The experimental tank was filled with conditioned water from the home tank to ensure that each animal was constantly exposed to uniform and familiar olfactory cues. Animals (N = 11 for both experiments) were transported from the home tank in covered buckets, gently transferred to the test arena using a 3-liter plastic pitcher, and allowed to habituate for 10min prior to the start of the experimental trials. Following habituation, video recording commenced and individuals were subjected to a 5min control period during which time no vibrational pulses were administered. The control period was followed by a 5min period or "stimulus package" that began with

20s of baseline silence and continued with the presentation of 11 randomly ordered pulse trains that were separated by 20s of silence (Figure 3.2).

Treatment order (control first, stimulus second) was not altered between trials because it was unclear how long the effect of the stimulus on the behavior of the animals, if any, would last. If the stimulus were to be presented before the control in these initial experiments, any continuing effect on the behavior of the animals would therefore reduce the legitimacy of the control data. After each trial was complete, the video recoding was stopped and the animal was returned to the home tank. The test aquarium was rinsed thoroughly between trials with fresh (non-saline) water to remove any residual individual olfactory cues.

3.2 Methods and Materials for Frequency Sensitivity Experiment

3.2.1 Experimental Apparatus

The experimental arena was a rectangular Plexiglas™ tank (41cm L x 21cm W x 26.8cm H), containing ~25cm standing water (Figure 3.3). To reduce background vibration, the tank was placed on four foam pads measuring a total of 14.5cm in height. Foam pads were substituted for the slate top and tennis ball table used in the previous experiments due to the unauthorized removal and unfortunate discard of this equipment. The foam pads were placed on a metal desk (115cm H x 77cm W x 73.5cm L).

One digital camera (Sony Digital Handycam, model DCR-VX1000) mounted on a tripod was positioned approximately 1.5m in front of the long axis of the tank and used to record each trial. No second camera was used during this experiment due

to logistical problems encountered when attempting to simultaneously record stimulus output from both cameras. To prevent visual contact between the animals and the observers to control for inadvertent cuing, a removable blind was placed along three sides of the tank and only the area containing the apparatus was illuminated. All other areas in the experimental room were kept dark and experimenters remained at least 3m from the uncovered portion of the tank avoiding moving in front of the tank during the trials.

3.2.2 Vibrating Stimulus

To generate the required frequencies, a spherical acrylic bead, 18.95mm in diameter, was attached in an identical fashion to that described in the Source-displacement Experiments (refer to section 3.1.2). Pre-selected frequencies of the same amplitude (a 0.37mm bead displacement was used) were delivered using a Gateway 450S laptop computer (2.0 GHz Pentium 4M processor, Irvine, California). Signal outputs were monitored with an analog oscilloscope (Tenma, model 72-320) (Figure 3.4).

Stimulus presentations were compiled and edited using CoolEdit Pro v.2.1 from Syntrillium Software Corporation (recently acquired by Adobe Systems Inc. and renamed Adobe Audition v.1.5). The 5min stimulus package consisted of 11 randomly ordered frequencies (10, 50, 75, 100, 150, 200, 300, 400, 500, 750 and 1000Hz) that were chosen based on existing literature including determining which frequencies might be most prevalent in the animal's natural habitat. Each frequency emission was 5s long and was separated by 20s of silence. A select frequency was

included only once per trial sequence and the presentation orders of the frequencies were randomized using the Microsoft Excel 2002 random-number-generator function.

3.2.3 Experimental Procedure

All trials were conducted on the same day between the hours of 0845h and 1500h. As in previous experiments, the experimental tank was filled with conditioned water from the home tank to ensure that each animal was exposed to uniform and familiar olfactory cues. Animals (N = 11) were gently transferred by hand from the home tank into the experimental tank for transport to the same testing room. Each *Nautilus* was habituated to the experimental apparatus for 10min prior to the start of the trials, after which video recording began. Trials consisted of a 5min control period (silence) and a 5min stimulus-set presentation consisting of 11 randomly ordered frequencies. The presentation of the treatment category (control or stimulus) was alternated between trials and a 5min "buffer period" was inserted between treatments to control for order effects.

After each trial was complete, the video recoding was stopped and each animal was returned to the home tank. The test aquarium was rinsed thoroughly between trials with fresh (non-saline) water to remove any residual individual olfactory cues.

3.3 Data Collection and Behavioral Analysis

Data were collected from the video recordings by two independent observers using a Sony DHR-1000 digital video-cassette recorder. Observers were aware of the control/stimulus treatment order but had no knowledge of the individual frequency

orders during stimulus presentation. A suite of six typical *Nautilus* behaviors was identified prior to the experiment (Table 3.1) but no *a priori* assumptions were made as to whether those behaviors would be evident or about their magnitude and polarity. Trials were subdivided into 5s bins and individual behavioral measurements were recorded in real-time for each bin. All typical behaviors such as rocking, touching the bottom of the tank (not just resting on the bottom), tentacle extension (expressed as a percentage of body length), and the "cat's whiskers" foraging posture were not detected in any of the trials. Ventilation rate proved to be the one robust measure and hence will be the focus of all analyses.

Ventilation rate was defined as the number of completed respirations per 5s interval. This behavior was recorded by observing the area of the mantle cavity bilaterally located posterior to the eye or by minor vertical oscillations of the entire animal produced by water expulsion through the hyponome (Fig. 1.3). A completed respiration was defined as either 1) the period between one closure of the mantle to the next, or 2) the deviation in movement of the animal from a standing position to a position either slightly above or below, and then the return to the initial standing position, which has proven to be another reliable indicator of ventilation in these animals.

3.3.1 Statistical Analysis

Univariate ANOVA and *post hoc t*-tests were applied to multiple levels of data beginning with overall comparisons between treatments (control vs. stimulus) to determine if any effect of vibration on behavior was evident. Additional analyses were then performed on data that were placed into categories based on the response of

the animals over distance and over time. Two "distance" categories were created: responses of animals less than 20cm (<20cm) and greater than 20cm (>20cm) from the source were analyzed separately to examine the function of distance from the source on behavior. Analysis of these categories was conducted across 15 trials from all three experiments. "Time" categories comprised 5s time-bins. Here, control data were compared to five 5s post-stimulus categories (5s stim, 5s post, 6-10s post, 11-15s post, and 16-20s post) to describe the reaction of the animal over time.

As an additional note, mean ventilation rates varied greatly between animals so numerical ventilation rates were converted into percentage change from the control to illustrate change in behavior. However, all statistical tests were performed on the actual ventilation values as opposed to the percentage values to avoid an artificial increase or decrease in probability due to the imposition of fixed limits (0-100) on the measure.

3.4 Overall Combined Results for All Experiments

Twenty trials using 11 animals were conducted. In fifteen trials, animals remained stationary for the duration of each trial and five trials had animals that were in constant motion throughout. Animals altered their behavior in the presence of vibrations. A significant decrease of 8.9% in ventilation rate occurred between control and stimulus treatments across all animals (ANOVA, $p = <.001$, $F = 24.573$) with an average control response of 3.70 ventilations/5s (SD = 1.59) and an average ventilation rate in the presence of a stimulus of 3.37 ventilations/5s (SD = 1.47; Figure 3.5).

Nautiluses also significantly decreased their ventilation rate over time (Figure 3.6). ANOVA and *post-hoc t*-tests revealed that the largest decrease of 9.2% was observed during the actual 5s stimulus presentation (p = .001) and the smallest decrease of 6.8% occurred 5 seconds after that (p = .017). The responses of animals in the remaining three 5s post-stimulus bins declined 8.5% in the 6-10s post-stimulus bin from the control (p = .004), followed by an 8.0% decrease from the control during the 11-15s post-stimulus bin (p = .007), and lastly decreasing by 7.8% from the control during the 16-20s post-stimulus bin (p = .004), respectively.

An additional analysis was performed on the 15 animals that remained stationary throughout the trial to determine if the results were somehow skewed by the inclusion of the five moving animals. Nearly identical to the results of the previous analysis, a significant decrease in ventilation rate of 8.8% (ANOVA, p = <.001, F = 38.986) was found to exist between control and stimulus conditions. This suggests that the inclusion of these animals into the overall analysis did not affect the results overall and has allowed for the entire presentation of the data from all three experiments.

The role distance played in the responses of animals to the stimulus was examined as well. Fifteen trials in which animals remained stationary were examined, so that distance was a constant throughout each the trial. A Spearman's Rank correlation test revealed a positive association between ventilation rate and distance from the vibrating stimulus in *Nautilus* (Spearman's rank coefficient = .206, p = <.001). Animals vented at a rate 6.8% lower when they were closer to the stimulus than when they were greater than 20cm from the origin of the vibrations.

Ventilation rate also decreased significantly (ANOVA and *post hoc t*-tests) from the control mean over time when the animals were less than 20cm from the source (N = 7; Fig 3.7). Significant decreases in ventilation rate were found for each of the temporal categories (5s stimulus, p = .002; 5s post-stimulus p = .007; 6-10s post-stimulus, p = .002; 11-15 post-stimulus, p = .002; and 16-20s post-stimulus, p = .012). For animals that remained further than 20cm from the source during the trials (N = 8), significant differences in ventilation rate were only obtained from three of the five temporal-stimulus categories and with no obvious pattern (5s stimulus, p = .001; 5s 6-10s post-stimulus, p = .005; and 16-20s post-stimulus, p = .015).

When source-displacement and source-velocity increased, animals exhibited a decrease in their ventilations. Pearson correlations compared ventilation rates in all animals from the SSDE and LSDE (Figure 3.8) that were less than 20cm from the source (N = 3) and greater than 20cm (N = 7), producing correlation coefficients of -.136 (p = <.001) and -.018 (p = .781), respectively. The same tests were used to evaluate the relationship between ventilation rate and source-velocity for animals tested in the FSE that were also less than 20cm from the source (N = 4; Pearson's correlation coefficient = -.253, p = <.001). Only one animal was found to be further than 20cm from the source during the entire experiment and, when the same correlation tests were applied, did not indicate a significant relationship between ventilation rate and source-intensity (N = 1; Pearson's correlation coefficient = .102, p = 291). Although this result supports trends revealed in the other two experiments, it cannot be viewed as having any statistical merit due to the inadequate sample size and must therefore be used descriptively (Figure 3.9).

Although the creation of distance "categories" was possible, precise distances for each animal from the source could not be obtained. Because no one potential point of reception could be consistently identified for each of the animals, it was not possible to establish a reliable end point that could be used to measure the distance from the bead. Even if a point of reception was arbitrarily chosen (*e.g.*, the eye of the animal or closest tentacle to the source), determining true particle displacements and velocities would be further impacted by each animal's position within the tank. The reason for this is that these quantities are dependent on the both the strength of the vibrating source as well as its direction, and weaken at different rates with regard to the animal's position.

3.5 Results for Small Source-Displacement Experiment: Bead Displacement 0.01-0.13mm

3.5.1 General Behavior

The general trend for a majority of the experimental subjects (N = 7) was to remain stationary throughout the entire trial. The animals would attach to a point on the tank wall with one or two tentacles and hang motionless (save respiration) for the entire trial. Only two animals deviated from this pattern, remaining in constant motion for the duration of both control and experimental treatments (these animals were discounted from any spatial analysis). This behavior can most likely be attributed to animal stress since they were equally motile during both control and experimental treatments.

3.5.2 Pooled Behavioral Analysis

Data collected from seven trials suggested that nautiluses significantly reduced their ventilation rates in the presence of a vibrating bead (ANOVA, p = <.001, F = 13.599). Ventilation rates throughout the entire experiment ranged from 1 ventilation/5s to 8 ventilations/5s. Overall, animals averaged 3.60 ± 0.06 ventilations/5s during the control period and decreased their rate to 3.31 ± 0.06 ventilations/5s after exposure to a vibrational stimulus (Figure 3.10), equivalent to a decrease of 8.1%. ANOVA and *post hoc* *t*-tests were used to determine temporal responses after the animals were split into distance categories. Animals less than 20cm from the source (N = 2) exhibited their greatest decrease in ventilation rate (15.7%) during the first 5s of the stimulus presentation (p = <.001). Additionally, significant decreases in ventilatory rate were seen during the 5s post- (10.1%, p = .002), 6–10s post- (11.3%, p = <.001), and 11–15s post-stimulus (10.1%, p = .002) temporal bins and are listed in Table 3.2. Animals greater than 20cm from the source (N = 3) also exhibited their greatest decrease in ventilation rate (14.6%) during the first 5s of the stimulus presentation (p = <.001) and exhibited smaller decreases after the 6–10s post- (9.2%, p = .021) and 16–20s post-stimulus periods (11.2%, p = .005) (Figure 3.11). These results suggest that animals that are closer to the source show a larger decrease in ventilation rate from the control condition and that time may also be a factor.

An additional analysis was performed on only the five animals that remained stationary throughout the trial to determine if the results were somehow skewed by the inclusion of the two moving animals. Similar to the results of the previous

analysis, a significant decrease in ventilation rate of 9.0% (ANOVA, $p = .001$, $F = 40.901$) was observed between the control and stimulus conditions. This suggests that the incorporation of these animals into the overall analysis did not impact the results overall and has allowed for the complete presentation of the data collected during this experiment.

3.5.3 Behavioral Analyses of Individuals

Three of the seven animals tested in this experiment showed a significant decrease in respiration rate after exposure to a vibrating sphere during and after presentation (one or more stimulus and post-stimulus temporal bins). Two of the animals (Animal 7 and Animal 9) showed a significant decrease in ventilation during each of the temporal bins (although no directional trend indicating a continuing decrease or increase in ventilation rate over time was evident) and all three animals exhibited the most dramatic response during the 5s stimulus presentation specifically. Lastly, Animal 2 exhibited a significant decrease in ventilation rate during three of the five temporal bins but, as before, no directional trend was evident. Two of the three animals that demonstrated a significant decrease in ventilation rate were less than 20cm from the vibrating sphere, underscoring that there is probably an added effect of proximity in their reaction to the stimulus. Additionally, a general trend was apparent since an additional three of the seven animals tested exhibited their lowest ventilation rate, albeit not statistically significant, when exposed the 5s stimulus presentation, suggesting that they demonstrate the strongest response in the presence of the stimulus.

Statistical Note

A statistically conservative approach was used when evaluating the results of all univariate ANOVA tests and pairwise comparisons (*post hoc t*-tests) between treatments for each animal. A Bonferroni correction was applied to reduce the overall error rate. The significance level was adjusted by sequentially dividing the *p* value (.05) by the total number of tests and then ordering the F statistical value from largest to smallest. For example, if seven animals were compared individually, the individual with the highest F statistic or lowest *p* value would be held to an error rate of .007 as opposed to .05 (as .05 / 7 = .007). The next highest F statistic would be held to an error rate of .008 (as .05 / 6 = .008), and so forth. This correction was applied to each experiment where individual results were reported.

Animal 2: A marked decrease in ventilation was observed in Animal 2 when the animal was presented with the stimulus package (Figure 3.12). The animal remained stationary for the duration of the entire trial at a distance that was less than 20cm from the source. Ventilation rates for the entire trial ranged from 2.40 ± 0.20 ventilations/5s to 3.00 ± 0.20 ventilations/5s. The overall average ventilatory rate was 2.97 ± 0.06 ventilations/5s during the control trial. Ventilation rate decreased significantly, however, in the presence of a vibrational stimulus (ANOVA, $p = .005$, $F = 8.135$). A significantly negative correlation was established between ventilation rate and source-displacement for this animal (Pearson's correlation coefficient = -.257, $p = .006$).

Animal 7: Animal 7 remained stationary for the duration of the entire trial less than 20cm from the vibrating sphere. The range of ventilation rates for the entire

trial was from 2.40 ± 0.18 ventilations/5s to 3.12 ± 0.05 ventilations/5s. The overall ventilatory rate during the control trial was 3.12 ± .05 ventilations/5s. Ventilation rate decreased significantly, however, in the presence of a vibrational stimulus (ANOVA, p = <.001, F = 26.118) as the mean value for the stimulus treatments was 2.73 ± .05 ventilations/5s (Figure 3.13). A significantly negative correlation was established between ventilation rate and source-displacement for this animal (Pearson's correlation coefficient = -.322, p = <.001).

Animal 9: Animal 9 remained stationary for the duration of the entire trial at a distance from the source that was greater than 20cm. Ventilation rates for the entire trial ranged from 1.80 ± 0.2 ventilations/5s to 2.75 ± 0.06 ventilations/5s, averaging 2.75 ± 0.06 ventilations/5s during the control trial. Ventilation rate decreased significantly in the presence of a vibrational stimulus (ANOVA, p = <.001, F = 48.867). The animal respired on average of 2.16 ± 0.06 ventilations/5s during the stimulus treatments (Figure 3.14) and ventilation rate for this animal had a significantly negative correlation to source-displacement (Pearson's correlation coefficient = -.412, p = <.001).

Animal 5: Animal 5 remained attached to the test arena for the length of the entire trial and exhibited a non-significant, although noteworthy, decrease in respiration after being exposed to a vibrational source. Animal 5 was greater than 20cm from the source and ventilation rates for the entire trial ranged from 2.80 ± 0.25 ventilations/5s to 3.40 ± 0.25 ventilations/5s. The average ventilatory rate for this animal during the control trial was 3.37 ± 0.08 ventilations/5s and decreased when exposed to vibration (ANOVA, p = .052, F = 3.868). Mean values for the stimulus

treatments were 3.16 ± 0.08 ventilations/5s, (Figure 3.15). The animal ventilated at its lowest rate during the 5s stimulus presentation and a general decrease in ventilation rate was seen when source-displacements increased, although no significant correlation was evident.

Animal 6: Although Animal 6 showed the smallest difference in ventilation rate between treatments of all the trials, a non-significant decrease after exposure to vibratory source was still evident. This animal, like the majority of the other experimental animals, remained still for the duration of the entire trial and maintained a distance of greater than 20cm from the source. Ventilation rates for this trial ranged from 3.00 ± 0.19 ventilations/5s to 3.60 ± 0.19 ventilations/5s. The overall average ventilatory rate during the control trial was 3.27 ± 0.06 ventilations/5s and it decreased to 3.21 ± 0.06 ventilations/5s during the presentation of the stimulus (Figure 3.16). The animal ventilated at its lowest rate during the 16-20s post-stimulus temporal bin and a general decrease in ventilation rate was seen when source-displacements increased, although no significant correlation was evident.

Animal 4: Animal 4 was one of the two animals that remained in constant motion for the duration of the entire trial and, because of an increase in swimming activity and presumably a subsequent demand for more oxygen, recorded the largest and highest range of respiratory rates of all seven trials. Ventilation rates for the entire trial ranged from 2.80 ± 0.47 ventilations/5s to 7.20 ± 0.47 ventilations/5s with a mean rate of 4.50 ± 0.17 ventilations/5s during the control. The ventilation rate for this animal decreased when it was in the presence of a vibrational stimulus but the difference was not significant. Mean values for the stimulus treatments were 4.29 ±

0.18 ventilations/5s (Figure 3.17) and the animal demonstrated its lowest ventilatory rates during the 5s stimulus presentation, and the 11-15s and 16-20s post-stimulus time bins. A general decrease in ventilation rate was seen when source-displacements increased, although no significant correlation was evident.

Animal 10: Animal 10, like all other animals in this experiment, showed a decrease in ventilatory response after being exposed to the stimulus package, the effect of which was not statistically significant. Ventilation rates for the entire trial ranged from 4.40 ± 0.33 ventilations/5s to 5.80 ± 0.33 ventilations/5s and the increase in respiration, compared to other trials, can be attributed to the fact that the animal remained in motion throughout the entire trial. The mean ventilatory rate was 5.17 ± 0.10 ventilations/5s during the control trial. The animal averaged 4.91 ± 0.10 ventilations/5s during the stimulus treatment (Figure 3.18) and achieved its lowest ventilation rate during the 5s stimulus presentation. A general decrease in ventilation rate was seen when source-displacements increased, although no significant correlation was evident.

3.6 Results for Large Source-Displacement Experiment: Bead Displacement 0.08-1.12mm

3.6.1 General Behavior

Consistent with the findings from the SSDE, no signature behaviors (rocking, touching the bottom of the tank, tentacle extension, and "cat's whiskers" foraging displays) were detected in any of the five animals tested. In addition, all of the experimental subjects were stationary for the duration of the entire trial. The animals

would, as before, attach to a point within the tank and remain there for the entire trial. Ventilation rate was used as the metric since it proved to be the most reliable measure in each of the five animals.

3.6.2 Pooled Behavioral Analysis

Animals exhibited a significant decrease in ventilation rate when compared to the control response (N = 5, ANOVA, p = .003, F = 8.857) (Figure 3.19). Pooled data from all of the trials indicated that nautiluses averaged a respiration rate of 2.98 ± 0.02 ventilations/5s during control trials that decreased to 2.88 ± 0.03 ventilations/5s during the stimulus period, representing a 3.4% decrease overall, the lowest differential of any of the experiments. *Post hoc t*-tests were used to determine temporal responses after the animals were split into distance categories. The animal less than 20cm from the source (N = 1) exhibited the greatest decrease in ventilation rate (22.1%) during the first 6-10s of post-stimulus period (p = <.001). Additionally, significant decreases in ventilatory rate (16.1%) were seen during the first 5s of the stimulus presentation (p = .004)). All of the animal responses over time and their probability values are listed in Table 3.2 (ANOVA and *post hoc t*-tests). Animals greater than 20cm from the source (N = 4) exhibited significant decreases in ventilation rate during the 6–10s post-stimulus time-bin (p = .018) and the 11–15s post-stimulus time-bin (p = <.005), exhibiting an overall reduction from the ventilatory control mean of 4.3% and 5.1%, respectively (Figure 3.11).

3.6.3 Behavioral Analyses of Individuals

Two of the five animals tested in this experiment (Animal 2 and Animal 8) showed a significant decrease in respiration rate when exposed to vibration, although

four of the five showed an overall trend of decreased ventilation. No temporal or distance pattern could be established between both animals since each of them exhibited their largest ventilatory decreases during different stimulus and post-stimulus time bins and each was in a different distance category. Additionally, a general temporal trend was apparent since an additional three of the five animals tested exhibited their lowest ventilation rate, albeit not statistically significant, 11–15s after the stimulus presentation and each of these animals were greater than 20cm from the source. Animals with significant results will be reported first.

Animal 2: Animal 2 was greater than 20cm from the source and significantly decreased its ventilation after being exposed to multiple vibrational stimuli (ANOVA, p = .002, F = 9.978). Ventilation rates for the entire trial ranged from 2.60 ± 0.18 ventilations/5s to 3.20 ± 0.18 ventilations/5s. When the animal was exposed to the control condition, mean respiration rate was 3.17 ± 0.06 ventilations/5s. During the stimulus treatment, respiration decreased to 2.91 ± 0.06 ventilations/5s (Figure 3.20). The animal ventilated at its lowest rate during the 11-15s post-stimulus period although no significant temporal correlation was evident.

Animal 8: Animal 8 was the only animal that was less than 20cm from the source and demonstrated a highly significant decrease in ventilation when subjected to the treatment condition (ANOVA, p = .005, F = 8.028). The range of ventilation rates for this trial was 2.33 ± 0.21 ventilations/5s to 2.68 ± 0.06 ventilations/5s. Mean values for the control and stimulus treatments were 2.68 ± 0.06 ventilations/5s and 2.43 ± 0.07 ventilations/5s, respectively (Figure 3.21). The animal ventilated at its

lowest rate during the 6-10s post-stimulus period although no significant temporal correlation was evident.

Animal 1: Animal 1 did not significantly decrease its ventilation rate in response to a multiple vibratory stimuli and remained at a distance greater than 20cm from the source. Ventilation rates for the entire trial ranged from 3.00 ± 0.13 ventilations/5s to 3.20 ± 0.14 ventilations/5s. Mean values for the control and stimulus treatments were 3.12 ± 0.04 ventilations/5s and 3.04 ± 0.04 ventilations/5s, respectively (Figure 3.22). The animal ventilated at its lowest rate during the 5s and 11-15s post-stimulus periods although no significant temporal correlations were evident.

Animal 6: No significant difference in ventilation rates was recorded for Animal 6 between the control and treatment conditions. This animal remained at a distance greater than 20cm from the source and ventilation rates for the entire trial ranged from 2.80 ± 0.08 ventilations/5s to 3.20 ± 0.08 ventilations/5s. The animal responded nearly identically to the control and stimulus treatment. The means were 2.98 ± 0.02 ventilations/5s and 2.98 ± 0.03 ventilations/5s, for the control and stimulus treatments, respectively (Figure 3.23). The animal ventilated at its lowest rate during the 5s stimulus presentation although no significant temporal correlation could be established.

Animal 7: Animal 7 remained stationary for the duration of the entire trial at a distance greater than 20cm from the source and is the only animal for which an overall increase in respiration during exposure to the vibrational stimuli can be observed. However, a univariate ANOVA test revealed no significant difference in

ventilation rates between the control and treatment conditions. Ventilation rates for the entire trial ranged from 2.80 ± 0.15 ventilations/5s to 3.40 ± 0.15 ventilations/5s. Mean values for the control and stimulus treatments were 2.98 ± 0.04 ventilations/5s and 3.04 ± 0.05 ventilations/5s, respectively (Figure 3.24). Although the animal increased its ventilatory rate overall, it still exhibited a decrease in ventilation rate during the end of the post-stimulus period, achieving its lowest rate during the 11-15s post-stimulus period and its next lowest rate during the 16-20s post-stimulus bin, however, no significant temporal correlations could be established.

3.7 Results for Frequency Sensitivity Experiment: Range 10–1000Hz

3.7.1 General Behavior

All of the experimental subjects remained stationary during the control period as well as the stimulus period. The animals would either attach to a point on the tank wall or would settle on the bottom of the tank. Only animal respiration could be observed since all other typical behaviors such as rocking, touching the bottom of the tank (not just resting on the bottom), tentacle extension, and the "cat's whiskers" foraging posture were absent in all of the trials. As before, ventilation rate proved to be a reliable measure and will be the focus hereafter. As in the preceding experiments, no data could be collected for two of the ten animals tested for the same reasons as stated previously.

3.7.2 Pooled Behavioral Analysis

Ventilation rate data collected from eight animals showed that nautiluses slow their respiration during vibrations of all frequencies presented (ANOVA, $p = <.001$, F

= 13.320). Pooled data from all eight trials indicated a lower rate of respiration during exposure to multiple frequencies (particle velocities) when compared to the control mean value (4.26 ± 0.10 ventilations/5s for the control response and 3.75 ± 0.10 ventilations/5s for the stimuli), a decrease equivalent to 12.0% overall when compared to the ventilatory control mean (Figure 3.25). The same analysis was performed on only the five animals that remained motionless throughout the trial to determine if the results were impacted by the inclusion of the 3 moving animals. Similar to the previous analysis, a significant decrease in ventilation rate of 14.0% (ANOVA, p = <.001, F = 12.651) was observed between control and stimulus conditions. This suggests that the inclusion of these animals into the overall analysis did not affect the results overall and has allowed for the presentation of the entire data set.

ANOVA and *post hoc t*-tests were used to determine responses of the animals over time after the animals were split into distance categories. Animals less than 20cm from the source (N = 4) showed a significant decrease in ventilation rate during the 5s (a decrease of 14.8%, p = .020), 11–15s (a decrease of 15.3%, p = .020), and 16–20s (a decrease of 13.2%, p = .025) post-stimulus bins. All temporal-based animal responses and their probability values are listed in Table 3.2 (ANOVA and *post hoc t*-tests). The animal greater than 20cm from the source (N = 1) exhibited a significant decrease in ventilatory rate during the first 5s of the stimulus presentation (5s stim), posting an overall reduction from the ventilatory control mean of 11.1%, and actually significantly increased its ventilation rate for each of the remaining temporal bins (Figure 3.11).

The same analysis was performed on only the five animals that remained motionless throughout the trial to determine if the results were impacted by the inclusion of the 3 moving animals. Similar to the previous analysis, a significant decrease in ventilation rate of 8.6% (ANOVA, p = 001, F = 12.651) was observed between control and stimulus conditions. This suggests that the inclusion of these animals into the overall analysis did not affect the results overall and has allowed for the presentation of the entire data set.

Statistical Note

A univariate ANOVA was applied to the entire sample population to determine if between-subject variability was significant. A significant interaction between animals was evident (p = <.001, F = 596.436). This justified further analyses at the level of the individuals to account for differences in response magnitude between individuals, which might otherwise be masked by a pooled analysis. Although the presence of significant inter-animal variation reduces the power of the ANOVA when comparing entire populations, it is still highly effective in establishing general behavioral trends across the population. Additional support for this trend can then be provided through individual examination and analysis.

To examine the possibility of habituation across trials in the nautiluses, an ANOVA was also conducted to determine if the presentation order (control first or stimulus first) had an effect on ventilation rate. Initially, the results of the test for habituation indicated that the presentation order had a significant effect on ventilation (p = .007, F = 7.287), suggesting that ventilation rates of animals that receive the stimulus treatment first may differ overall from those that experience the control first.

Further comparisons of the means indicated that, regardless of the presentation order, the treatment values were always lower than the control values. A reason for this result may be that in the separate presentation groups (four animals experienced the control first and four animals experienced the stimulus package first) the group that experienced the control first generally ventilated at greater rates (control mean = 5.19 ± 0.13; stimulus mean 4.31 ± 0.13) than those exposed to stimuli first (control mean = 3.34 ± 0.13 ventilations/5s; stimulus mean = 3.17 ± 0.13 ventilations/5s). It may be that the 5 min buffer that occurred between conditions was not a sufficient length of time to allow for the animals to reestablish a normal respiratory pattern. However, this result does reinforce the notion that exposure to a vibrational stimulus, or set of stimuli, lowers ventilation rate of nautiluses for a period of time afterwards.

3.7.3 Behavioral Analyses of Individuals

Four of the eight animals exhibited a significant decrease overall in ventilation rates after being exposed to multiple frequencies. Two of the animals (Animal 3 and Animal 6) showed a significant decrease in ventilation during each of the temporal bins and all four animals exhibited significant decreases in ventilation rate during the 5s post-stimulus, 11–15s post-stimulus, and 16–20s post-stimulus periods. Two of the four animals that demonstrated a significant decrease in ventilation rate were less than 20cm from the vibrating sphere and the other two animals remained in motion throughout the trial. Of all the animals that responded in a statistically significant way, three received the control treatment first and the remaining individual received the stimulus treatment first. The results of the animals that received the control treatment followed by the stimulus treatment are reported first and then the group that

was administered the stimulus portion before the control treatment follows. In each group, statistically significant findings are stated first.

Control Treatment First

Animal 3: A clear decrease in respiration rate was observed in Animal 3 when presented with the stimulus package (ANOVA, p = <.001, F = 71.895). Ventilation rates for the entire trial ranged from 5.60 ± 0.32 ventilations/5s to 8.80 ± 0.32 ventilations/5s as the animal remained in constant motion throughout the trial. The average ventilatory rate was 8.31 ± 0.13 ventilations/5s during the control period. The animal decreased its respiratory rate to 6.76 ± 0.13 ventilations/5s when exposed to multiple frequencies (Figure 3.26). Animal 3 averaged significantly lower respiratory rates during each of the stimulus and post-stimulus time bins.

Animal 6: Animal 6 remained within 20cm of the source and decreased its ventilation rates between the control and treatment conditions significantly (ANOVA, p = <.001, F = 301.863). The animal's ventilation rate ranged from 2.40 ± 0.21 ventilations/5s to 2.72 ± 0.08 ventilations/5s over the course of the trial. Mean respiration rates for the control and stimulus treatments were 4.72 ± 0.08 ventilations/5s and 2.82 ± 0.08 ventilations/5s, respectively, representing the largest disparity observed throughout the experiment (Figure 3.27). Animal 6 averaged significantly lower respiratory rates during each of the stimulus and post-stimulus time bins.

Animal 8: Animal 8 also demonstrated a highly significant decrease in ventilation when subjected to the treatment condition and maintained a distance of less than 20cm from the source (ANOVA, p = .001, F = 26.177). The range of

ventilation rates for this trial was 1.20 ± 0.17 ventilations/5s to 2.00 ± 0.05 ventilations/5s. Mean values for the control and stimulus treatments were 2.00 ± 0.05 ventilations/5s and 1.64 ± 0.05 ventilations/5s, respectively (Figure 3.28). Animal 8 averaged significantly lower respiratory rates during the 5s post-, 11–15s post-, and 16–20s post-stimulus time bins.

Animal 1: No significant difference in ventilation rates was recorded for Animal 1 between the control and treatment conditions although an overall increase during the stimulus presentation was observed. Animal 1 remained in constant motion throughout the trial and ventilation rates for the entire trial ranged from 5.40 ± 0.42 ventilations/5s to 6.60 ± 0.42 ventilations/5s. The means were 5.74 ± 0.13 ventilations/5s and 6.04 ± 0.13 ventilations/5s, for the control and stimulus treatments, respectively (Figure 3.29). Animal 1 increased its ventilation rate during all but one temporal bin exhibiting an average decrease in respiration rate 5s during the stimulus presentation (5s stim), none of which were statistically significant.

Stimulus Treatment First

Animal 4: Animal 4 significantly decreased its ventilation after being exposed to multiple vibrational stimuli and remained in constant motion throughout the trial (ANOVA, $p < .001$, $F = 32.199$). Ventilation rates for the entire trial ranged from 3.00 ± 0.34 ventilations/5s to 4.35 ± 0.10 ventilations/5s. When the animal was exposed to the control condition, mean respiration rate was 4.35 ± 0.10 ventilations/5s. During the stimulus treatment, respiration decreased to 3.52 ± 0.10 ventilations/5s (Figure 3.30) and the animal averaged significantly lower respiratory

rates during the 5s post-, 6–10s post-, 11–15s post-, and 16–20s post-stimulus time bins.

Animal 11: No significant difference in ventilation rates was recorded for Animal 11 between the control and treatment conditions. The animal stayed within 20cm of the source and its ventilation rates for the entire trial ranged from 3.60 ± 0.39 ventilations/5s to 5.80 ± 0.39 ventilations/5s. The animal responded nearly identically to the control and stimulus treatment. The means were 4.87 ± 0.14 ventilations/5s and 4.85 ± 0.14 ventilations/5s, for the control and stimulus treatments, respectively (Figure 3.31). Animal 11 experienced its lowest ventilatory rate on average during the 6–10s post-stimulus period.

Animal 2: Animal 2 did not significantly decrease its ventilation rate in response to a multiple vibratory stimuli and was the only animal to remain further than 20cm from the source. Ventilation rates for the entire trial ranged from 32.00 ± 0.23 ventilations/5s to 2.80 ± 0.23 ventilations/5s, and mean values for the control and stimulus treatments were 2.45 ± 0.07 ventilations/5s and 2.46 ± 0.07 ventilations/5s, respectively (Figure 3.32). Animal 2 increased or maintained its ventilation rate during all but one temporal bin exhibiting an average decrease in respiration rate during the 5s stimulus presentation (5s stim), none of which however, were statistically significant.

Animal 9: Animal 9 remained within 20cm of the source and exhibited an overall increase in respiration during exposure to the vibrational stimuli, the difference of which was not significant. Ventilation rates for the entire trial ranged from 1.60 ± 0.21 ventilations/5s to 2.00 ± 0.21 ventilations/5s. Mean values for the

control and stimulus treatments were 1.69 ± 0.06 ventilations/5s and 1.83 ± 0.06 ventilations/5s, respectively (Figure 3.33). Animal 9 increased its ventilation rate during all but one temporal bin exhibiting an average decrease in respiration rate 6–10s after the stimulus presentation (6–10 post-stim), none of which were statistically significant.

3.8 Discussion

The major finding revealed by these experiments is that nautiluses are capable of responding to vibrational stimuli. The behavioral response is almost always a decrease in ventilation rate subsequent to vibration exposure when compared to the control condition. Although the overall decrease differed between experiments, with the smallest difference occurring in the LSDE and the largest in the FSE, it is important to note that nine of the 20 trials analyzed (across all three experiments) revealed significant decreases in ventilation rate when the animal was exposed to vibratory stimuli. Additionally, no significant increases in ventilation were discovered throughout the course of these experiments, supporting the general trend of post-exposure reduction in respiration. Furthermore, the following conclusions are supported by the results of these experiments: 1) an increase in signal intensity is significantly correlated to a decrease in *Nautilus* ventilation rate (Fig. 3.8); 2) an increase in signal velocity results is also significantly correlated to a decrease in ventilation rate (Fig. 3.9); and 3) *Nautilus* respiratory rates are significantly correlated with their proximity to the source, decreasing as the animal nears the source or the source nears the animal (Fig. 3.11).

Another noteworthy result revealed that the largest ventilation rate differential among experiments occurred during the FSE (a decrease from the control condition of 0.51 ventilations/5s). This may be an artifact of longer stimulus exposure (5s stimulus pulses were administered during the FSE, whereas multiple 2ms clicks over a 5s period were used during the SSDE and LSDE) or a simple indication that nautiluses respond more strongly to pure tones than to clicks. In terms of animal response to individual source-displacements and frequencies, it is difficult if not impossible (as a result of this experimental design) to establish a concrete threshold of sensitivity considering the complete range of responses demonstrated by all of the animals and their varying distances from the source (see the end of section 3.4 for a more in depth explanation). But a range of stimuli was used to describe the overall responses of animals to a suite of environmentally relevant vibrations.

Comparatively speaking, these findings are relevant to research conducted previously on other invertebrates, such as Williamson's (1988) investigation into the vibrational sensitivity of the statocyst in the northern Octopus (where a minimum particle-displacement threshold of 0.12μm was determined) and the study conducted by Klages *et al*. (2002) which noted that the deep-water amphipod, *Eurythenes gryllus*, produces particle displacements of 0.05–0.3μm between 70–200Hz when feeding and swimming. Nautiluses are capable of responding well within these ranges of displacements and frequencies and future work should focus on determining practical applications of this system in the wild. The detection of signals in the wild can benefit *Nautilus* in many ways. The observed response (a decrease in ventilation rate) could quite possibly serve as a mechanism for predator avoidance. These

experiments revealed that no patterned temporal response to vibrational signals was evident, since significant decreases in ventilation rate ranged from the stimulus presentation to the 16–20s post-stimulus period. The lack of uniformity suggests that these animals can respond to the stimulus for up to at least 20s post-presentation, and that the distance from the source and the components of the signal are both important factors.

From a biological standpoint, it seems probable that decreasing respiratory rates may best serve as a defense mechanism. Such a mechanism would work most effectively in concert with their cryptic coloration by reducing their overall rocking movement as the predator nears and the signal strength increases, thereby drawing less predatory attention. Conversely, decreasing respiration may benefit an animal's predatory success. This is not to imply that *Nautilus* are formidable hunters-- but an argument in support of a sit-and-wait strategy is plausible. These animals spend most of their lives attached to coral reefs that are teeming with potential prey items. Perhaps nautiluses, upon detection of a certain chemical/vibrational cue (assuming they can be coupled), decrease their rate of ventilation in order to make themselves less conspicuous to an unsuspecting prey and continue to shallow their respiration as the prey moves closer.

3.8.1 Possible Mechanisms of Transmission

It is difficult to suggest a physiological mechanism responsible for this behavior based on these experiments. It is evident that these animals are capable of exhibiting a response to a mechanical source, the mechanism of which would most likely involve epithelial tactile receptors on the tentacles, mechanoreceptors below

the rhinophore, or some other innervated system. Such is the case with some recent cuttlefish research (Komak *et al.*, 2005) that has demonstrated that epidermal lines along the mantle and arms containing polarized hairs are able to detect local water movements and subsequently integrate that information into behavioral responses (also noteworthy is the fact that a similar randomized frequency experiment was conducted and lower confidence intervals were adopted, $p < 0.10$, due to the exploratory nature of the research). The location of these potential receptors could not be ascertained by these experiments but perhaps these are not the only possibilities.

Another possible mechanism of transmission involves the nautiloid statocyst and the cilia that line its externally-connected duct, Kölliker's Canal. Since there is no evidence suggesting that these cilia are innervated, a plausible function could be that they act as a filter or somehow transmit hydrodynamic disturbances or pressure differences to the inside of the lumen where they can be appropriately acted on via statoconia displacement or direct manipulation of the hair cells.

Hypotheses regarding the evolutionary benefit of the ability to detect vibration are inextricably linked to the observable measure, ventilation rate, and are elaborated on in the following section. Irrespective of the behavioral response, it seems that any additional sensory system that an animal can use, whether it is in conjunction with alternate systems or serving as a primary system, would be beneficial to its survival. Based on the average depth in which these animals live, coupled with their nektobenthic niche, it seems reasonable that an evolutionary argument can be made

for the benefits of possessing a mechanosensory system capable of detecting hydrodynamic disturbances and/or substrate-borne vibrations.

Nautilus clearly can detect and respond to vibrational stimuli based on these experiments. To what end this sensory system serves, whether it is mate selection, prey acquisition, predator avoidance, etc., can only be examined within the context of ventilation. Without establishing that a decrease in ventilation rate is a primary response to vibrational stimuli, or that the stimuli were "complete" in their presentation as they would be in the wild, it is difficult to speculate on the likely adaptations of the mechanism. Furthermore, it is necessary to address a few issues arising from these experiments that could be of likely contention or critique. Further explanation regarding sample size and the selection of the source-displacement used in the Frequency Sensitivity Experiment (0.37mm) are addressed in the following paragraphs.

3.8.2 Sample Size

One of the most common critiques of most scientific studies (and not just behavioral) is small sample sizes and their statistical validity. As opposed to other disciplines, ethologists who maintain experimental animals are often faced with a unique set of circumstances that arise purely from the animals with which they work. The Chambered *Nautilus* is no exception. Little effort has been put forth on the behalf of these animals in the area of population dynamics, and the acquisition of a large sample is not feasible and possibly not ecologically responsible. That being said, I am a proponent of statistical viability regardless of sample size. In fact, using a within-subject design is a powerful experimental tool, since the animal's behavior

under treatment is compared to its own behavior without treatment. Initially, a sample size of twelve was proposed for each of the experiments which would have amply sufficed. For reasons explained previously, data from seven (SSDE), five (LSDE), and eight (FSE) trials were successfully collected and data from five trials for each experiment were considered for any type of analysis regarding distance from the source. Although I would have preferred having data from all of the trials in the interest of reducing inter-animal variation, these sample sizes are still adequate and defendable considering the conservative statistical approach used (Bonferroni correction).

3.8.3 Selection of 0.37mm Source-displacement for FSE

The selection of the source-displacement value of 0.37 was based on animal responses that were observed during the LSDE. A larger value was specifically chosen in order to avoid any possible interference that may be caused by background noise. Additionally, an approximate decrease in ventilation rate of 9.50% was observed during the LSDE which proved to be the largest difference from the control ventilation rate. Vindication for this selection lies in the fact that the FSE elicited the largest average decrease overall (0.51 ventilations/5s or 10.4%) when compared to the SSDE (8.5% decrease) and LSDE (4.7% decrease).

It is possible, however, that any of the individual displacements tested would have sufficed, especially when taking into consideration that the displacement value falls off at a rate of $1/r^3$ (Kalmijn, 1988), where r is distance from the source. Since the animals were not held at a predetermined distance from the source (and some of them remained in constant motion throughout the trial), it is likely that their responses

to particular stimuli were impacted by their distances from the source (evidenced by the significantly positive correlation between distance and ventilation that was discussed previously). More specifically, animals that remained closer to the source experienced larger particle displacements then the ones that remained at further distances. All things considered, this simply means that the particle-displacement sensitivity threshold for *Nautilus* is probably much lower than the actual values reported here and does not preclude the fact that *Nautilus* do demonstrate a behavioral response to vibratory signals.

4.0 General Conclusions and Future Considerations

The most challenging aspect of this research that I encountered was effectively interpreting the results from the animal's perspective. Anthropomorphic bias often precludes researchers from depicting an accurate picture of the system in question, and statistical evidence, although present, may not always be relevant. It is quite difficult if not impossible to actually see the situation from the animal's point of view, simply because we are not the animal. The situation is exacerbated when little information exists pertaining to the lifestyles of the model organism, as is the case with the Chambered *Nautilus*. Although *Nautilus* are far from neglected in a research sense, little in the way of data gathered in a wild or natural setting exists. The absence of these data made it difficult to speculate on the behavioral relevance of the conclusions of these experiments. Nonetheless, potential evolutionary benefits do exist and further research should focus on examining these possibilities within a natural setting.

The experiments described in this thesis were aimed at further defining the sensory capabilities of the animal; capabilities that had previously been dismissed. In light of the results, I feel that it can be said with confidence that these animals possess the necessary components to clearly detect and respond to vibrational stimuli by processing environmental signals and then acting on that information as evidenced by a behavioral response. I also believe that further research into the unique anatomy of their statocyst is warranted; more specifically, Kölliker's canal and the epidermal pore that links it to the exterior and the role it may play in defining an animal's response to angular accelerations. Admittedly, this research is not exhaustive and

falls short of defining sensitivity thresholds accurately. This is merely the first step in what will hopefully be a multi-discipline research effort focused on delineating the extent of this mechanosensory ability.

The proximate mechanisms of this system are yet to be defined and would benefit greatly from physiological and neurological experimentation. Many behavioral questions have arisen as a result of this research and further investigation into the applications of this system in natural settings need to be conducted. Initially, when these experiments were conceived, I proposed a third experiment that would incorporate the methodologies of both the Angular Acceleration Experiment and the Vibration Sensitivity Experiments in order to determine if Kölliker's canal also contributed to the reception of waterborne vibrations. Eventually, after evaluating the results of the first two experiments, it became evident that a third experiment was unwarranted. This decision was based mostly on the unconvincing results obtained during the Angular Accelerations Experiment and the uncertainty of the extent of the impact, if any, that Kölliker's canal has on the system. A similar argument can be made based on the results of the Vibration Experiments for which precise sensitivity thresholds for both source-displacement and stimulus velocity were not able to be defined. In the future, a more effective way of accurately determining those ranges would be to keep the animal stationary and perhaps to incorporate some more sophisticated equipment such as hydrophones and signal processing software. Animal restraint was intentionally avoided considering the exploratory nature of the research and having no established behavioral baseline. By incorporating these additional techniques and attracting the interests of other areas of expertise, advances

can be made in truly defining the limitations of these creatures; advances that may not only shed light on their past, but possibly contribute to their conservation and ensure their survival for another few hundred million years to come.

As an additional and final note, another discovery concerning *Nautilus* anatomy was made that, to this author's knowledge, has not been reported in the literature thus far. While reviewing the video data collected during the Angular Acceleration Experiment, we discovered that nautiluses have two sets of hyponome configurations. As explained previously, the hyponome of a *Nautilus* is completely flexible as it is made from overlapping mantle tissue. Interestingly, the overlap itself can begin from either the left or right side of the animal and it varies between animals (refer to Fig. 2.2 for an example of an animal with a right overlap). Initially, this anatomical incongruity seemed like a plausible explanation as to why nautiluses demonstrated lateral positional preferences when exposed to control conditions but, after attempting to correlate this finding with the experimental results, no conclusive determinations could be made. A sex specific hypothesis was also posed to account for the variation. That hypothesis was ultimately rejected after no significant relationship between sex and hyponome overlap could be established. Although there is no explanation as to why such a configuration exists, a seemingly inconspicuous clue like this may lead to many larger discoveries, reaffirming the importance of conducting future work in this field.

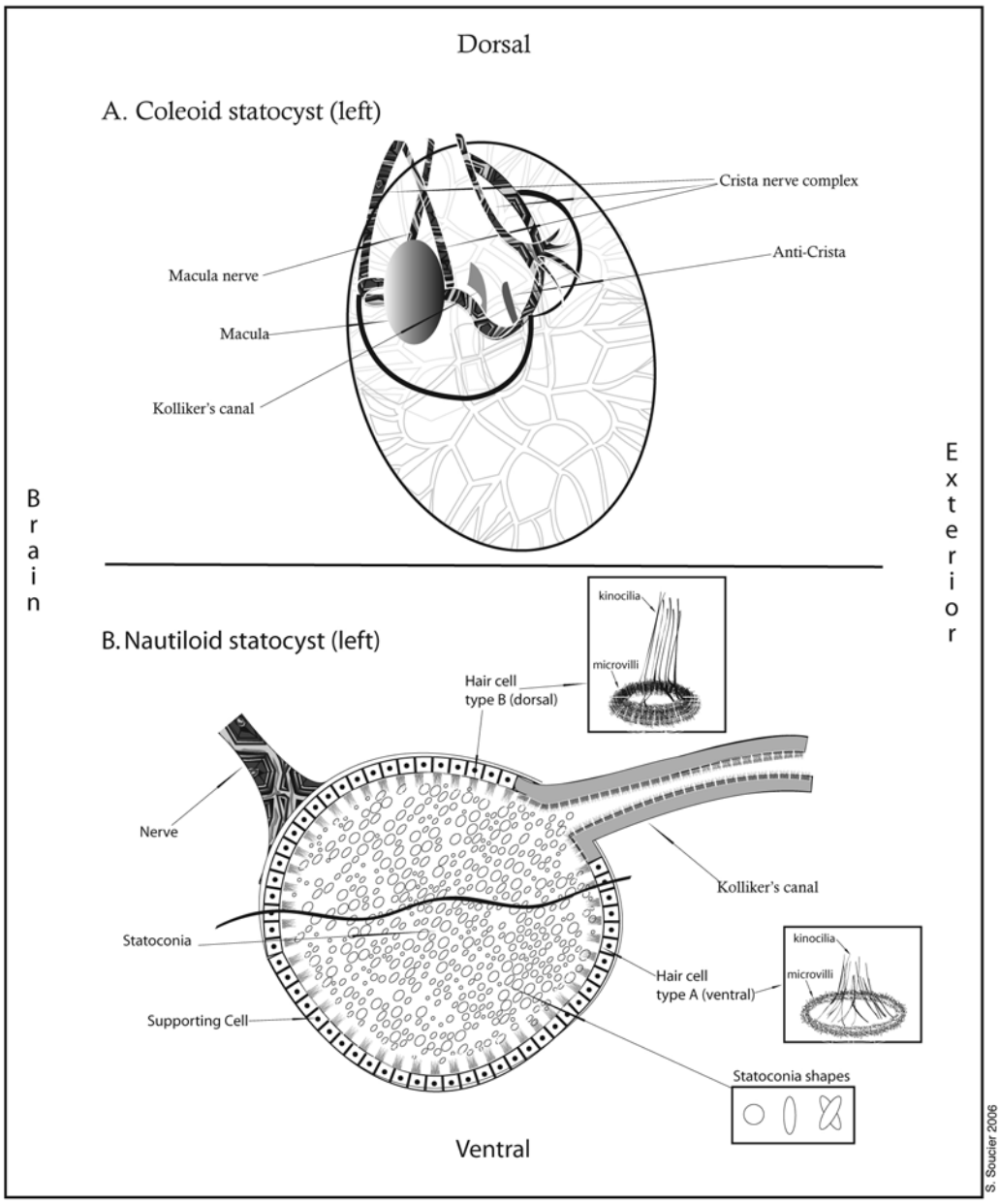

Figure 1.1. (A) Anterior view of a coleoid statocyst (*Octopus vulgaris*) depicting the macula and crista systems that are absent in *Nautilus*. (B) Anterior view of a *Nautilus* statocyst and the extension of Kölliker's canal to the exterior. Wavy line is an approximate demarcation of dorsal/ventral split (figure not to scale).

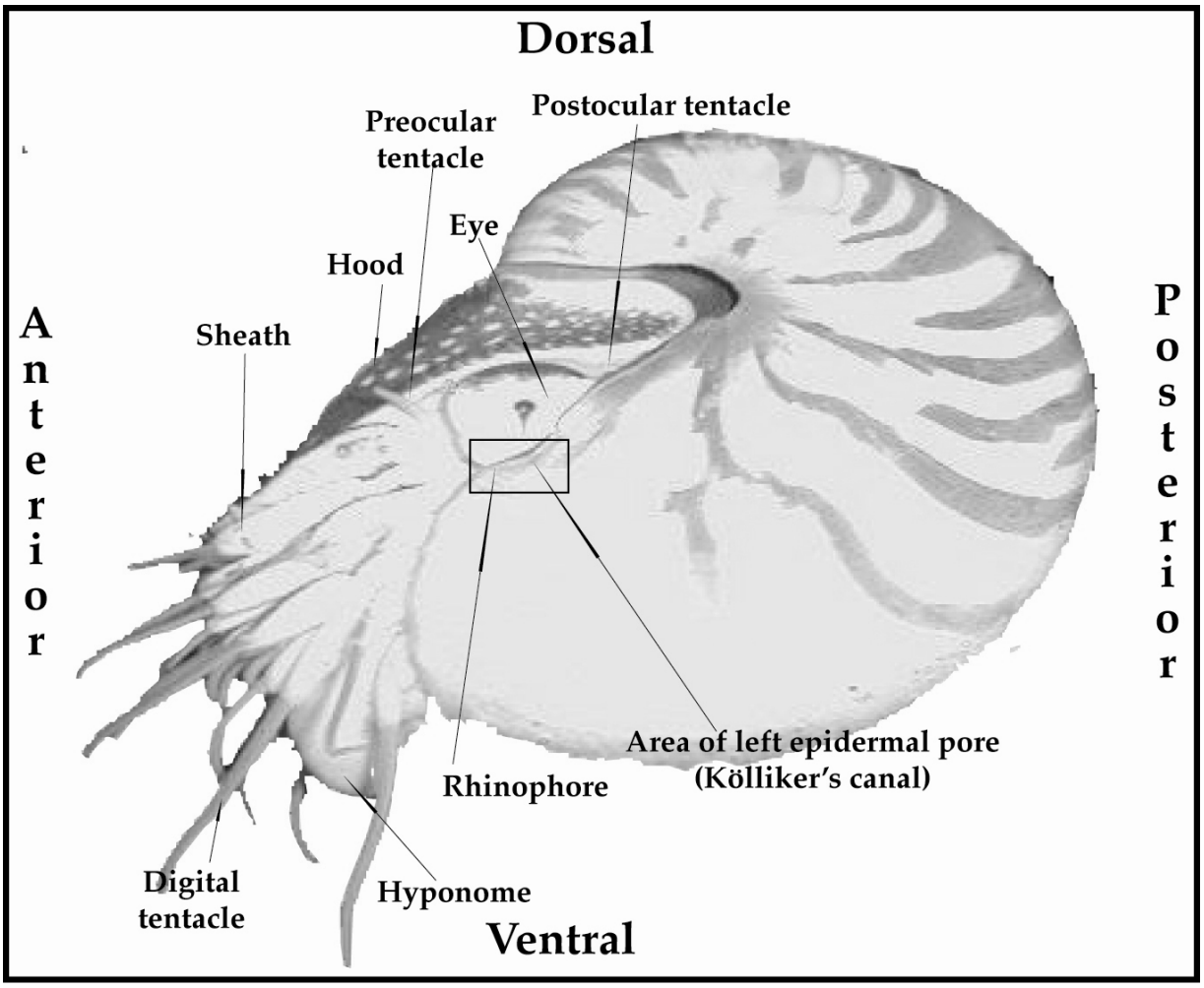

Figure 1.2. Lateral view of *Nautilus* depicting various external components with emphasis on the location of the epidermal pore that connects Kölliker's canal with the left statocyst.

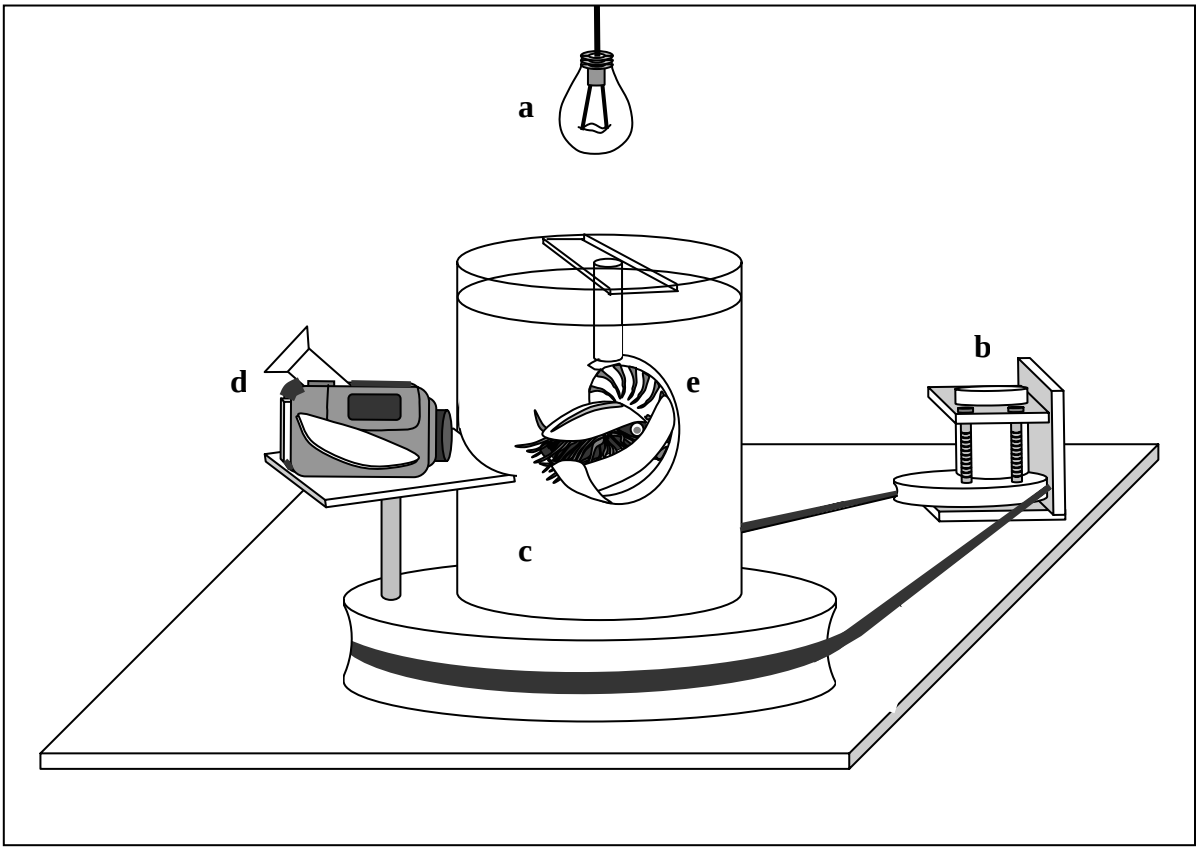

Figure 2.1. Figure 2.1 is a schematic of the angular acceleration experimental apparatus; a.k.a. The SpinMaster. Components are listed as follows: a) 20-watt lamp, b) reversible motor with pulley, c) cylindrical tank with pulley, d) camera platform and camera, and e) animal harness.

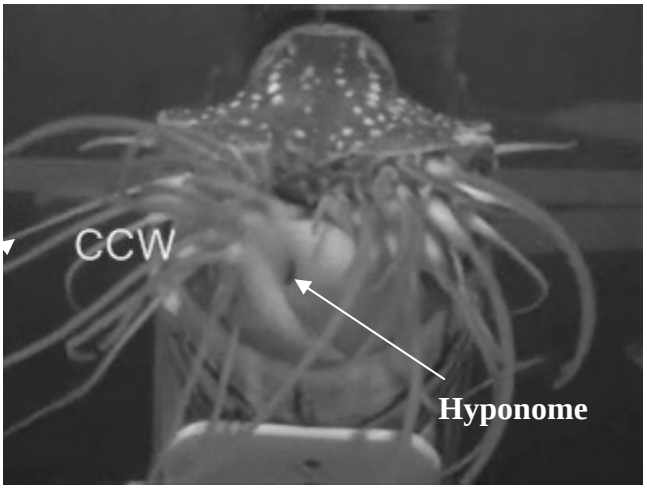

Figure 2.2. Figure 2.2 is an image of an experimental animal extracted from video that shows the position of the hyponome (right-handed) during a counter clockwise rotation. The arrow approximately indicates the corresponding coordinates of measure for this frame.

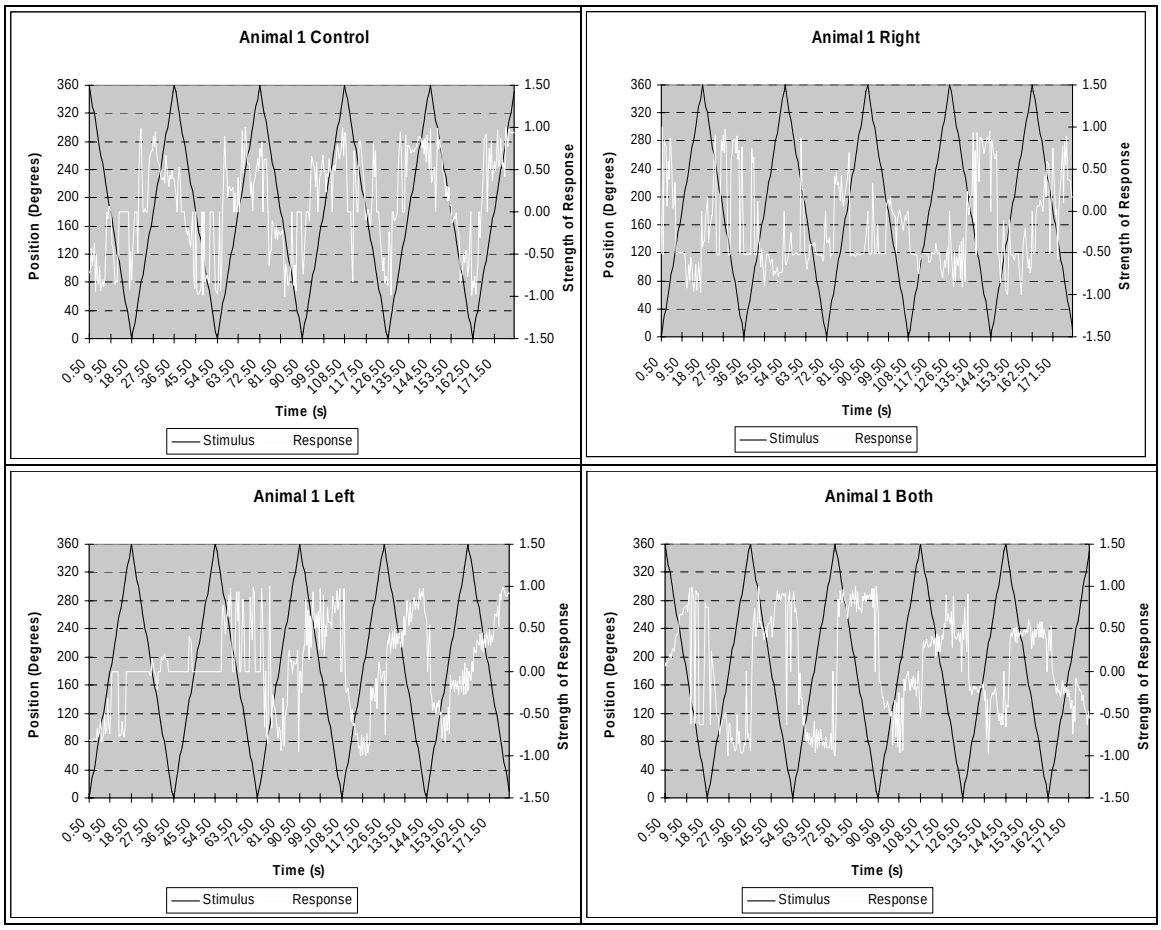

Figure 2.3. Animal 1. Hyponome position in respect to a rotating stimulus for different blockage treatments. Increasing position values (0–360°) indicate a CCW rotation whereas decreasing values (360–0°) reflect a CW rotation. (+) Response values indicate hyponome positioning to the animal's left whereas (-) values indicate hyponome positioning to the animal's right. Compensatory responses are seen when the values of both variables are synchronized with respect to time.

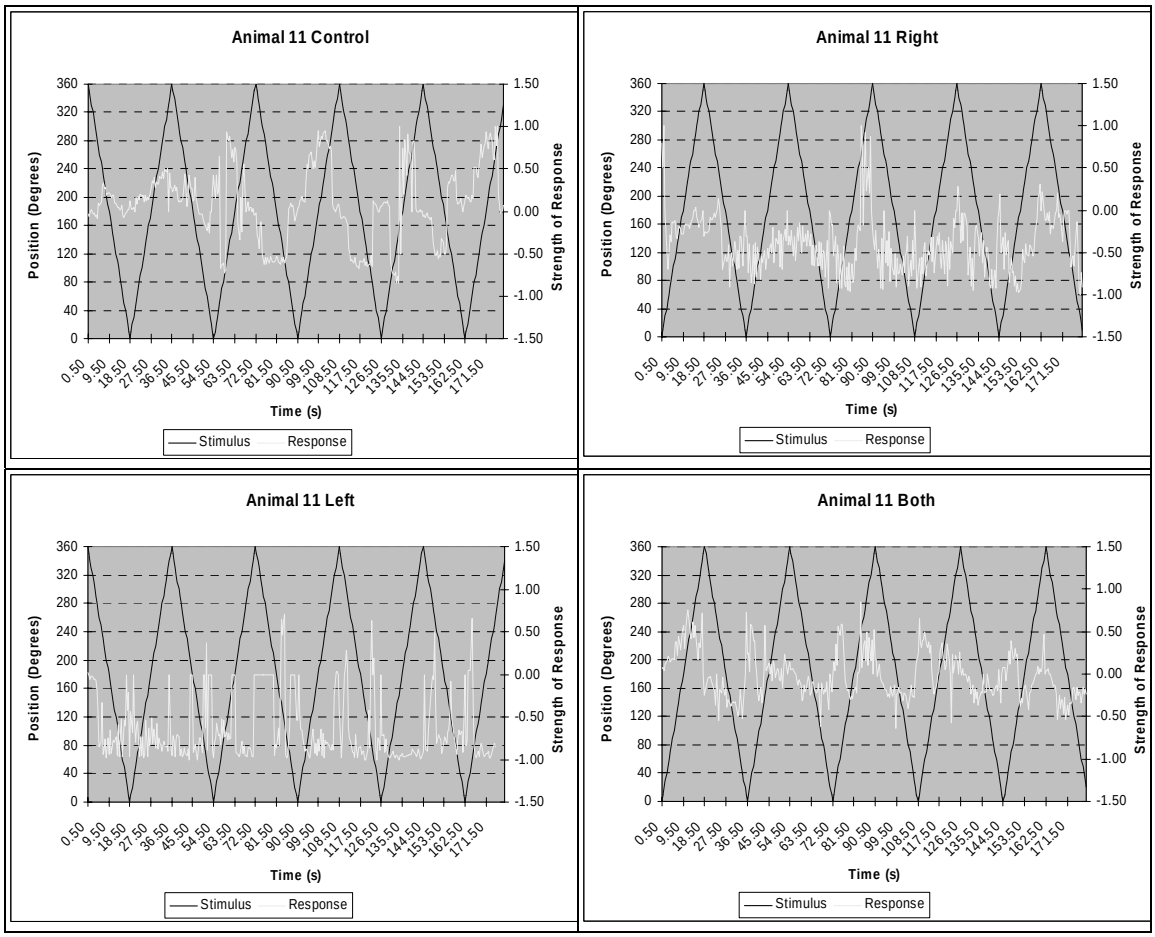

Figure 2.4. Animal 11. Hyponome position in respect to a rotating stimulus for different blockage treatments. Increasing position values (0–360°) indicate a CCW rotation whereas decreasing values (360–0°) reflect a CW rotation. (+) Response values indicate hyponome positioning to the animal's left whereas (-) values indicate hyponome positioning to the animal's right. Compensatory responses are seen when the values of both variables are synchronized with respect to time.

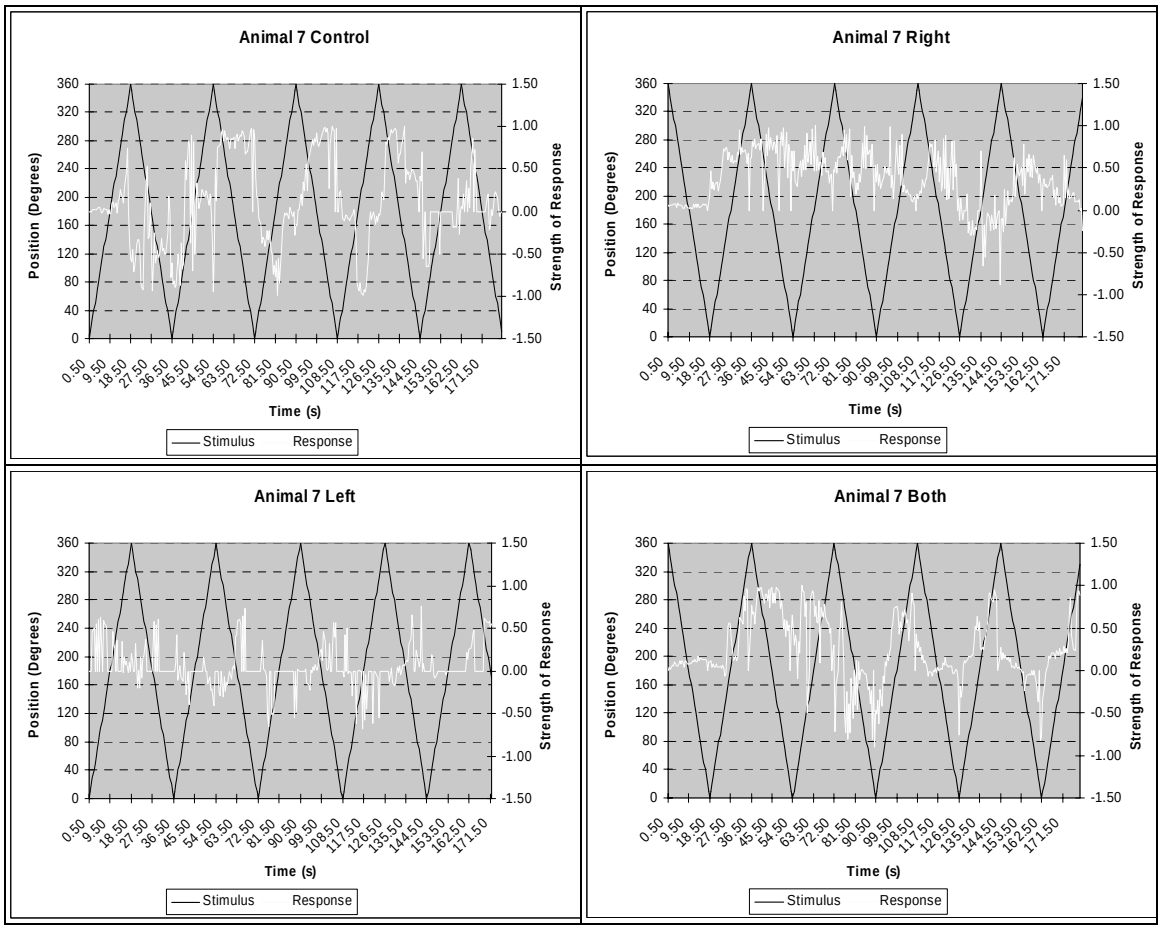

Figure 2.5. Animal 7. Hyponome position in respect to a rotating stimulus for different blockage treatments. Increasing position values (0–360°) indicate a CCW rotation whereas decreasing values (360–0°) reflect a CW rotation. (+) Response values indicate hyponome positioning to the animal's left whereas (-) values indicate hyponome positioning to the animal's right. Compensatory responses are seen when the values of both variables are synchronized with respect to time.

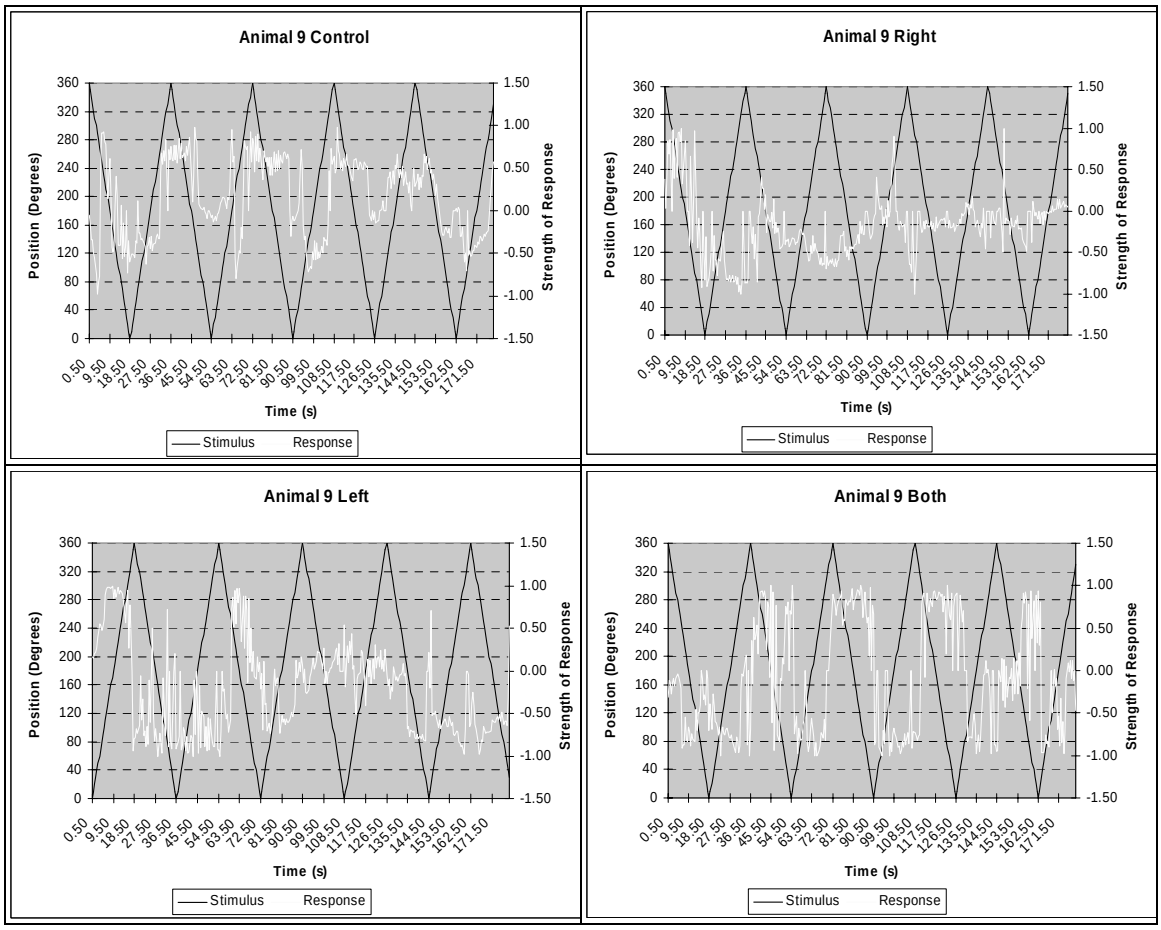

Figure 2.6. Animal 9. Hyponome position in respect to a rotating stimulus for different blockage treatments. Increasing position values (0–360°) indicate a CCW rotation whereas decreasing values (360–0°) reflect a CW rotation. (+) Response values indicate hyponome positioning to the animal's left whereas (-) values indicate hyponome positioning to the animal's right. Compensatory responses are seen when the values of both variables are synchronized with respect to time.

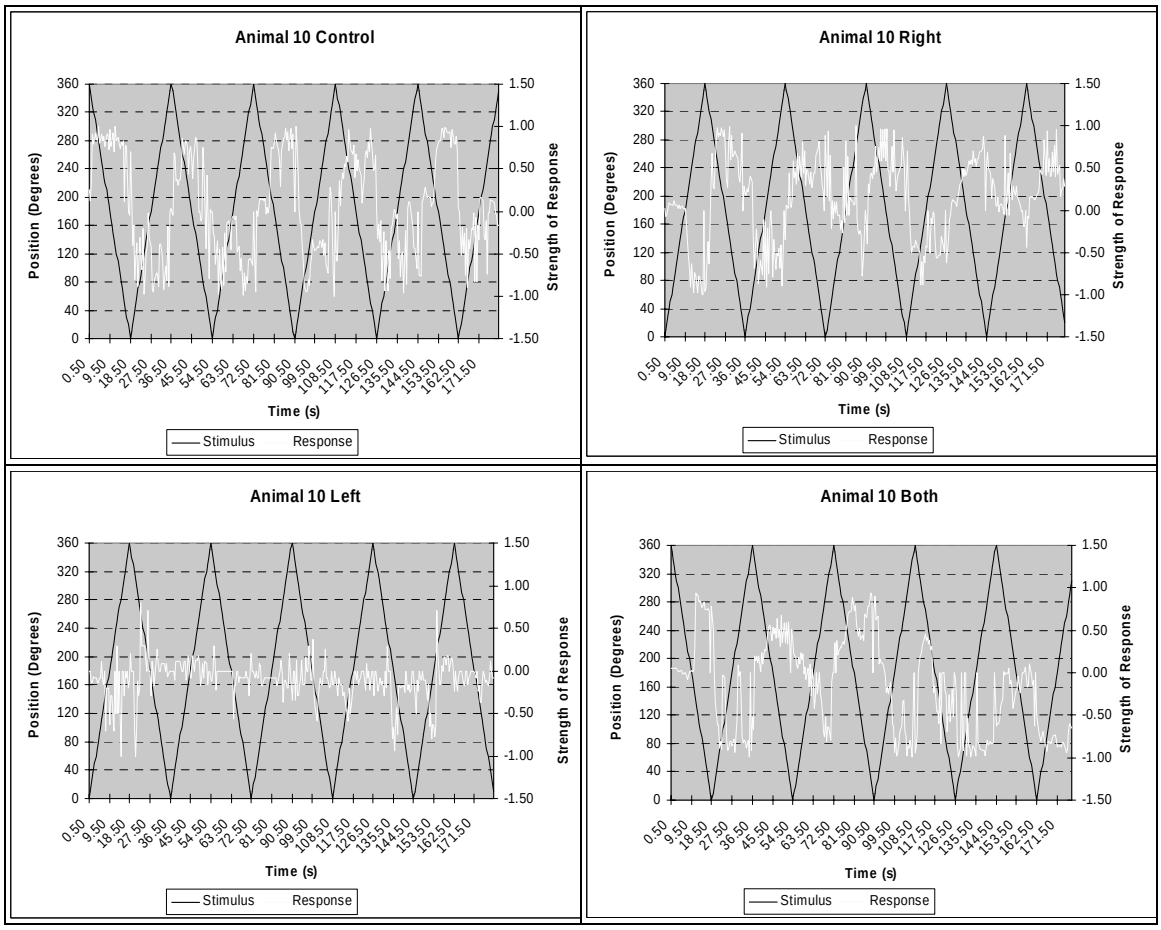

Figure 2.7. Animal 10. Hyponome position in respect to a rotating stimulus for different blockage treatments. Increasing position values (0–360°) indicate a CCW rotation whereas decreasing values (360–0°) reflect a CW rotation. (+) Response values indicate hyponome positioning to the animal's left whereas (-) values indicate hyponome positioning to the animal's right. Compensatory responses are seen when the values of both variables are synchronized with respect to time.

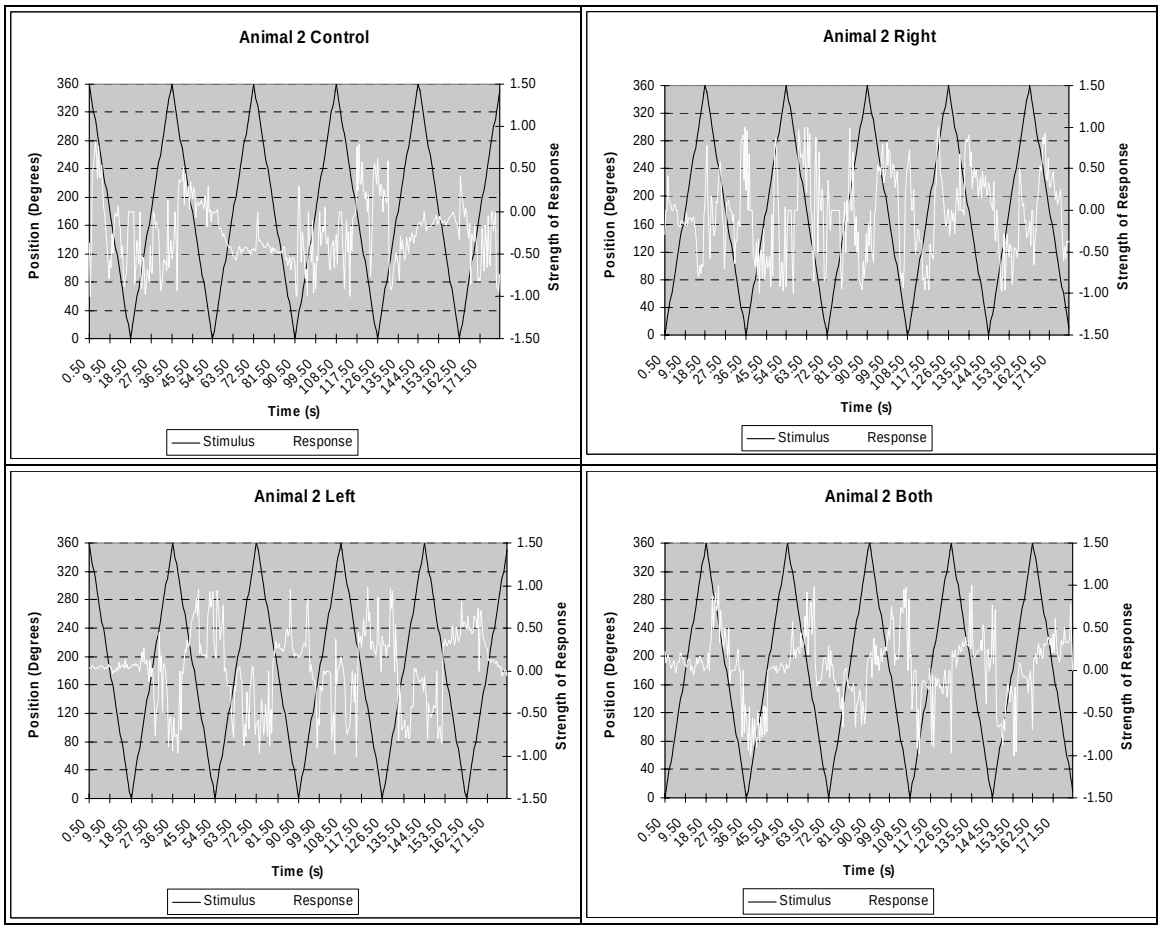

Figure 2.8. Animal 2. Hyponome position in respect to a rotating stimulus for different blockage treatments. Increasing position values (0–360°) indicate a CCW rotation whereas decreasing values (360–0°) reflect a CW rotation. (+) Response values indicate hyponome positioning to the animal's left whereas (-) values indicate hyponome positioning to the animal's right. Compensatory responses are seen when the values of both variables are synchronized with respect to time.

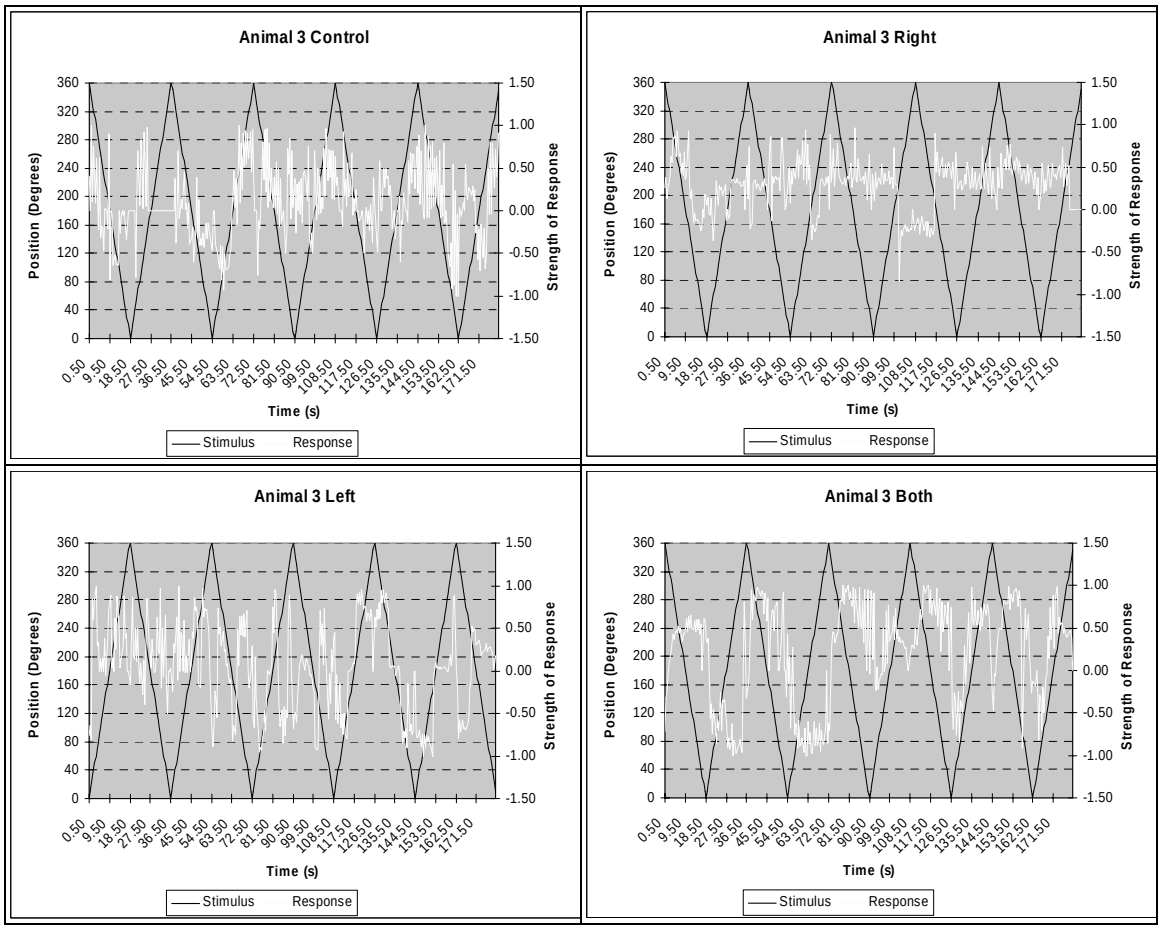

Figure 2.9. Animal 3. Hyponome position in respect to a rotating stimulus for different blockage treatments. Increasing position values (0–360°) indicate a CCW rotation whereas decreasing values (360–0°) reflect a CW rotation. (+) Response values indicate hyponome positioning to the animal's left whereas (-) values indicate hyponome positioning to the animal's right. Compensatory responses are seen when the values of both variables are synchronized with respect to time.

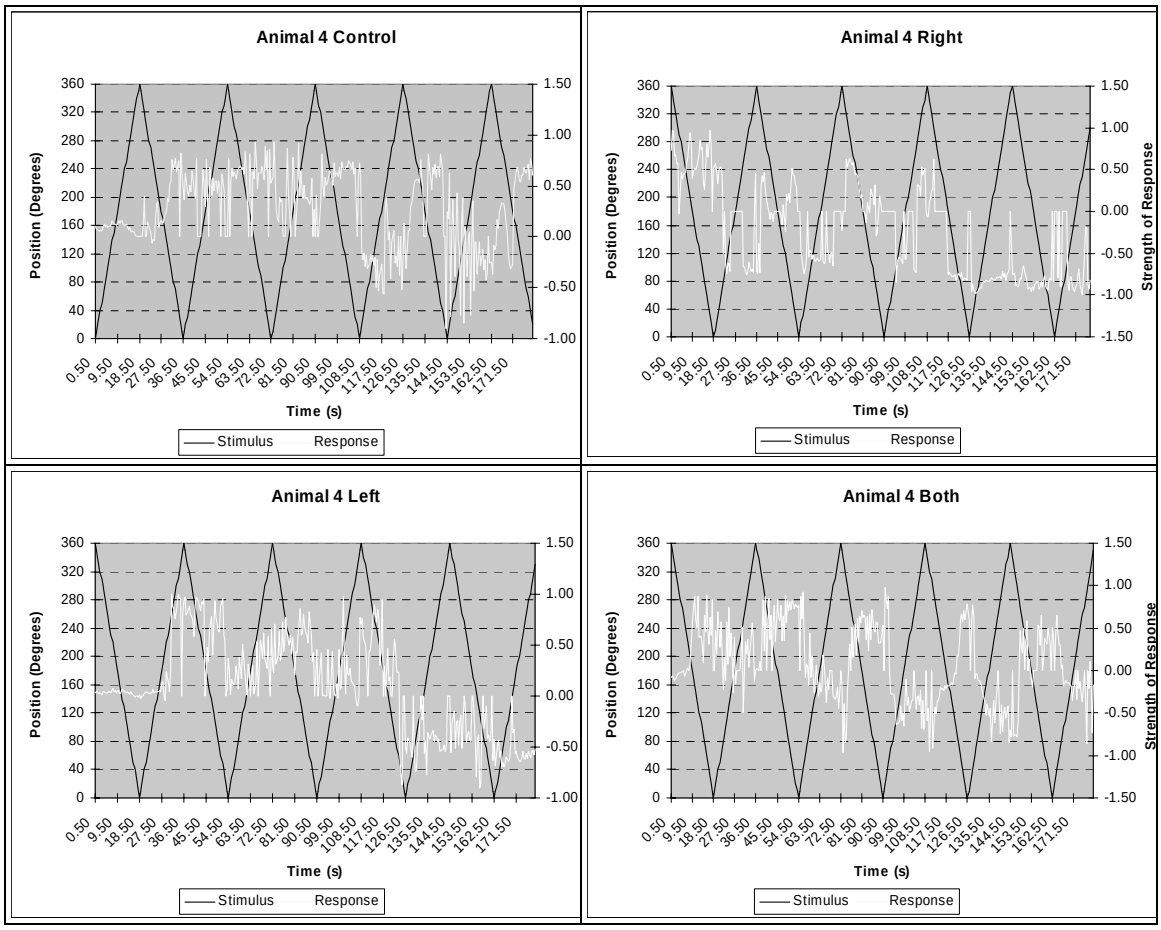

Figure 2.10. Animal 4. Hyponome position in respect to a rotating stimulus for different blockage treatments. Increasing position values (0–360°) indicate a CCW rotation whereas decreasing values (360–0°) reflect a CW rotation. (+) Response values indicate hyponome positioning to the animal's left whereas (-) values indicate hyponome positioning to the animal's right. Compensatory responses are seen when the values of both variables are synchronized with respect to time.

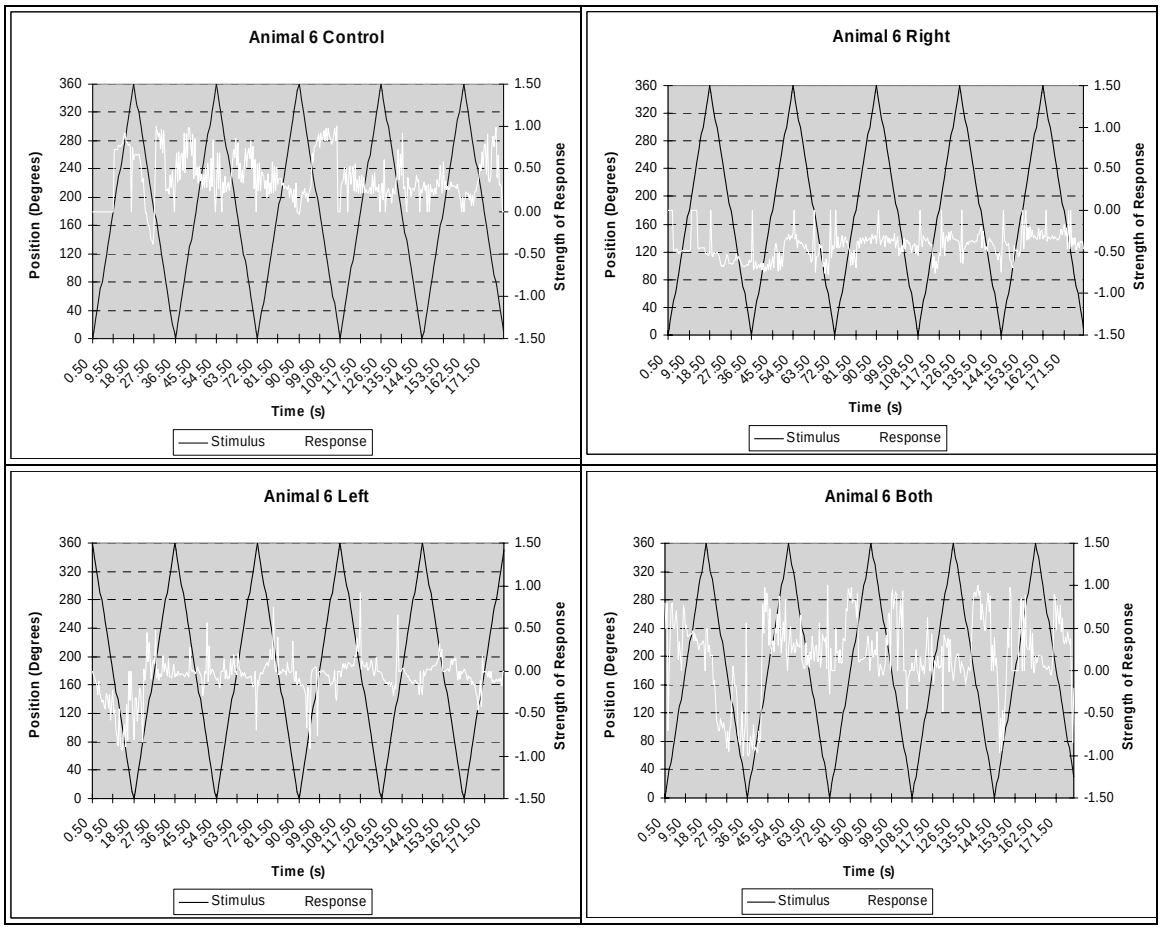

Figure 2.11. Animal 6. Hyponome position in respect to a rotating stimulus for different blockage treatments. Increasing position values (0–360°) indicate a CCW rotation whereas decreasing values (360–0°) reflect a CW rotation. (+) Response values indicate hyponome positioning to the animal's left whereas (-) values indicate hyponome positioning to the animal's right. Compensatory responses are seen when the values of both variables are synchronized with respect to time.

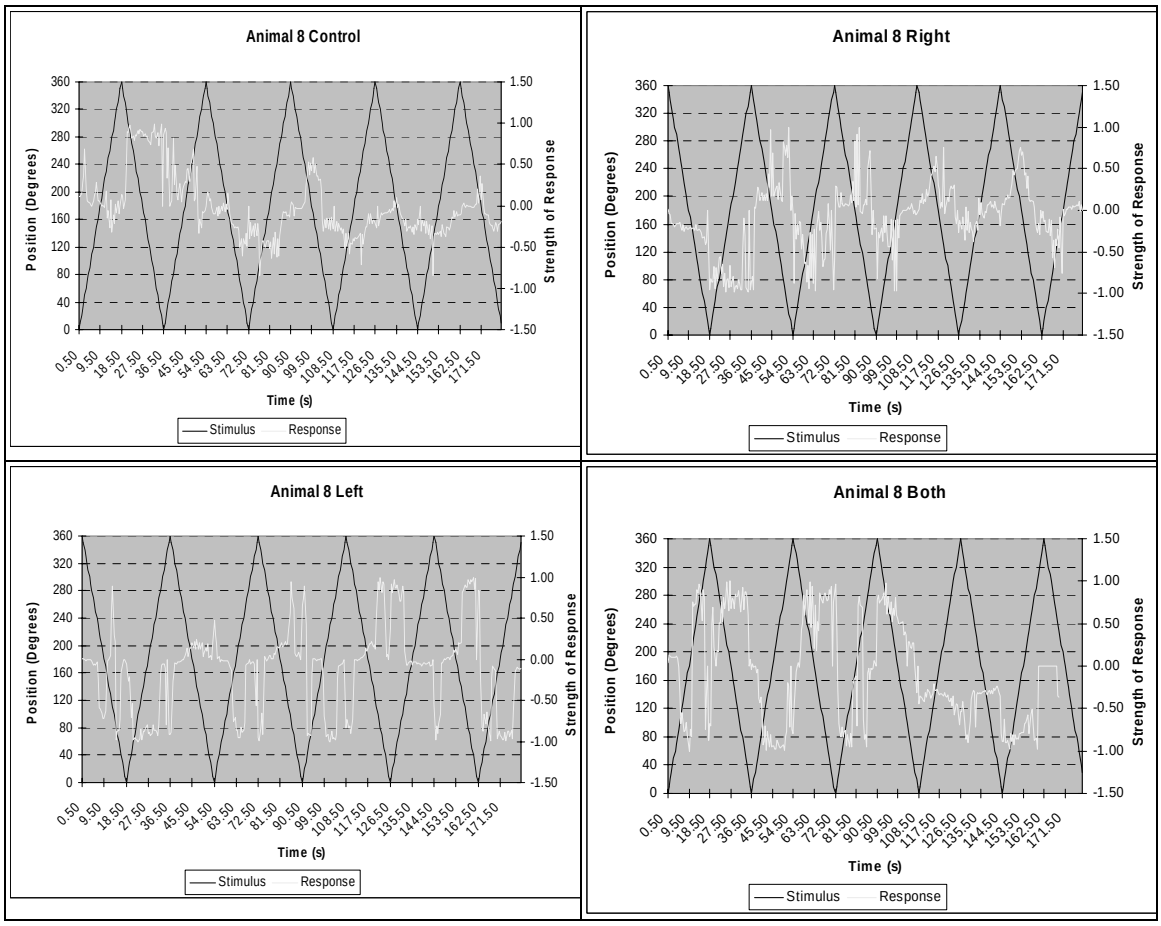

Figure 2.12. Animal 8. Hyponome position in respect to a rotating stimulus for different blockage treatments. Increasing position values (0–360°) indicate a CCW rotation whereas decreasing values (360–0°) reflect a CW rotation. (+) Response values indicate hyponome positioning to the animal's left whereas (-) values indicate hyponome positioning to the animal's right. Compensatory responses are seen when the values of both variables are synchronized with respect to time.

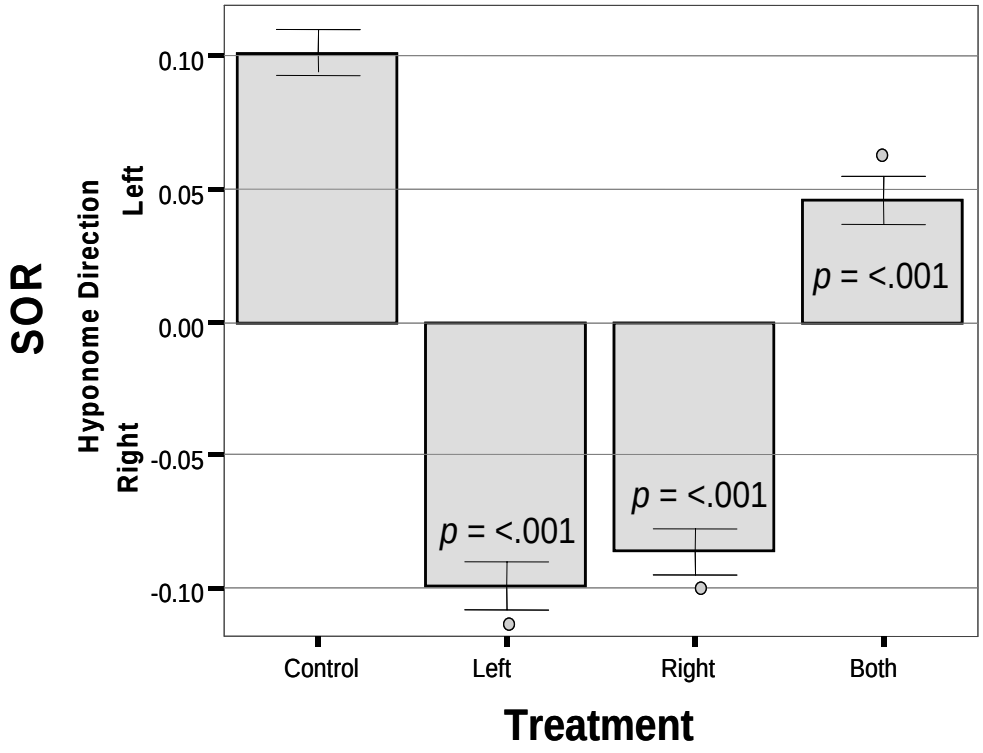

Figure 2.13. Strength of Response (SOR) comparisons for all animals (N = 10) across all treatments. Probability values reflect significant differences of mean SOR between individual blocking treatments and the control.

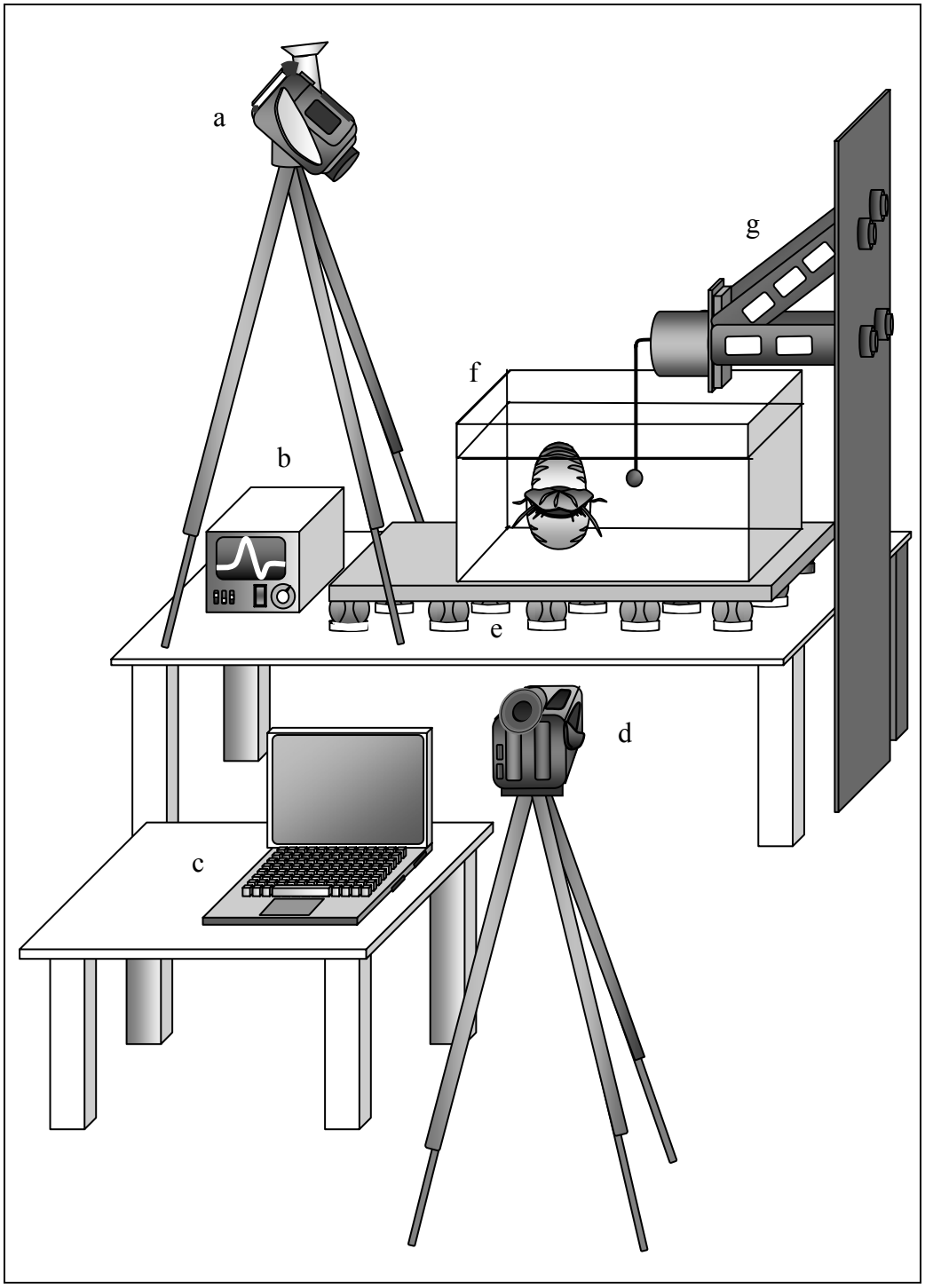

Figure 3.1. Experimental setup for source-displacement experiments: a) top-view camera, b) oscilloscope, c) laptop computer, d) side-view camera, e) vibration absorption table, f) experimental tank with animal, and g) wall mount with mini-shaker and shaft/bead.

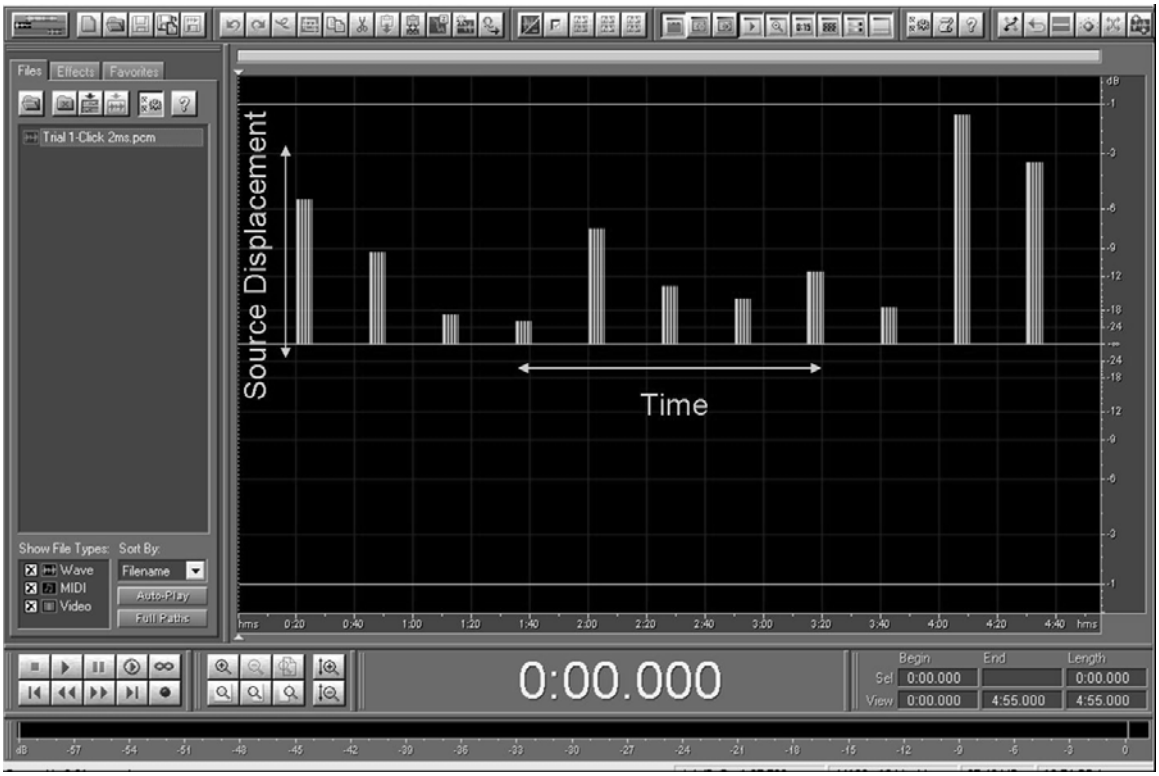

Figure 3.2. Fig. 3.2 is a screenshot of a computer-generated stimulus package that was used in the source-displacement experiments. Each signal is a composition of ten 2ms bursts of equal displacement amplitudes administered over a 5s period. Intervals consisting of 15s of silence were placed between each signal.

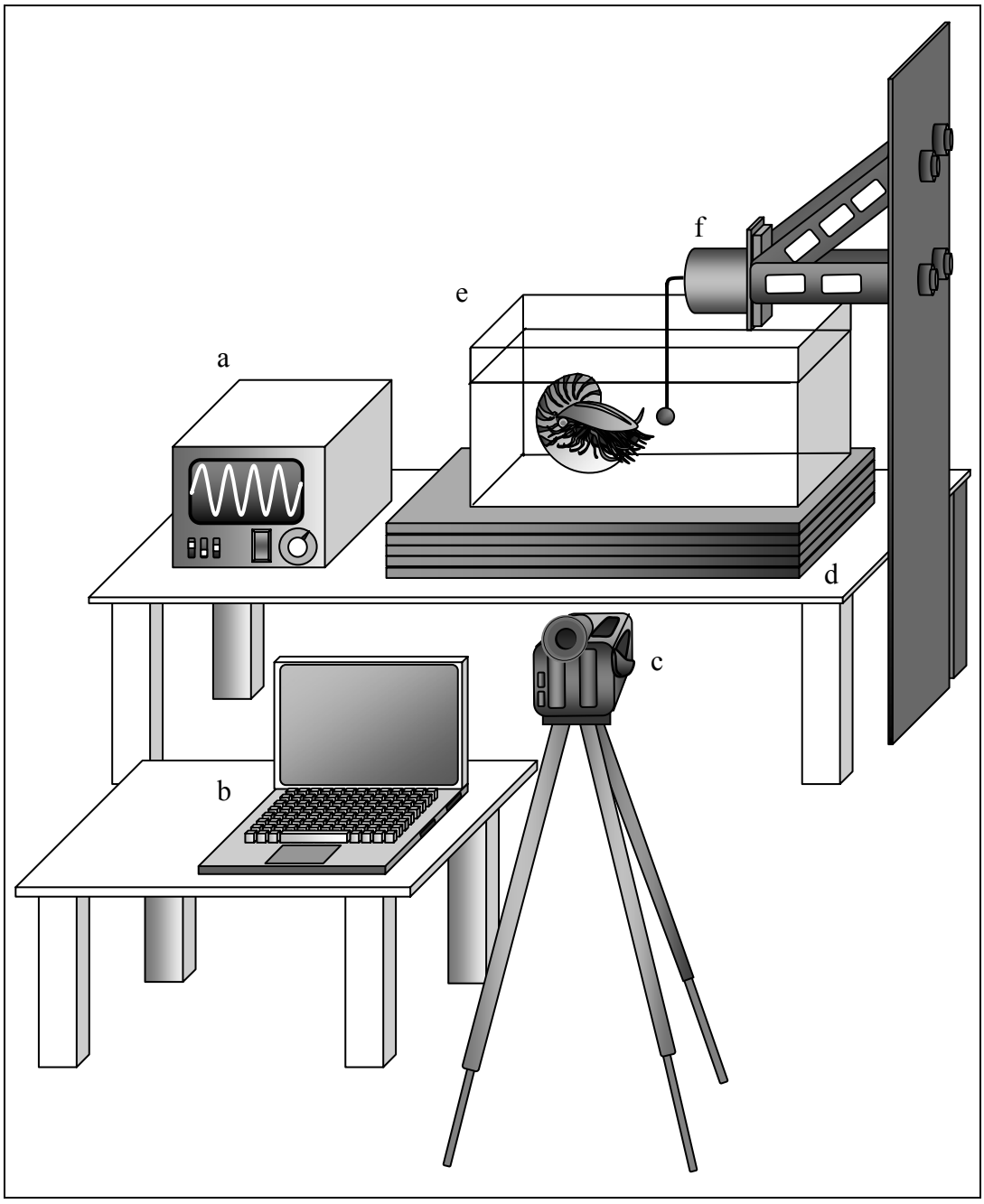

Figure 3.3. Experimental apparatus for frequency sensitivity experiments: a) oscilloscope, b) laptop computer, c) side-view camera, d) foam vibration absorption layer, e) experimental tank with animal, and f) wall mount with mini-shaker and attached shaft/bead.

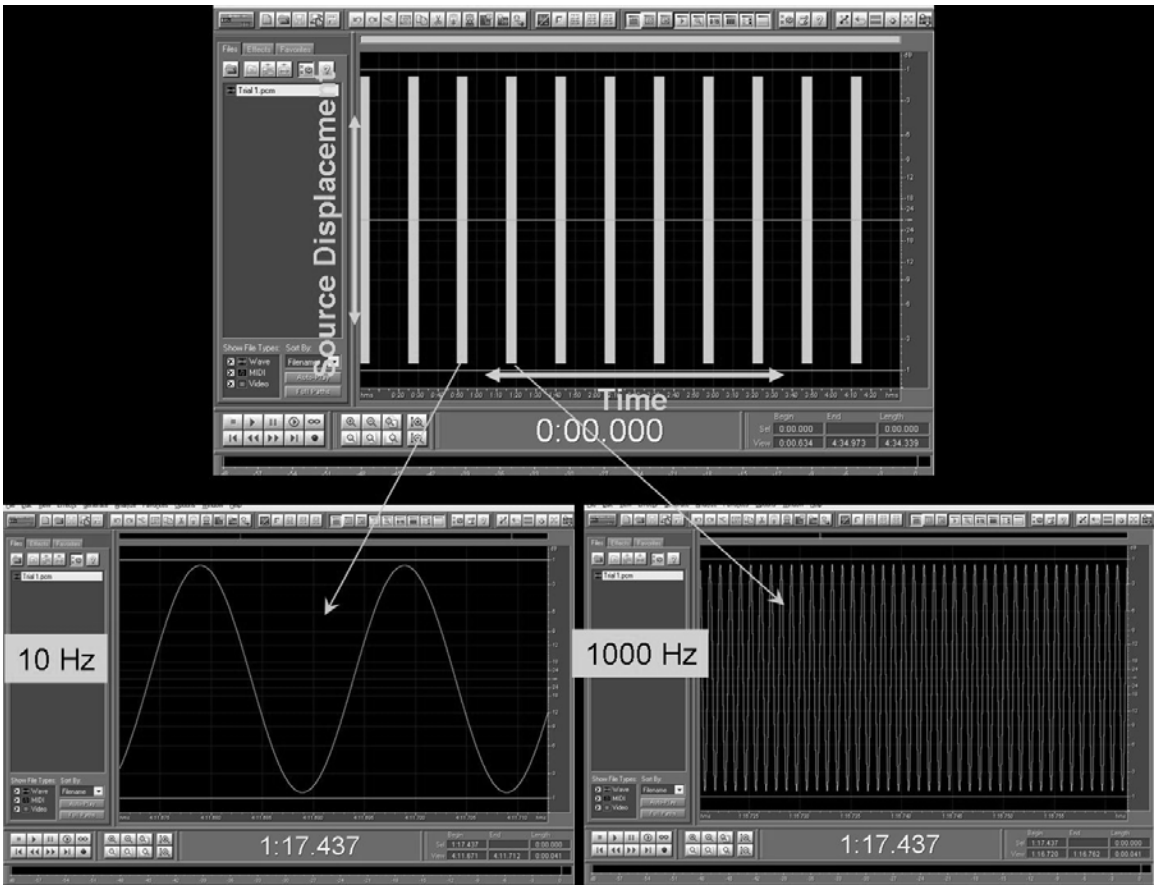

Figure 3.4. Fig. 3.4 is a screen shot of a computer-generated representation of a randomized frequency presentation package (top). Arrows point to the bottom half of the figure that is a comparison between two different frequencies (10Hz and 1000Hz) of the same displacement amplitudes.

Table 3.1. A list of six typical *Nautilus* behaviors, their corresponding index values, and their levels of measurement that were intended to be used in statistical analysis. Ventilation rate proved to be the only observable behavior and was therefore the only behavior that was incorporated into the analysis.

Behavior	**Index Score**		**Level of Measurement (Scale)**
Ventilation Rate	Frequency		Interval
Rocking	Yes = 1	No = 0	Nominal
Touch Bottom	Yes =1	No = 0	Nominal
Cat's Whiskers	Yes = 1	No = 0	Nominal
Movement	Yes = 1	No = 0	Ordinal
a. Towards	Yes = 2		
b. Away from	Yes = -2		
c. None	None = 0		
Tentacle	Yes = 1	No = 0	Ordinal
a. <1/3 Body	Yes = 2		
b. >1/3 Body	Yes = -2		

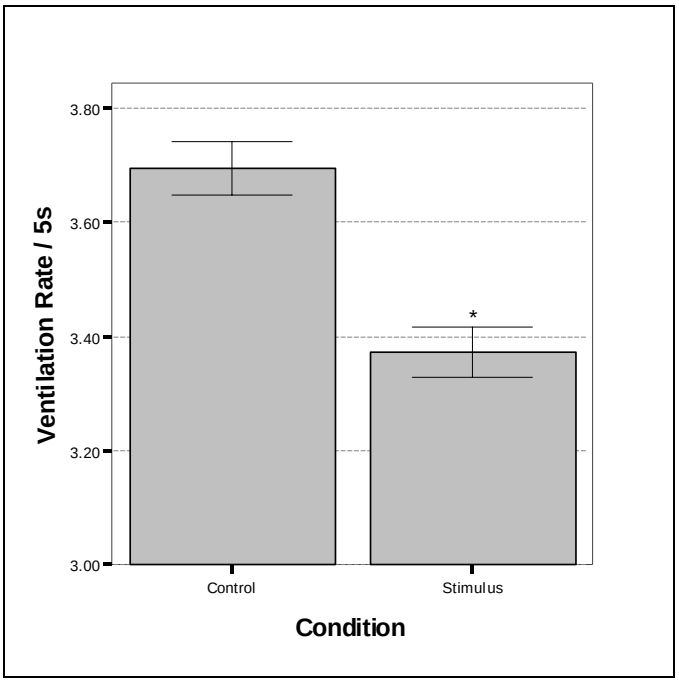

Figure 3.5. Bar graph depicts mean ventilation rates / 5s between control and stimulus treatments for all three experiments (N = 20). The asterisk indicates a significant difference from the control treatment. Error bars show mean ± 1.0 SE.

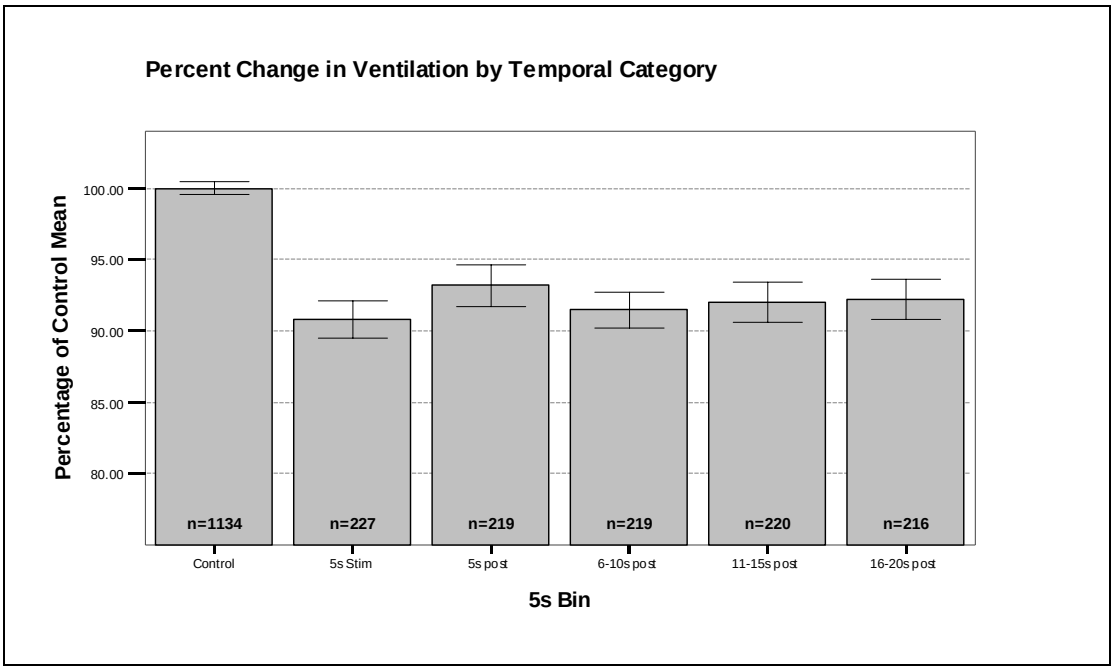

Figure 3.6. Bar graph depicts the average percent change in ventilation from the control to five stimulus and post-stimulus time categories. Each bin, except for the control, represents a 5s period of time that begins with the presentation of the stimuli and continues for 20s post-stimuli period. N = the number of 5s bins that were included in each category. Significant decreases between the control and stimuli bins were found for each of the five time categories. Error bars show mean ± 1.0 SE.

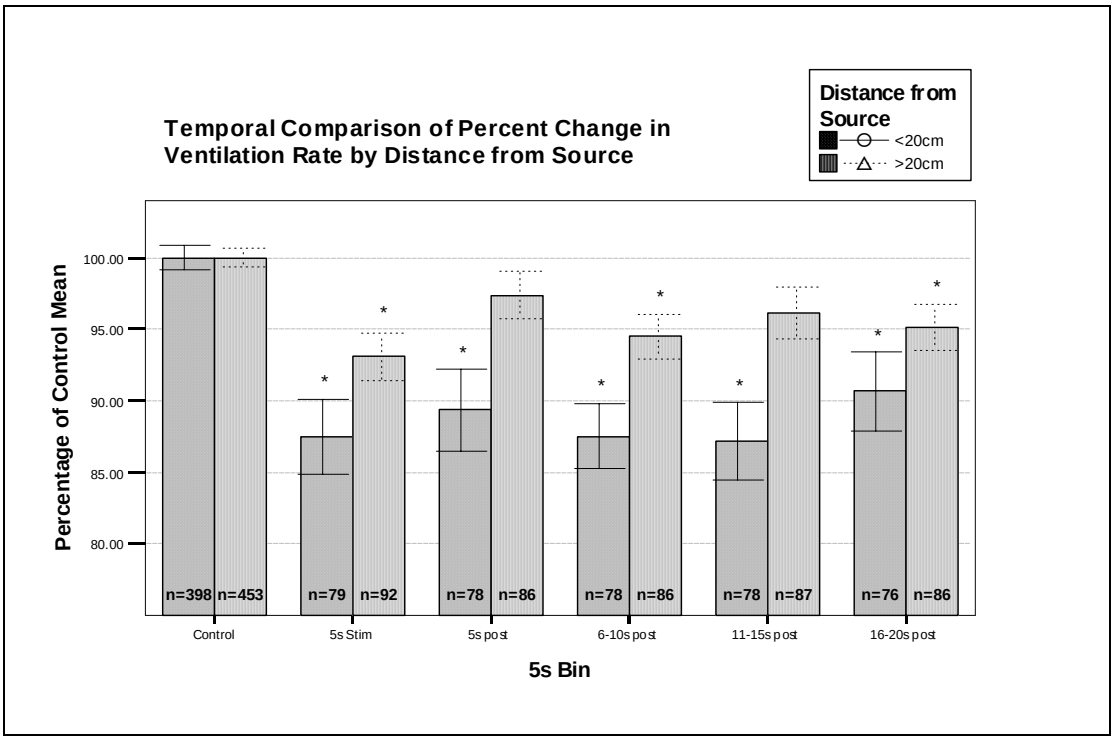

Figure 3.7. Bar graph depicts the percent change in ventilation/5s from the control for two distance categories over time. Each bin, except for the control, represents a 5s period of time that begins with the presentation of the stimulus and continues for 20s post-stimuli period (seven trials were included in the analysis). Significant decreases between the control and stimuli bins (marked by asterisks) were found for each of the <20cm categories and for the 5s Stimulus, 6–10s post-stimulus, and 16–20s post-stimulus categories (eight trials were included in the analysis). Error bars show mean ± 1.0 SE.

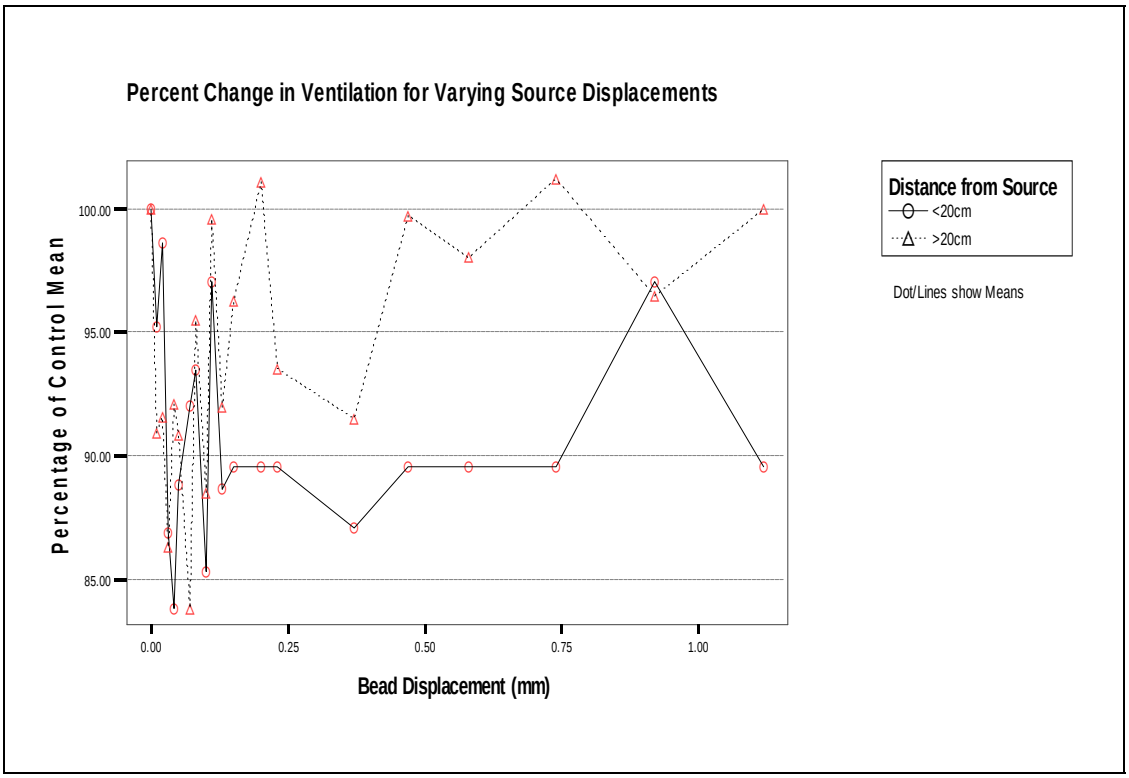

Figure 3.8. Figure 3.8 depicts the impact of the distance the animal is from the source on ventilation rate. Data shown is from two experiments, SSDE and LSDE, and accounts for 10 trials. Bead displacement refers to the distance traveled by the leading edge of the bead and does not include bead diameter.

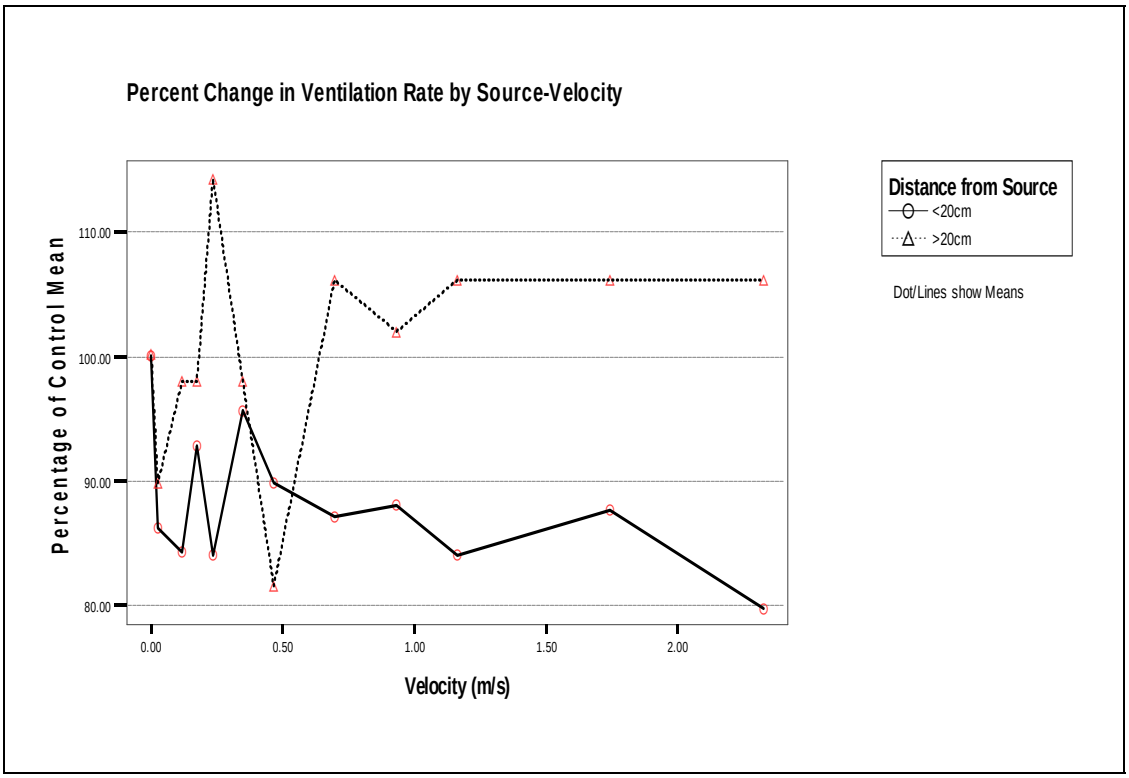

Figure 3.9. Figure 3.9 shows the percent change in ventilation across five animals after exposure to randomized source velocities (N= 4 for the <20cm of the source and N = 1 for the >20cm). Significant decreases in ventilation from the control (0.00 m/s) were identified for 0.2 and 2.32m/s.

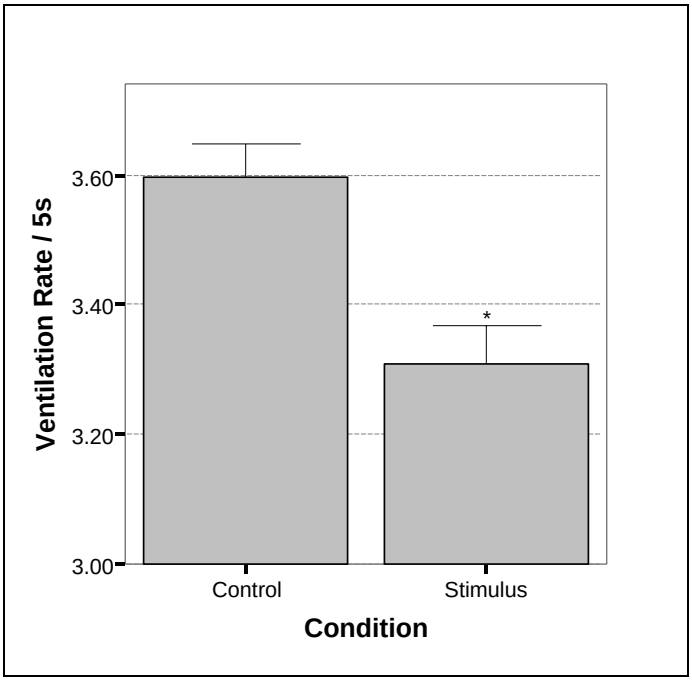

Figure 3.10. Bar graph depicts mean ventilation rates / 5s between control and stimulus treatments for all SSDE trials. The asterisk indicates a significant difference from the control treatment. Error bars show mean ± 1.0 SE.

Table 3.2. Table 3.2 lists changes in ventilation rate (VR) from the control mean for each stimulus and post-stimulus time bin according to three different experiments. Probability values are also given and maximum percentage values are bolded for each experiment.

	Bin	*p* value	% VR change	Bin	*p* value	% VR change
SSDE	**<20cm (N = 2)**			**>20cm (N = 3)**		
	5s stim	**<.001**	**-15.7**	**5s stim**	**<.001**	**-14.6**
	5s post	0.002	-10.1	5s post		-7.6
	6-10s post	<.001	-11.3	6-10s post	0.021	-9.2
	11-15s post	0.002	-10.1	11-15s post		-6.1
	16-20s post		-4.2	16-20s post	0.005	-11.2
LSDE	**<20cm (N = 1)**			**>20cm (N = 4)**		
	5s stim	0.004	-16.1	5s stim		0
	5s post		4.1	5s post		0.4
	6-10s post	**<.001**	**-22.1**	6-10s post	0.018	-4.3
	11-15s post		-8.5	**11-15s post**	**0.005**	**-5.1**
	16-20s post		-5.1	16-20s post		-2.3
FSDE	**<20cm (N = 4)**			**>20cm (N = 1)**		
	5s stim		-9.8	**5s stim**		**-11.1**
	5s post	0.02	-14.8	5s post		0.2
	6-10s post		-10.6	6-10s post		0.2
	11-15s post	**0.02**	**-15.3**	11-15s post		7.4
	16-20s post	0.025	-13.2	16-20s post		4.9

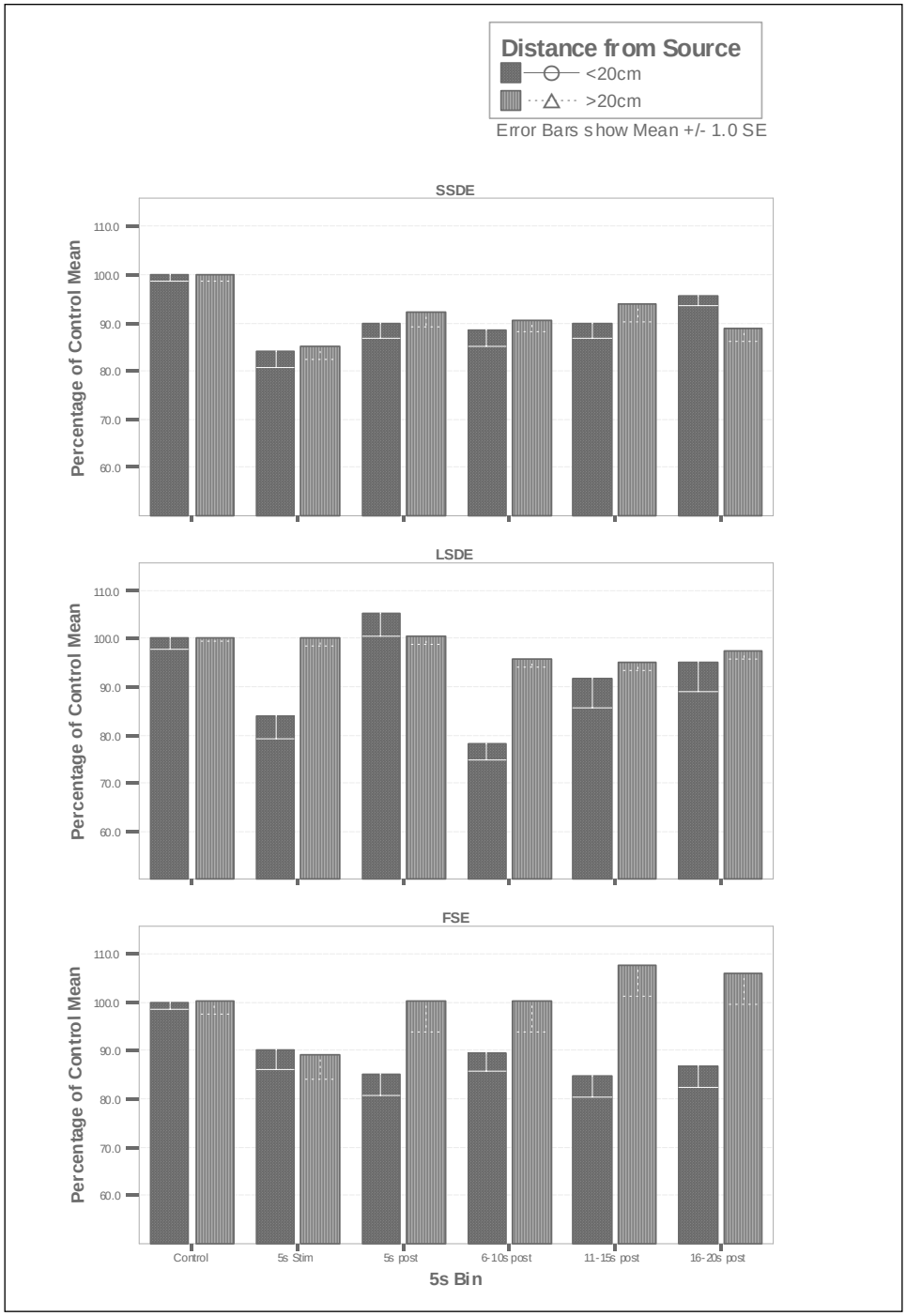

Figure 3.11. Figure 3.11 compares ventilation responses to different stimulus and post-stimulus bins at different distances for each of three experiments.

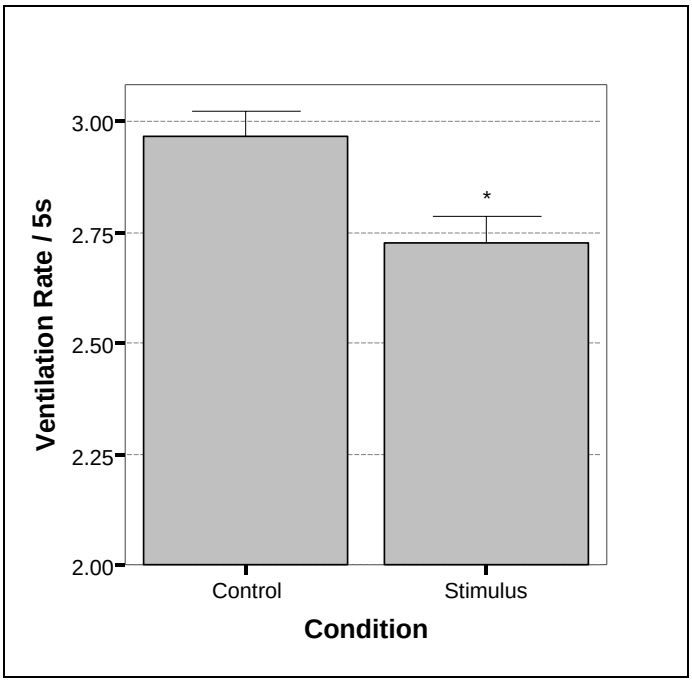

Figure 3.12. Bar graph depicts mean ventilation rates / 5s between control and stimulus treatments for animal 2. The asterisk indicates a significant difference from the control treatment. Error bars show mean ± 1.0 SE.

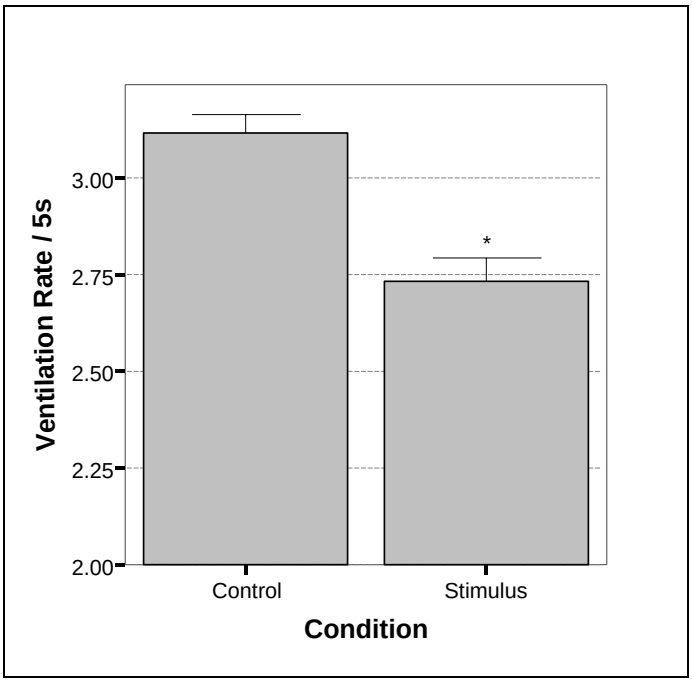

Figure 3.13. Bar graph depicts mean ventilation rates / 5s between control and stimulus treatments for animal 7. The asterisk indicates a significant difference from the control treatment. Error bars show mean ± 1.0 SE.

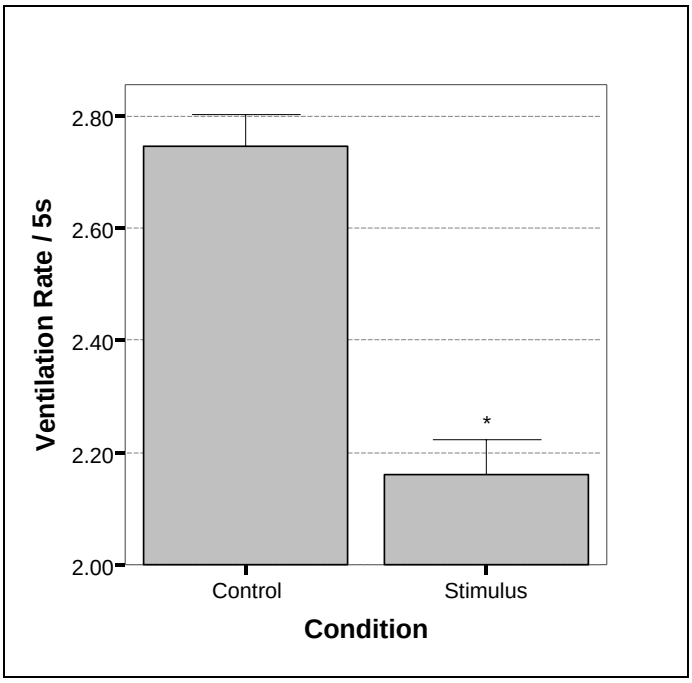

Figure 3.14. Bar graph depicts mean ventilation rates / 5s between control and stimulus treatments for animal 9. The asterisk indicates a significant difference from the control treatment. Error bars show mean ± 1.0 SE.

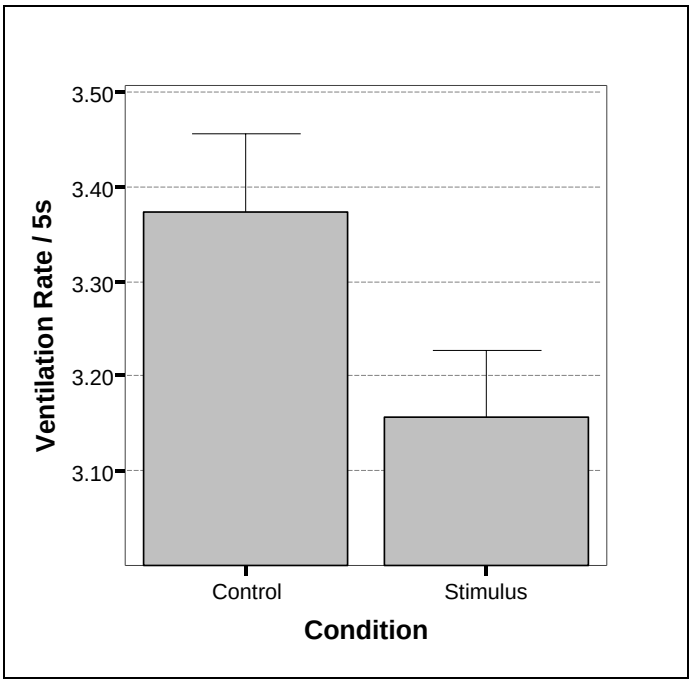

Figure 3.15. Bar graph depicts mean ventilation rates / 5s between control and stimulus treatments for animal 5. No significant difference from the control treatment was found. Error bars show mean ± 1.0 SE.

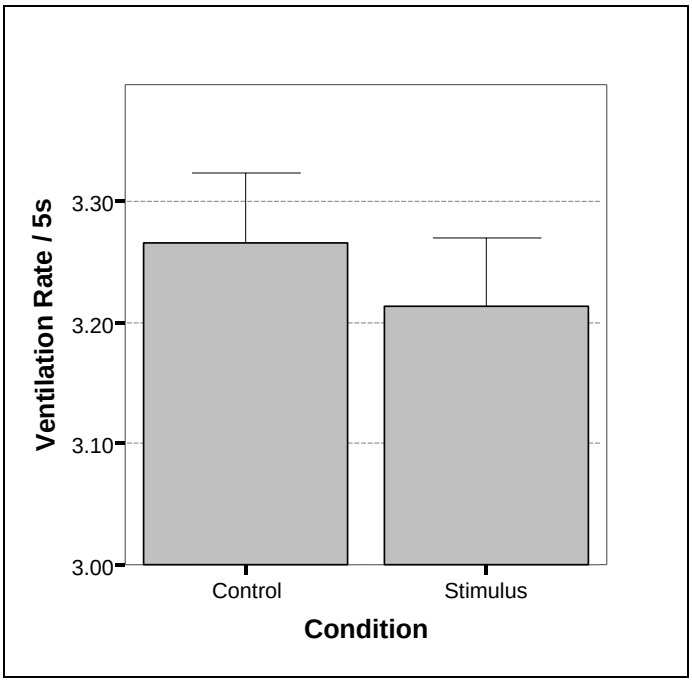

Figure 3.16. Bar graph depicts mean ventilation rates / 5s between control and stimulus treatments for animal 6. No significant difference from the control treatment was found. Error bars show mean ± 1.0 SE.

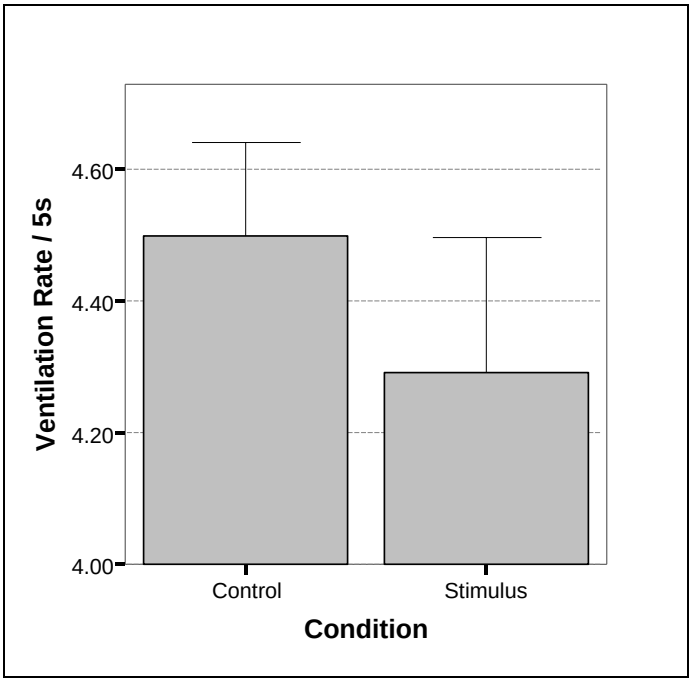

Figure 3.17. Bar graph depicts mean ventilation rates / 5s between control and stimulus treatments for animal 4. No significant difference from the control treatment was found. Error bars show mean ± 1.0 SE.

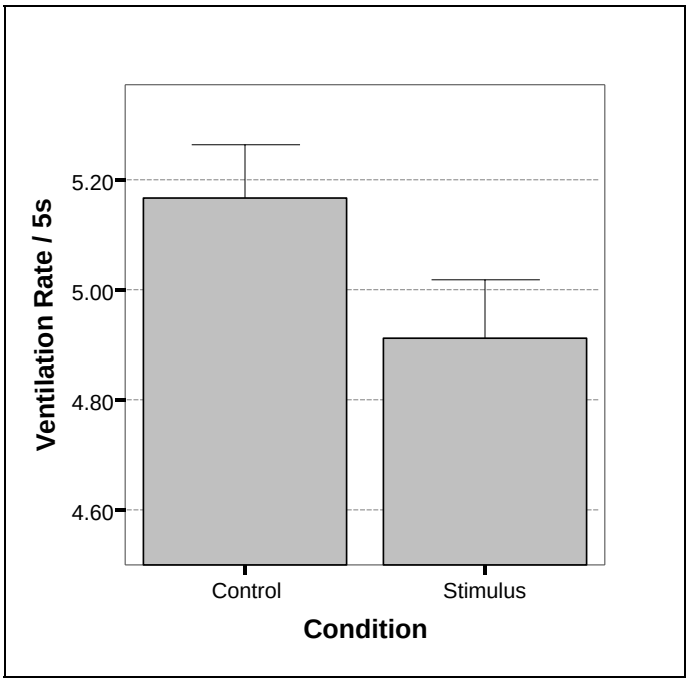

Figure 3.18. Bar graph depicts mean ventilation rates / 5s between control and stimulus treatments for animal 10. No significant difference from the control treatment was found. Error bars show mean ± 1.0 SE.

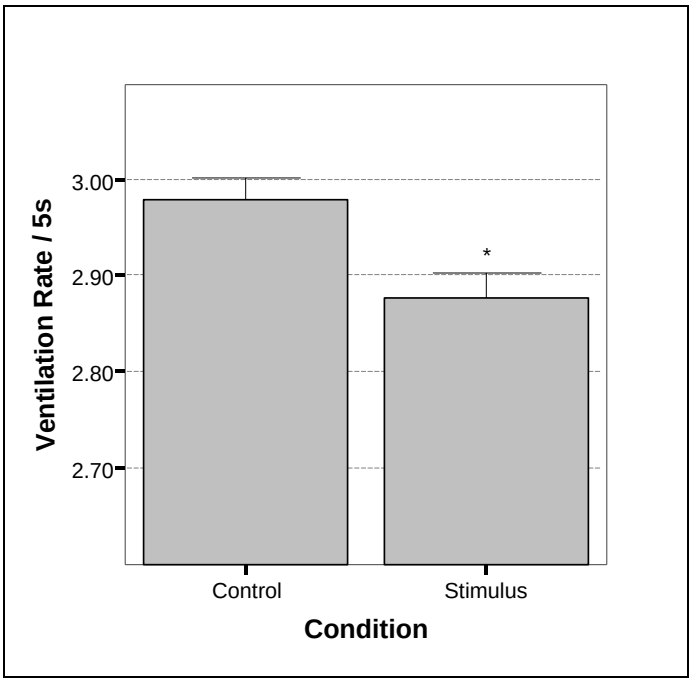

Figure 3.19. Bar graph depicts mean ventilation rates / 5s between control and stimulus treatments for all LSDE trials. The asterisk indicates a significant difference from the control treatment. Error bars show mean ± 1.0 SE.

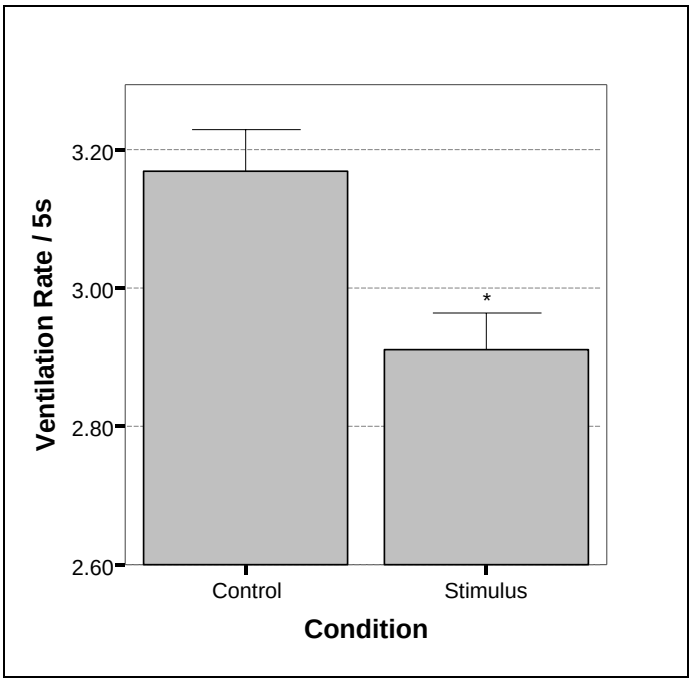

Figure 3.20. Bar graph depicts mean ventilation rates / 5s between control and stimulus treatments for animal 2. The asterisk indicates a significant difference from the control treatment. Error bars show mean ± 1.0 SE.

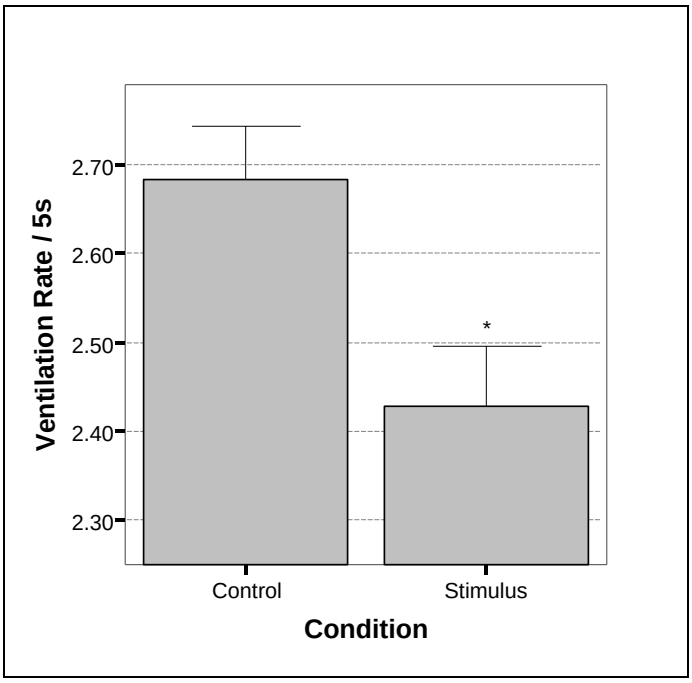

Figure 3.21. Bar graph depicts mean ventilation rates / 5s between control and stimulus treatments for animal 8. The asterisk indicates a significant difference from the control treatment. Error bars show mean ± 1.0 SE.

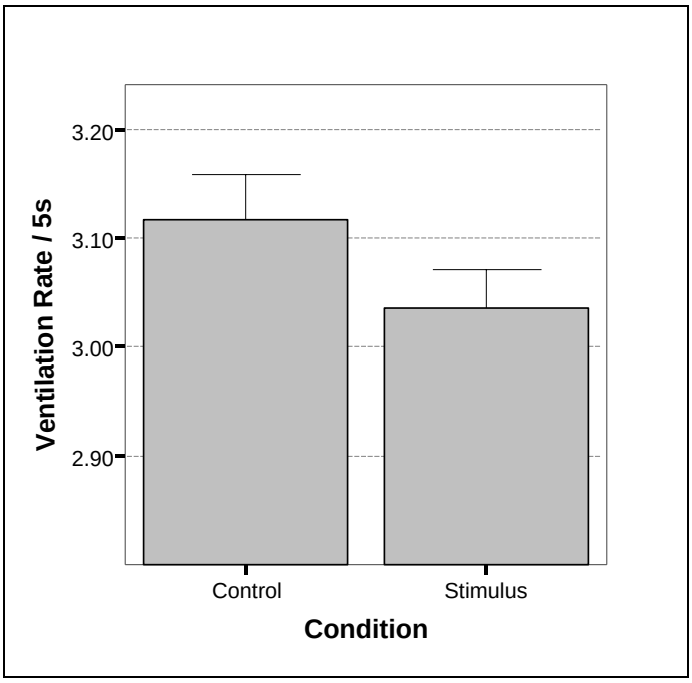

Figure 3.22. Bar graph depicts mean ventilation rates / 5s between control and stimulus treatments for animal 1. No significant difference from the control treatment was found. Error bars show mean ± 1.0 SE.

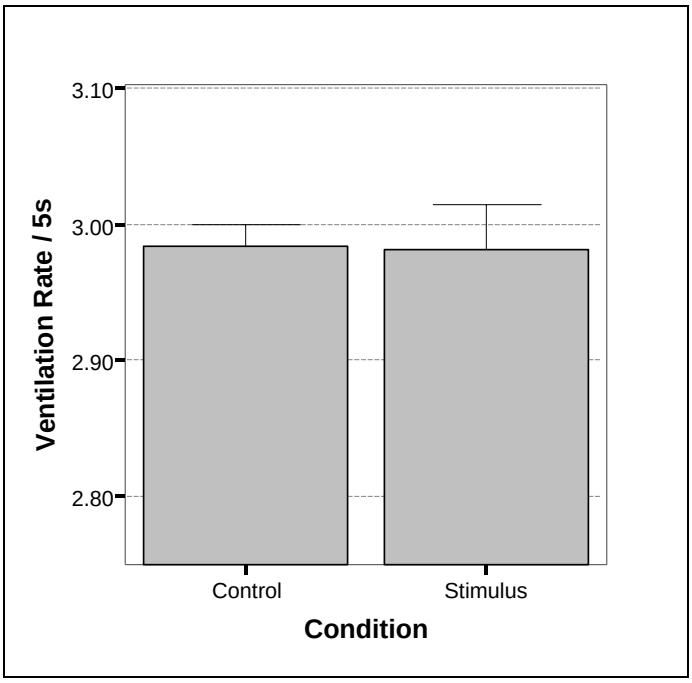

Figure 3.23. Bar graph depicts mean ventilation rates / 5s between control and stimulus treatments for animal 6. No significant difference from the control treatment was found. Error bars show mean ± 1.0 SE.

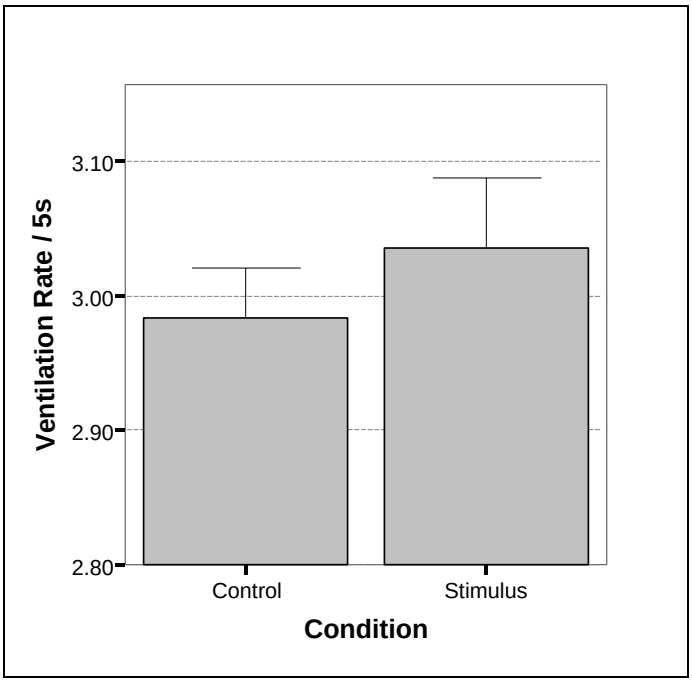

Figure 3.24. Bar graph depicts mean ventilation rates / 5s between control and stimulus treatments for animal 7. No significant difference from the control treatment was found. Error bars show mean ± 1.0 SE.

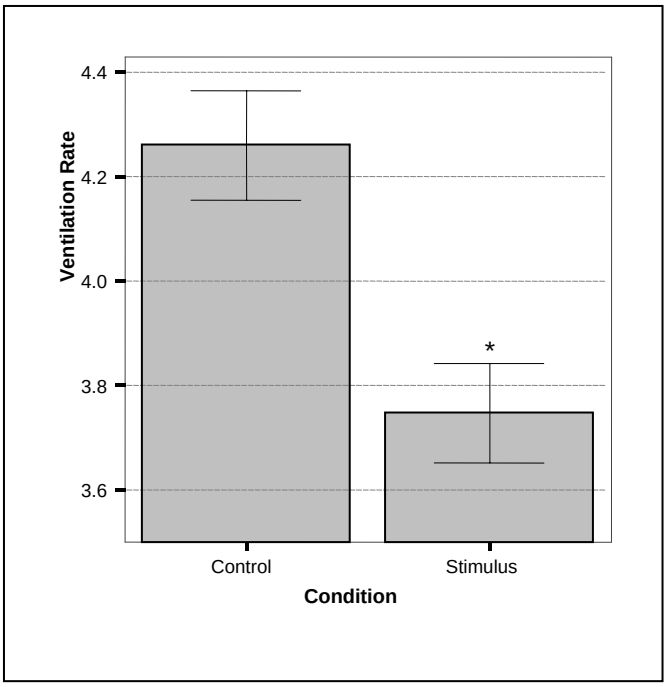

Figure 3.25. Bar graph depicts mean ventilation rates between control and stimulus treatments for all FSE trials. The asterisk indicates a significant difference from the control treatment. Error bars show mean ±1.0 SE.

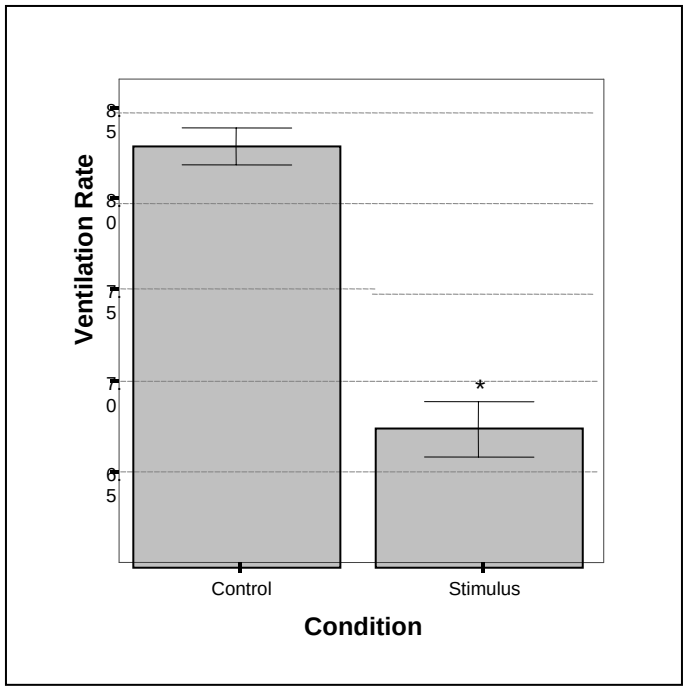

Figure 3.26. Bar graph depicts mean ventilation rates between control and stimulus treatments for Animal 3 (control administered first). The asterisk indicates a significant difference from the control treatment. Error bars show mean ±1.0 SE.

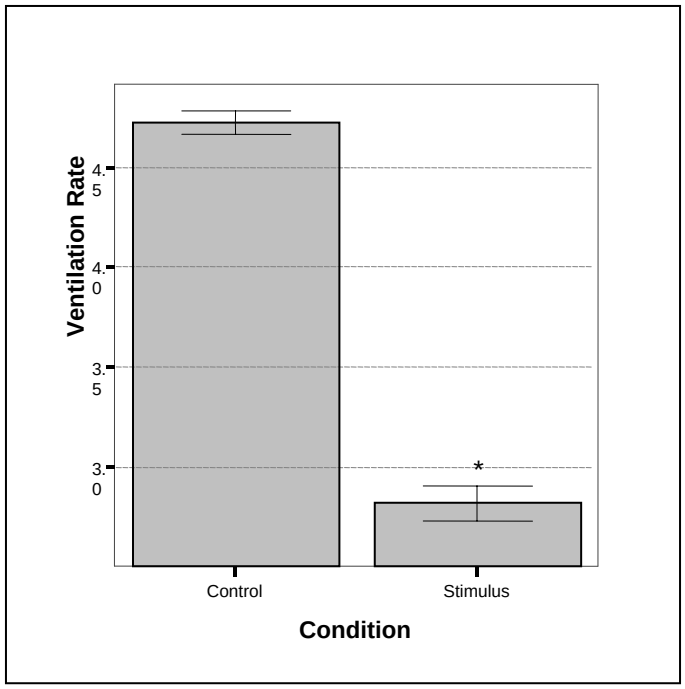

Figure 3.27. Bar graph depicts mean ventilation rates between control and stimulus treatments for Animal 6 (control administered first). The asterisk indicates a significant difference from the control treatment. Error bars show mean ±1.0 SE.

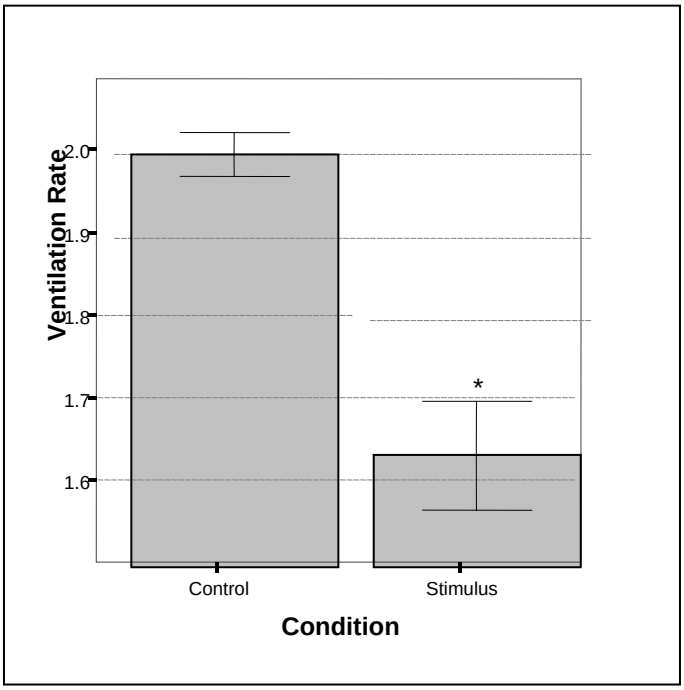

Figure 3.28. Bar graph depicts mean ventilation rates between control and stimulus treatments for Animal 8 (control administered first). The asterisk indicates a significant difference from the control treatment. Error bars show mean ±1.0 SE.

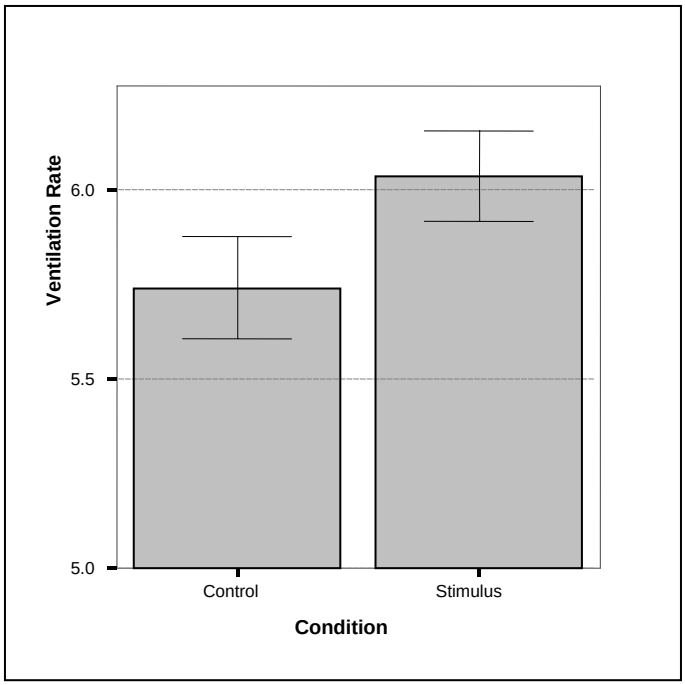

Figure 3.29. Bar graph depicts mean ventilation rates between control and stimulus treatments for Animal 1 (control administered first). Pairwise comparisons revealed no significant difference from the control treatment. Error bars show mean ±1.0 SE.

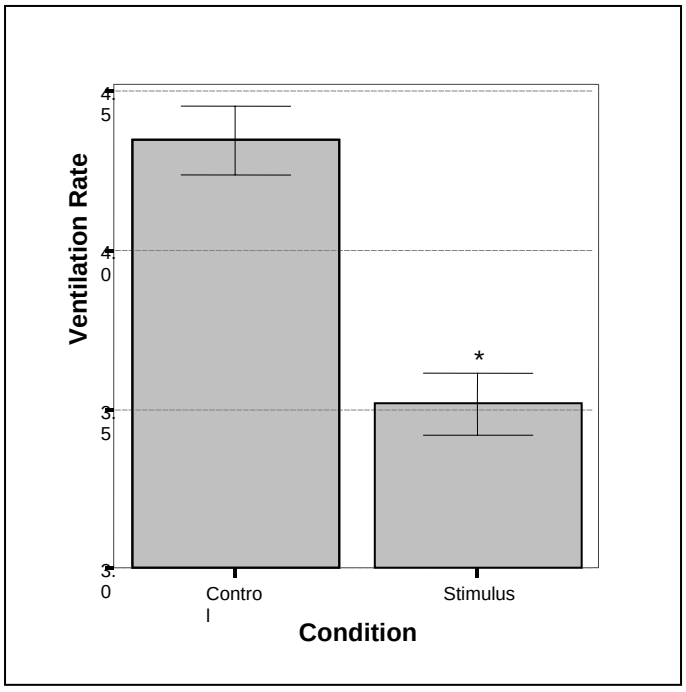

Figure 3.30. Bar graph depicts mean ventilation rates between control and stimulus treatments for Animal 4 (stimulus administered first). The asterisk indicates a significant difference from the control treatment. Error bars show mean ±1.0 SE.

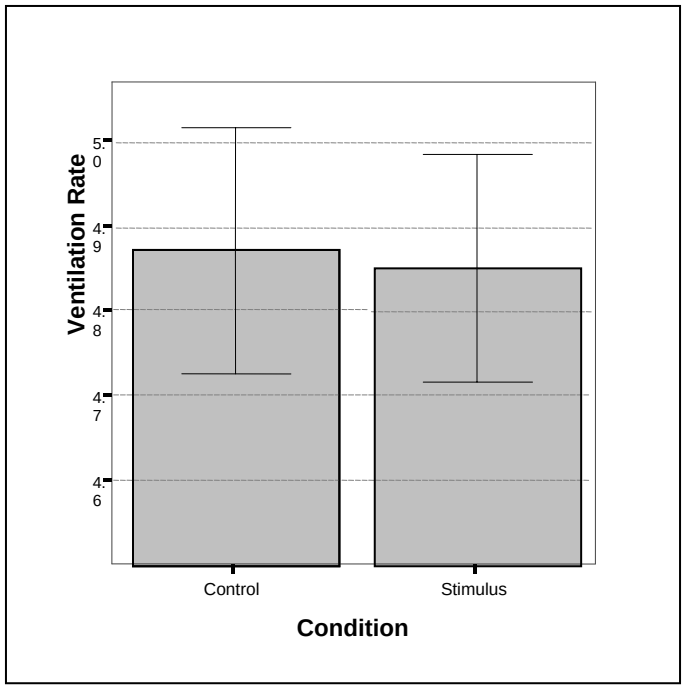

Figure 3.31. Bar graph depicts mean ventilation rates between control and stimulus treatments for Animal 11 (stimulus administered first). Pairwise comparisons revealed no significant difference from the control treatment. Error bars show mean ±1.0 SE.

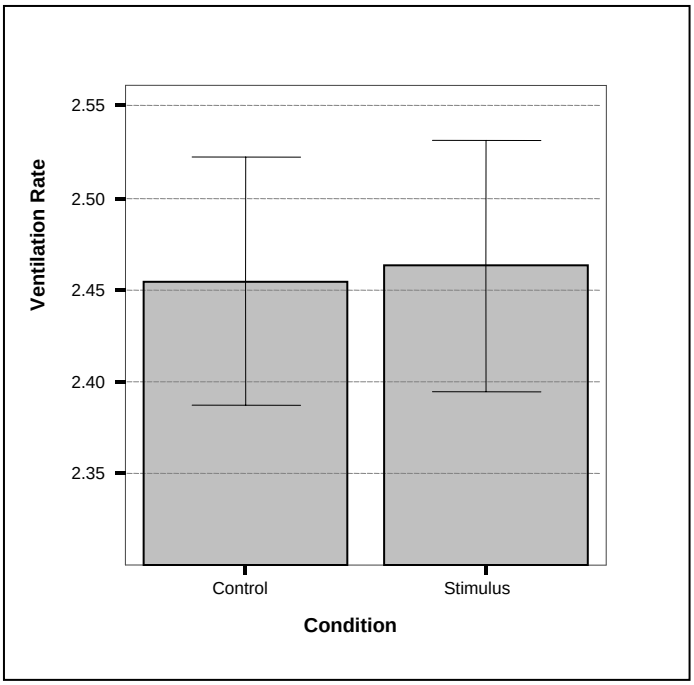

Figure 3.32. Bar graph depicts mean ventilation rates between control and stimulus treatments for Animal 2 (stimulus administered first). Pairwise comparisons revealed no significant difference from the control treatment. Error bars show mean ±1.0 SE.

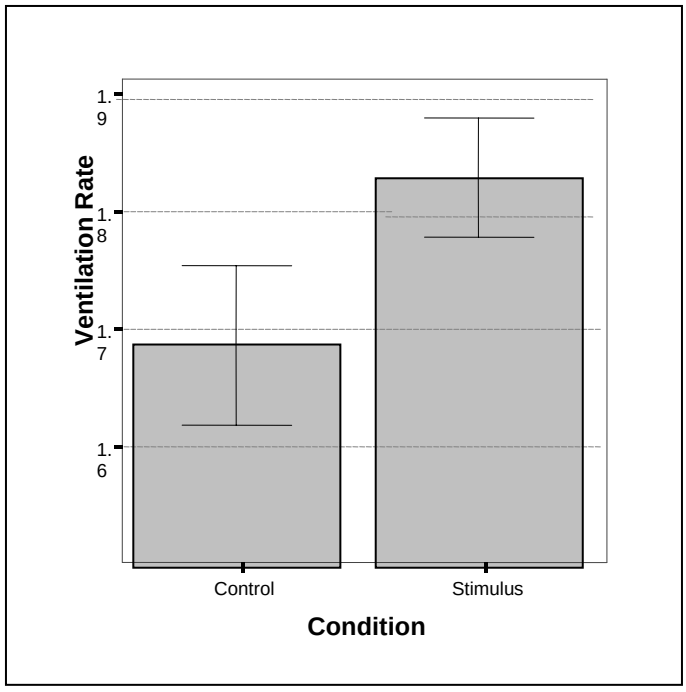

Figure 3.33. Bar graph depicts mean ventilation rates between control and stimulus treatments for Animal 9 (stimulus administered first). Pairwise comparisons revealed no significant difference from the control treatment. Error bars show mean ±1.0 SE.

Literature Cited

Arnold, J.M., Awai, M., and Carlson, B. 1990. Hatching of *Nautilus* embryos in the Waikiki Aquarium. *J. Ceph. Biol.* **1**: 117.

Arnold, J.M., Awai, M., and Carlson, B. 1993. *Nautilus* embryology: Egg capsule formation, deposition, and hatching. *J. Ceph. Biol.* **2**: 51–56.

Barber, V.C. 1968. The structure of mollusc statocysts, with particular reference to cephalopods. *Symp. Zool. Soc. Lond.* **23**: 37–62.

Barber, V.C., and Wright, D.E. 1969. The fine structure of the sense organs of the cephalopod mollusc *Nautilus*. *Z. Zellforsch*. **102**: 293–312.

Basil, J.A., Bahctinova, I., Kuroiwa, K., Lee, N., Mims, D., Preis, M., and Soucier, C. 2005. The Function of the Rhinophore and the Tentacles of *Nautilus pompilius* L. (Cephalopoda, Nautiloidea) in Orientation to Odor. *Marine and Freshwater Behavior and Physiology*. **38**(3): 209-221.

Basil, J.A., Hanlon, R.T., Sheikh, S.I., and Atema, J. 2000. Three-dimensional odor tracking by *Nautilus pompilius*. *J. Exp. Biol.* **203**(9): 1409–1414.

Basil, J.A., Lazenby, G.B., Nakanuku, L., and Hanlon, R.T. 2002. Female *Nautilus* are attracted to male conspecific odor. *Bulletin of Marine Science*. **70**(1): 217–225.

Bidder, A.M. 1962. Use of the tentacles, swimming, and buoyancy control in the pearly nautilus. *Nature*. **196**: 451–454.

Bleckmann, H. 1994. *Reception of Hydrodynamic Stimuli in Aquatic and Semiaquatic Animals* (Progress in Zoology). VCH Publishing, NewYork. **41**: 115 p.

Boal J.G., Wittenberg K.M. and Hanlon, R.T. 2000. Observational learning does not explain improvement in predation tactics by cuttlefish (Mollusca: Cephalopoda). *Behavioural Processes*. **52**: 141–153 (http://www.cephbase.com/refdb/refsrch3.cfm).

Braun, C.B., Coombs, S., and Fay, R.R. 2001. Multisensory integration in the octavolateralis system. Symposium contribution: Multimodal Sensory Guidance of Complex Behaviors. Part of the 5th meeting of the International Society of Neuroethologists.

Budelmann, B.U. 1977. Structure and function of the angular acceleration receptor systems in the statocysts of cephalopods. *Symp. Zool. Soc. London.* **38**: 309–324.

Budelmann, B.U. 1988. Morphological diversity of equilibrium receptor systems in aquatic invertebrates. *In* Sensory Biology of Aquatic Animals (eds. Atema, J., Fay, R.R., Popper, A.N., and Tavolga, W.N.). Springer-Verlag, New York. Pp. 757–782.

Budelmann, B.U. and Tu, Y. 1997. The statocyst-oculomotor reflex of Cephalopods and the vestibulo-oculomotor reflex of vertebrates: A tabular comparison. *Vie milieu*. **47**(2): 295–99.

Cheng, M.W. and Caldwell, R.L. 2000. Sex identification and mating in the blue-ringed octopus, *Hapalochlaena lunulata. Animal Behaviour.* **60**: 27–33.

Collins, D., Ward, P.D. and E.G. Westermann. 1980. Function of cameral water in *Nautilus*. *Paleobiology*. **6**(2): 168–172.

Coombs, S. 1994. Nearfield detection of dipole sources by the goldfish (*Carassius auratus*) and the mottled sculpin (*Cottus bairdi*). *J. Exp. Biol.* **190**: 109–129.

Everest, F.A. 2001. *The Master Handbook of Acoustics*, 4th ed. McGraw-Hill, New York.

Fukada, Y. 1987. Histology of the long digital tentacles. *In* Nautilus: *The Biology and Paleobiology of a Living Fossil* (eds. Saunders, W.B. and Landman, N.H.). Plenum Press, New York. Pp. 249–256.

Hamada, T., Deguchi, Y., Fukuda, Y., Habe, T., Hirano, H., Kanie, Y., Kawamoto, N., Mikami, S., Obata, I., Okutani, T. and K. Tanabe. 1978. Recent advancement of the rearing experiments of *Nautilus* in Japan. *Venus, the Japanese Journal of Malacology*. **37** (3): 131–136.

Hanlon, R.T. and Messenger, J.B. 1996. *Cephalopod Behaviour*. Cambridge University Press, Cambridge.

Haven, N. 1977. The reproductive biology of *Nautilus pompilius* in the Philippines. *Marine Biology*. **42**: 177–184.

Jordan, M., Chamberlain, Jr., J.A., and Chamberlain, R.B. 1988. Response of *Nautilus* to variation in ambient pressure. *J. Exp. Biol*. **137**: 175–189.

Kalmijn, A.J. 1988. Hydrodynamic and acoustic field detection. *In* Sensory Biology of Aquatic Animals (eds. Atema, J., Fay, R.R., Popper, A.N., and Tavolga, W.N.). Springer-Verlag, New York. Pp. 83–130.

Kinsler, L.E., Frey, A.R., Coppens, A.B., and Sanders, J.V. *Fundamentals of Acoustics*, 3rd ed. John Wiley and Sons, New York.

Klages, M., Muyakshin, S., Soltwedel, T., and Arntz, W.E. 2002. Mechanoreception, a possible mechanism for food fall detection in deep-sea scavengers. *Deep Sea Research Part I: Oceanographic Research Papers.* **49**(1): 143–155.

Komak, S., Boal, J.G., Dickel, L., and Budelmann, B.U. 2005. Behavioral responses of juvenile cuttlefish (Sepia officinalis) to local water movements. *Marine and Freshwater Behaviour and Physiology.* **38**(2): 117–125.

Landman, N.H. and Cochran, J.K. 1987. Growth and longevity of *Nautilus*. *In* Nautilus: *The Biology and Paleobiology of a Living Fossil* (eds. Saunders, W.B. and Landman, N.H.). Plenum Press, New York. Pp. 401–417.

Martin, A.W., Catala-Stucki, I., and Ward, P.D. 1978. The growth rate and reproductive behavior of *Nautilus macromphalus*. *Neues. Jahrb. Geol. Palaontol. Abh.* **156**(2): 207–25.

Messenger, J.B. 2001. Cephalopod chromatophores: neurobiology and natural history. *Biol. Rev.* **76**: 473–528.

Mikami, S., and Okutani, T. 1977. Preliminary observations on maneuvering, feeding, copulating, and spawning behaviors of *Nautilus macromphalus* in captivity. *Venus*. **36**: 29–41.

Morris, C.C. 1989. Preliminary observations on the ultrastructure of statoliths from *Nautilus*. *J. Ceph. Biol*. **1**(1): 15–20.

Muntz, W.R.A. 1991. Anatomical and behavioural studies on vision in *Nautilus* and *Octopus*. *Am. Malacological Bul.* **9**(1): 69–74.

Muntz, W.R.A. 1994a. Effects of light on the efficacy of traps for *Nautilus pompilius*. *Marine Behaviour and Physiology*. **24**:189–193.

Muntz, W.R.A. 1994b. Spatial summation in the phototactic behaviour of *Nautilus pompilius*. *Marine Behaviour and Physiology*. **24**:183–187.

Neumeister, H. and Budelmann, B.U. 1997. Structure and function of the *Nautilus* statocyst. *Phil. Trans. R. Soc. Lond.* B. **352**: 1565–1588.

O'Dor, R. K., Forsythe, J., Webber, D. M., Wells, J. and Wells, M. J. 1993. Activity levels of *Nautilus*. *Nature.* **362**: 626–627.

Pojeta, Jr., J., and Gordon, Jr., M. 1985. Class Cephalopoda. *In Fossil Invertebrates* (eds. Boardman, R.S., Cheetham, A.H., and Rowell, A.J.,). Blackwell Scientific Publications, Oxford; Boston. Pp. 329–358.

Popper, A.N., Salmon, M., and Horch, K.W. 2001. Acoustic detection and communication by decapod crustaceans. *J. Comp. Physiol.* A. **187**: 83–89.

Rogers, P.H. and Cox, M. 1988. Underwater sound as a biological stimulus. *In* Sensory Biology of Aquatic Animals (eds. Atema, J., Fay, R.R., Popper, A.N., and Tavolga, W.N.). Springer-Verlag, New York. Pp. 131–149.

Ruth, P., Schmidtberg, H., Westermann, B., and Schipp, R. 2002. The sensory epithelium of the tentacles and the rhinophore of *Nautilus pompilius* L (Cephalopoda, Nautilodea). *J. Morp.* **251**: 239–255.

Saunders, W.B. 1984. The role and status of *Nautilus* in its natural habitat: Evidence from deepwater remote camera photosequences. *Paleobiology*. **12**: 469–486.

Saunders, W.B. 1985. Studies of living *Nautilus* in Palau. *Nat. Geog. Soc. Res. Rep.* **18**: 669–682.

Saunders, W.B. and Landman, N.H. 1987. Nautilus: *The Biology and Paleobiology of a Living Fossil*. Plenum Press, New York.

Saunders, W.B. and Ward, P.D. 1987. Ecology, distribution, and population characteristics of *Nautilus*. *In* Nautilus: *The Biology and Paleobiology of a Living Fossil* (eds. Saunders, W.B. and Landman, N.H.). Plenum Press, New York. Pp. 137–162.

Saunders, W.B. and Spinosa, C. 1978. Sexual dimorphism in *Nautilus* from Palau. *Paleobiology.* **4**: 349–358.

Shigeno, S. and Yamamoto, M. 2002. Organization of the nervous system in the pygmy cuttlefish, *Idiosepius paradoxus* Ortmann (Idiosepiidae, Cephalopoda). *J. Morp.* **254**: 65–80.

Ward, P.D. 1987. *The Natural History of* Nautilus. London: Allen & Unwin Press.

Ward, P.D. and Saunders, W.B. 1997. *Allonautilus*: A new genus of living nautiloid cephalopod and its bearing on phylogeny of the Nautilida. *J. Paleont.* **71**: 1054–1064.

Ward, P.D. and Wicksten, M.K. 1980. Food sources and feeding behavior of *Nautilus macromphalus*. *The Veliger*. **23**: 119–124.

Williamson, R. 1988. Vibration sensitivity in the statocyst of the northern octopus, *Eledone cirrosa*. *J. Exp. Biol.* **134**: 451–454.

Wood, J.B. 2002. What we don't know about nautilus. *Tentacle*. **10**: 22–23.

Wood, J.B. and O'Dor, R.K. 2000. Do larger cephalopods live longer? Effects of temperature and phylogeny on interspecific comparisons of age and size at maturity. *Marine Biology*. **136**: 91–99.

Wray, C.G., Landman, N.H., Saunders, W.B., and Bonacum, J. 1995. Genetic divergence and geographic diversification in *Nautilus*. *Paleobiology*. **21**(2): 220–28.

Young, J.Z. 1965. The central nervous system of *Nautilus*. *Philos Trans R Soc Lond B Biol Sci*. **249**:1–39.

Young, J.Z. 1989. The angular acceleration receptor system of diverse cephalopods. *Philos Trans R Soc Lond B Biol Sci*. **325**:189–237.